# The Role of CHAP in Muscle Development, Heart Disease and Actin Signaling

*Willemijn van Eldik*

**Colophon**

The Role of CHAP in Muscle Development, Heart Disease and Actin Signaling

Willemijn van Eldik

Thesis Leiden University Medical Center


| | |
|---|---|
| Cover illustration and lay-out: | Merel Schouten (www.merelschouten.nl) |
| Printed by: | Gildeprint Drukkerijen |
| ISBN: | 9789461084187 |

# The Role of CHAP in Muscle Development, Heart Disease and Actin Signaling

Proefschrift

ter verkrijging van

de graad van Doctor aan de Universiteit Leiden,

op gezag van Rector Magnificus prof.mr. C.J.J.M. Stolker, volgens besluit van

het College voor Promoties

te verdedigen op donderdag 25 april 2013

klokke 11:15 uur

door

Willemijn Lisette van Eldik

geboren te Cothen

in 1982

**Promotiecommissie**

| | |
|---|---|
| Promotor | Prof. Dr. C.L. Mummery |
| Co-promotor | Dr. P.C.J.J. Passier |
| Overige leden | Prof. Dr. M.C. de Ruiter |
| | Prof. Dr. M.J. Goumans |
| | Prof. Dr. E.E. van der Wall - ICIN, Utrecht |
| | Dr. J. van der Velden - VUmc, Amsterdam |

The work presented in this thesis was carried out at the department of Anatomy and Embryology at the Leiden University Medical Center and Hubrecht Institute, Utrecht.

The research described in this thesis was supported by a grant of the Dutch Heart Foundation (DHF-2006B209). Financial support by the Dutch Heart Foundation for the publication of this thesis is gratefully acknowledged.

*funded by the dutch heart foundation*

Hartstichting

# Contents

# Chapter 1

*General introduction*

# Development of the different muscle types

Muscles can be broadly divided into three types: heart, skeletal and smooth muscle. Their common features include contractility and the presence of sarcomeres, but they differ significantly in their developmental origin and functional characteristics. This thesis concerns a novel protein important for contractile function in all muscle cell types.

*Development of the heart*

The heart is the first functional organ in the embryo[1]. In mammals and birds the cardiac crescent, the first distinct cardiac structure, is formed from cardiac precursor cells that originate from the anterior lateral plate mesoderm[2-4]. The cells in the cardiac crescent are specified by multiple inhibiting and inducing signals which result in a defined area of cardiac cells, known as the first heart field. Inhibitory canonical Wnt signals (Wnt3a and Wnt8) from the ectoderm and Noggin and Chordin (bone morphogenetic protein (BMP) antagonists) from the notochord prevent formation of cardiac mesoderm. On the other hand, cardiac mesoderm is induced by signals activated by BMP2, fibroblast growth factor 8 and sonic hedgehog homolog (Ssh) secreted from the pharyngeal endoderm[1]. Fusion of the cardiac crescent at the midline of the embryo (Figure 1) results in the formation of a linear heart tube that shows polarity at the outset, with anterior (ventricular) and posterior (atrial) specification[2, 3]. In all vertebrates the linear heart undergoes rightward looping (Figure 1) and in higher vertebrates, the looped heart subsequently undergoes septation at the level of the atrium, ventricle and arterial pole. At embryonic day 8 (E8) in the mouse embryo and Hamburger-Hamilton (HH) stage 24 in the chick embryo, new myocardium is added to the outflow tract of the heart. These cells are derived from the second heart field (SHF), which is located in the pharyngeal mesoderm (Figure 1)[2-5]. The first heart field (FHF) gives rise to the linear heart tube, definitive left ventricle and part of the inflow region of the heart, whereas the second heart field (SHF) gives rise to right ventricular and outflow tract myocardium and part of the inflow region[4, 5].

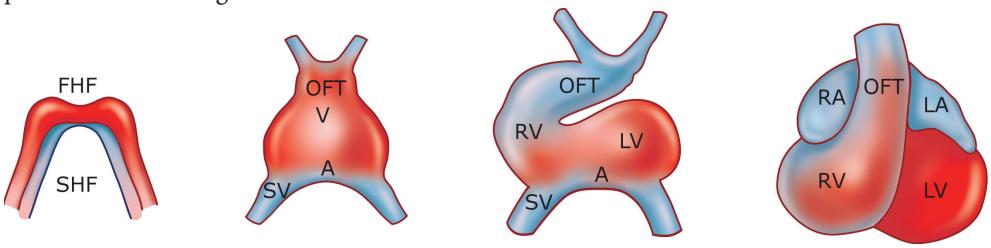


**Figure 1: Schematic overview of heart development. In the cardiac crescent stage two pools of cardiac progenitors can be identified; the first heart field (FHF) and second heart field (SHF). In the linear heart tube stage polarization of the heart can already be recognized. In third stage there is rightward cardiac looping and in the last stage there is chamber formation and septation. Ventricle (V), sinus venosus (SV), atrium (A), left ventricle (LV), right ventricle (RV), outflow tract (OT), left atrium (LA) and right atrium (RA).**

*Skeletal muscle development*

In vertebrates, muscles are formed from the paraxial mesoderm, which segments into somites. The ventral part of the somite, the sclerotome, gives rise to the cartilage and bone of the vertebral column and ribs, whereas the dorsal part of the somite, the dermomyotome, give rise to skin and muscles of the trunk and the limbs. The dermomyotome can be divided into epaxial and hypaxial parts (Figure 2)[6-8], which give rise to different muscle groups and

differ in the way myogenesis is induced. The epaxial part is located adjacent to the neural tube and notochord and will form the muscles of the back. The hypaxial part forms the muscles of the limbs, body wall and tongue. In the epithelium of the hypaxial dermomyotome, that is located opposite to the limb buds, muscle progenitor cells delaminate and migrate into the limb buds, forming the muscles of the limbs[6, 8]. Myogenesis is regulated largely by the MyoD family of basic helix-loop-helix factors[6, 8]. In the epaxial part, paired homeobox gene 3 (Pax3), myogenic factor (Myf) 5 and 6 induce myogenic differentiation 1 (MyoD1). In the hypaxial part, on the other hand, Pax3 induces MyoD indirect, via activation of Myf5 expression (see figure 2). These signaling cascades are induced by Shh from the ventral neural tube and notochord and (non-)canonical Wnt signals from the neural tube (Figure 2). Two phases of myogenesis can be distinguished. The primary myotome is formed from the dermomyotome. The epithelium of the dermomyotome is formed as a central sheet that is surrounded by four lips. During the first myogenic phase, cells of the four epithelial lips of the dermomyotome delaminate and locate between the dermomyotome and sclerotome to form the primary myotome[7] (primary fibers); this occurs between E11 and E14 in the mouse[6]. In the second myogenic phase the central part of the dermomyotome epithelializes, resulting in a second phase of muscle formation[7] (secondary fibers), which occurs between E14 and E16 in the mouse[6]. Generally speaking, the primary fibers tend to become slow fibers, whereas the secondary fibers become fast fibers[6]. In the postnatal period the muscle mass increases by

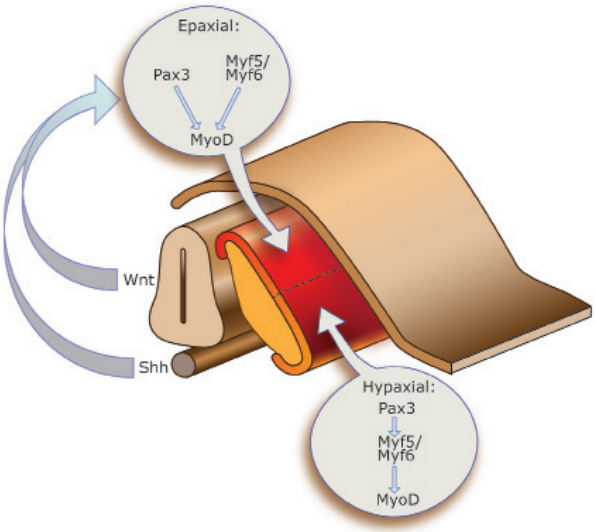


**Figure 2: Schematic overview of myogenic induction in the mouse. In the epixial part myogenic differentiation 1 (MyoD1) is induced by synergetic action of paired box gene 3 (Pax3), myogenic factor (Myf) 5 and 6, which are induced by Sonic hedgehog and Wnt1 from the notochord and neural tube , respectively. In the hypaxial part , on the other hand, Pax3 induces Myf5 and 6, which in turn induces MyoD1.**

hypertrophy (growth of individual cells) of existing muscle fibers[8].

Adult myogenesis is achieved by activation of quiescent satellite cells, which are marked by expression of Pax7, c-met proto-oncogene and M-cadherin. After muscle injury, these cells commit to a muscle-progenitor fate and activate transcription factors such as Pax3 and Myf5[6, 7], leading to differentiation of skeletal muscle cells. The satellite cells only have limited capacity of self-renewal, therefore skeletal muscle degenerates under pathological conditions[6].

*Vascular smooth muscle cell differentiation*

Vascular smooth muscle cells (VSMCs) have different embryonic origins which are reflected in their distribution in different tissues and organs. The walls of the great arteries (pulmonary artery, dorsal aorta, carotid and subclavian arteries) for example are derived from progenitor cells that migrate from the dorsal surface of the neural tube (neural crest) into the pharyngeal arch complex between E8.5 and 9.5 in the mouse. VSMCs of the coronary arteries arise from the epicardium, which forms during embryonic development from pro-epicardial cells (pro-epicardial organ) and grow over the surface of the myocardium to form a single layer of epicardial cells. Between E13.5 and E14.5 some of these cells undergo epithelial-to-mesenchymal transition and form the VSMCs of the coronary arteries[9, 10]. A third source of VSMC progenitors is an Islet-1 positive cell population, which produces the VSMC in the walls of the pulmonary trunk, aortic root and the branching coronary arteries[10].

Development of VSMCs from embryonic progenitors is regulated in three phases. During the first phase, vasculogenesis occurs and angioblasts differentiate into endothelial cells that assemble in a capillary vascular network. In the second phase (E10.5 in the mouse), increased cardiac output demands a more active vascular network, which leads to the production of chemo-attractants by the endothelial cells, this in turn attracts progenitors of VSMCs, the mesenchymal cells, to surround the vessel wall. Close contact between mesenchymal cells and endothelial cells, mediated by platelet derived growth factor, initiates SMC differentiation. In the last phase the cells further mature and form the vascular extracellular matrix[10].

Differentiated VSMCs are defined by expression of a specific subset of cytoskeletal and contractile proteins, such as α-smooth muscle actin (ASMA), smooth muscle calponin and smooth myosin heavy chain (MHC), SM22-α, desmin and smoothelin[10, 11]. The function of mature differentiated VSMCs is contraction, regulation of vascular tone, important for the regulation of blood pressure and blood flow distribution. Adult VSMCs proliferate very slowly, have a very low synthetic activity (low production of extracellular matrix) and are non-migratory[11]. However, unlike cardiac and skeletal muscle cells, adult SMCs can undergo reversible changes in phenotype between a contractile and synthetic state in response to changes in the local environment[9-11]. For example, after vascular injury contractile SMCs are capable of undergoing a transient modification of their contractile phenotype to a synthetic phenotype and in this way play an essential role in the repair of the vascular injury by producing extracellular matrix [11].

## Sarcomeres: contracting units of striated muscle and function in cardiac disease

In adult animals these three types of muscle cells can be recognized: heart, skeletal muscle and smooth muscle. In heart and skeletal muscle cells are 'striated', a striped pattern visible microscopically made up of sarcomeres. In these muscles sarcomeres form the basis for contraction. The function of sarcomeres in healthy and diseased muscle is discussed in the following section.

*Structure of sarcomeres*

Sarcomeres are multi-protein complexes responsible for the contraction of striated muscle. Contraction is regulated by two filament systems, the thin actin and the thick myosin filaments, that slide over each other. The sarcomere is a highly organized structure which can be divided

into several subcompartments. The Z-discs form the boundary of each sarcomere, the I-band (for isotropic) surrounds the Z-disc and is composed of only actin filaments, the A-band (for anisotropic) is composed of actin and myosin filaments and the M-band (middle) forms the centre of each sarcomere (Figure 3)[12, 13].

Protein composition of the sarcomere is determined by the specific muscle type. In the heart the giant protein titin is the structural backbone of the sarcomere and two of these molecules run from Z-disc to Z-disc. Titin determines the stiffness of the sarcomere and keeps the A-band in the middle of the sarcomere during contraction. Via T-cap, titin is connected to α-actinin[14, 15], the major component of the Z-disc. There are four α-actinin isoforms (1-4), of which α-actinin-2 and -3 are the only isoforms expressed in striated muscle. In cardiac tissue only α-actinin-2 is expressed. In the Z-disc, α-actinin-2 is organized as homodimers in an antiparallel manner and in this way cross-links actin[16]. Furthermore, α-actinin-2 functions in binding several proteins that are involved in stretch-sensor function of the Z-disc[12]. This will be discussed in more detail later in this chapter.

Actin is a ubiquitously expressed protein important in many fundamental processes, such as cell cycle regulation, cell motility and muscle contraction. In striated muscle, two actin forms are present, cardiac actin and skeletal actin. In adult cardiomyocytes cardiac actin is the major isoform present [16]. Via CapZ, a protein composed of α and β subunit, actin filaments are connected to α-actinin-2, linking the thin filaments to the Z-disc[12, 16]. Mutations in sarcomeric proteins can lead to the development of cardiomyopathy.

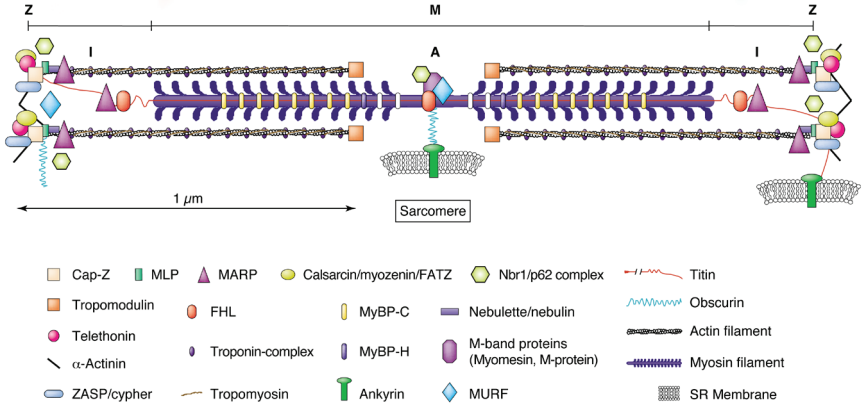


**Figure 3: Schematic overview of a sarcomere. The Z-disc forms the boundary of the sarcomere and is composed of α-actinin homodimers that bind several signaling molecules (see text). The I-band is composed of only actin filaments and the A-band is composed of actin and myosin filaments. The M-band forms the middle of the sarcomere. Adapted from[13].**

*Mutations in sarcomeric proteins result in cardiomyopathy*

Cardiomyopathy is a group of disorders of the heart that result in inadequate pumping of blood around the body. Hypertrophic cardiomyopathy (HCM) and dilated cardiomyopathy (DCM) are mainly caused by mutations in sarcomeric proteins. HCM is characterized by left ventricular hypertrophy (resulting from increased cell size or volume), increased systolic function and decreased diastolic function. At the histological level, hypertrophy and disarray of cardiomyocytes and interstitial fibrosis is observed[17, 18]. DCM, on the other hand, is characterized by ventricular dilation and contractile dysfunction of the left and/or right ventricles. Depending on the location of the mutation, HCM or DCM is induced; in HCM regions of sarcomeric proteins are mutated that are directly involved in force generation,

whereas the regions that are mutated in DCM are involved in force transmission from the sarcomere to the extrasarcomeric cytoskeleton[17].

Several mouse models for HCM and DMC have been generated, which reflect the pathology of the human disease. For example in a mutant mouse with a truncation in myosin binding protein C (MyBP-C), a mild HCM phenotype was observed [19], while a mutation (R403Q) in α-MHC resulted in a more severe HCM phenotype [19-21]. Mouse models with mutations in cardiac troponin T (cTnT) at different domains, R92Q (transgenic) [22]and ΔK210 (knock-out)[23], resulted in HCM and DCM, respectively.

Several mouse models for HCM and DCM have been reviewed in Beqqali et al and are summarized in table 1[24].

**Table 1: Overview of animal models of hypertrophic and dilated cardiomyopathy. Adapted from[24].**

| *Disease model* | *Gene* | *Mutation* | *Species* | *Approach* | **Reference** |
|---|---|---|---|---|---|
| *HCM* | α-MHC | R403Q/+ | Mouse | Knock-in | [19-21, 25] |
| | β-MHC | R403Q | Rabbit | Transgenic | [26] |
| | MyBP-C | truncation | Mouse | Knock-in | [19, 27-29] |
| | cTnT | R92Q | Mouse | Transgenic | [22, 30-33] |
| *DCM* | cTnT | ΔK210 | Mouse | Knock-in | [34] |
| | cTnT | R141W | Mouse | Transgenic | [31, 35] |

*The Z-disc as stretch-sensor*

α-actinin-2 anchors several proteins to the Z-disc, which act as stretch sensor. Several Z-disc proteins have been associated with cardiomyopathies, for example interacting proteins of α-actinin-2 such as calcineurin, muscle-specific LIM protein (MLP), T-cap, calcarcin-1, cypher and Enigma homologue protein (ENH) [12]. MLP has been found to be an essential component of the T-cap and titin complex, stabilizing the interaction between these proteins, which then can sense increase in stretch and activate downstream signals for hypertrophy [36].

The phospatase calcineurin, a heterotrimer consisting of a catalytic subunit A (CnA), calcineurin B and calmodulin, is a key regulator of hypertrophy. In the calcineurin pathway hypertrophic stimuli lead to an elevation in the intracellular $Ca^{2+}$ levels and subsequent activation of calcineurin. Activated calcineurin dephosphorylates nuclear factor of activated T-cells (NFAT), which then translocates to the nucleus to activate genes that are associated with stress, such as atrial natriuretic factor (ANF) and brain natriuretic peptide (BNP), and genes that encode fetal isoforms of contractile proteins such as β-myosin heavy chain (β-MHC) [37]. Molketin et al. generated transgenic (Tg) mice that express a constitutively active form of the catalytic subunit of calcineurin in the heart, by using of the α-MHC promoter to drive the calcineurin construct[38]. Hearts of calcineurin Tg mice show massive hypertrophy, disorganized cardiomyocytes, fibrosis and enlarged nuclei. Furthermore, with ageing calcineurin Tg mice show dilatation of the ventricles and are highly susceptible to sudden cardiac death[38]. NFATc2 [39] and NFATc3[40], are essential mediators of the calcineurin induced hypertrophy, which is reduced in $NFATc2^{-/-}$ or $NFATc3^{-/-}$ mice. However, $NFATc4^{-/-}$ mice do not exhibit reduced calcineurin induced hypertrophy, suggesting that NFATc4 does not play an important role in the calcineurin-dependent hypertrophy pathway [40].

Calsarcin, a novel target for calcineurin, binds to both calcineurin and α-actinin [41]. Overexpression of Calsarcin-1, both *in vitro* and *in vivo*, has protective effects on hypertrophy by interfering with calcineurin-NFAT signaling [42], while lack of calsarcin-1 enhances this signaling pathway[43].

In addition to the interaction with calsarcin and calcineurin, α-actinin has also been shown to interact with several PDZ-LIM proteins. Cypher (or Oracle/ZASP) is expressed in heart and

skeletal muscle during mouse and zebrafish development[44-46], and interacts with α-actinin-2[44] and calsarcin[47]. Deletion of cypher in mice and zebrafish results in disruption of the Z-disc structure and leads to the development of DCM[46-48]. However, in mice only deletion of the long isoform of cypher leads to development of late-onset DCM, whereas deletion of the short isoform has no effect[49]. More interestingly, mutations in cypher have been identified in humans that cause DCM[50]. These results indicate cypher as an essential component of the α-actinin-calcineurin-calsarcin complex to maintain cardiac structure and function.
ENH is another PDZ-LIM protein which interacts with α-actinin-2 [51], calsarcin and cypher. In ENH$^{-/-}$ mice expression of the short cypher isoform and calsarcin is lost, which leads to disruption of the Z-disc and development of DCM[52].
These data show an essential role for the Z-disc in the development of cardiomyopathies and targeting these components could reveal strategies for possible new therapies for the treatment of these diseases. Therefore, it will be necessary ultimately to identify all Z-disc components and in this way, increase understanding of Z-disc function in the development of cardiomyopathies. Work in this thesis has identified one new protein that is part of the Z-disc complex.

# Actin signaling

*Regulation of cardiac development and disease via actin signaling pathway*
The actin cytoskeleton is important in regulation cell shape changes and gene expression during development and disease. Polymerization of monomeric globular actin (G-actin) in filamentous actin (F-actin) is regulated by several actin binding proteins[53].
Rho GTPases (RhoA, Rac and Cdc42) induce actin polymerization via the Rho-associated kinase (ROCK)-LIM kinase-cofilin pathway[53-56]. RhoA can be induced by phosphorylation of ezrin/radixin/moesin (ERM), proteins that function in linking the membrane to the actin cytoskeleton[57]. RhoA is highly expressed in embryonic hearts, downregulated in adults and re-expressed during cardiac hypertrophy[58]. Heart-specific overexpression of RhoA leads to the development of a DCM-phenotype[59], whereas inhibiting ROCK protects the heart after aorta constriction[60].
Serum response factor (SRF) is a member of the MADS (MCM1, Agamous, Deficiens, SRF) family of transcription factors, which share a conserved motif of 57 amino acids mediating homodimerization, association with other factors and DNA-binding activity[61]. SRF is expressed in many cell types and functions in many biological processes, including gastrulation, development and function of the cardiovascular system, T-cell and B-cell activities in the immune system and neuronal functions of the developing and adult brain. Homodimeric SRF binds to a palindromic DNA sequence (CC(A/T)$_6$GG), which is called the CArG box[53]. Several SRF-mouse models have shown that SRF is essential for cardiac development, as well as maintaining adult cardiomyocytes. SRF is responsible for maintaining the sarcomeric integrity in cardiomyocytes[62-64] and disruption of its expression results in DCM in mice[65, 66]. Therefore, it is not surprising to find several sarcomeric genes, such as skeletal and cardiac actin, α-MHC and β-MHC, myosin light chain (MLC)2a and 2v, myomesin, troponin C, and titin, to be targets of SRF[62].
Myocardin and myocardin related transcription factors (MRTFs) function as co-activators of SRF resulting co-activator specific gene transcription determining skeletal and smooth muscle

differentiation. Furthermore, these factors also have distinct functions in pathophysiological remodeling of the heart[61].

Myocardin, MRTF-A and -B share a conserved so-called RPEL domain, which in MRTFs functions as G-actin binding domain. In myocardin, the RPEL domain does not bind G-actin, therefore myocardin is localized exclusively in the nucleus[61]. Myocardin is essential for smooth muscle differentiation and activates expression of smooth muscle genes in promoters with two adjacent CArG boxes by binding these as homodimers[67]. Tracing studies show that myocardin specifically marks cardiac, smooth and skeletal muscle lineages during embryonic development. In skeletal muscle precursors, myocardin expression leads to inhibition of differentiation, whereas in smooth muscle cell precursors it induces differentiation[68]. Myocardin$^{-/-}$ mice die around E10.5 and these mutant embryos show vascular abnormalities which result from impaired smooth muscle cell differentiation[69, 70]. Cardiac specific deletion (α-MHC-Cre) of myocardin leads to decreased expression of sarcomeric genes (α-cardiac actin, MLC2v, and tropomyosin) and connexin 43 and desmin, which results in disruption of the structural organization of the sarcomere and intercalated discs, respectively. Furthermore, the hearts of α-MHC-Cre-myocardin$^{f/f}$ showed left atrial enlargement, hypertrophy, interstitial fibrosis and a decreased cardiac function (decreased ejection fraction)[71]. Myocardin also has an essential function during pathophysiological events in the heart; it is upregulated in several *in vivo* and *in vitro* models of hypertrophy, as well as in human patient hearts with idiopathic DCM. The hypertrophic marker ANF is a direct target of myocardin and over-expression of myocardin in cardiomyocytes *in vitro* leads to a hypertrophic response, which can be abolished by expression of a dominant negative isoform lacking the transcriptional activation domain[72].

MRTF-A$^{-/-}$ mice are viable and show no cardiac defects. Female MRTF-A$^{-/-}$ mice are unable to nurse their offspring effectively, due to a failure in myoepithelial cell differentiation. These are cells that posses characteristics of both epithelial and SMC and surround the milk producing cells giving structural and contractile support[73]. Deletion of MRTF-A in the heart has a protective effect on the heart and shows that MRTF-A has a role in controlling the expression of a fibrotic gene program and smooth muscle cell differentiation. Scar formation and fibrosis are decreased in MRTF-A$^{-/-}$ mice after myocardial infarction or Angiotensin II treatment[74].

MRTF-B is expressed in derivatives of the neural crest. Therefore, MRTF-B knockout mice show cardiovascular abnormalities, resulting from impaired smooth muscle cell differentiation[75, 76].

Myocyte Enhancer Factor-2 (MEF2) is another MADS-box transcription factor. Four isoforms of MEF2 exist (A-D), of which isoforms A, C and D have distinct functions in the heart. Knockout studies show that MEF2A is essential for energy metabolism and sarcomeric organization in adult hearts[77], MEF2C is involved in cardiac morphogenesis[78], and MEF2D is a mediator of stress-dependent pathological remodeling of the adult heart[79]. On the other hand, overexpression of these factors induce (dilated) cardiomyopathy in mice[80, 81].

Transcriptional activity of SRF is regulated by Striated Muscle Activator of Rho Signaling (STARS). STARS binds to actin and activates RhoA in this way promoting actin polymerization and depletion of the G-actin pool. Subsequently, MRTFs translocate to the nucleus and activate gene expression by acting as co-factor for SRF. SRF induces actin genes, in this way providing a negative feed back loop [82, 83]. STARS is a direct target of MEF2, STARS expression is induced by MEF2 in several models of hypertrophy[84]. Thus, the formation of actin bundles is not only necessary for cell movement and polarization, but also leads to the induction of signal-transduction pathways important for cardiac development and hypertrophy. The actin

signaling pathway is summarized in figure 4.

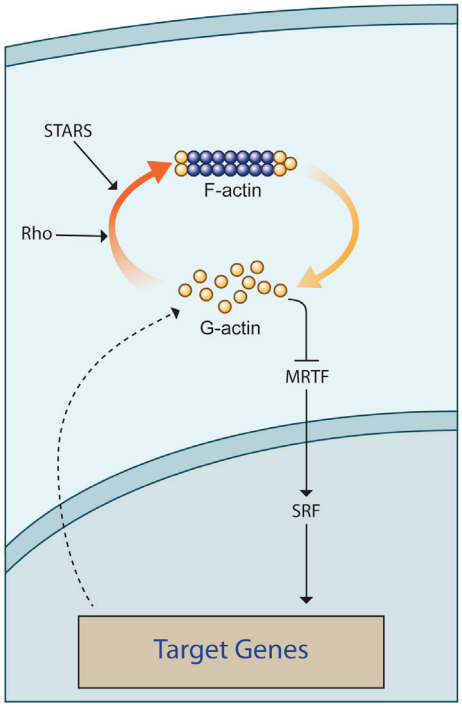


**Figure 4: The actin signaling pathway. Rho is activated by Striated Muscle Activator of Rho (STARS) which leads to polymerization of G-actin into F-actin and subsequent deletion of the G-actin pool. Myocardin Related Transcription Factors (MRTFs), normally inhibited by G-actin, translocate to the nucleus to act as transcriptional co-activator of Serum Response Factor (SRF). Actin is a target of SRF, in this way providing a negative feedback loop mechanism.**

*The synaptopodin gene family: role in actin polymerization*

Proteins belonging to the synaptopodin gene family are involved in actin signaling. Synaptopodin is the founding member of the synaptopodin gene family. Three isoforms (of one gene) of synaptopodin exist: Synpo-short (685 aa) expressed in the brain, Synpo-long (903 aa) and Synpo-T (181 aa) which are both expressed in kidney podocytes. Both Synpo-long and Synpo-short interact with α-actinin-2 and -4 resulting in elongation and bundling of actin filaments[85], which is regulated by preventing proteasomal degradation of RhoA[86]. Synaptopodin$^{-/-}$ mice lack 'spine apparatus', an organelle present in dendritic spines, which leads to defects in behavior. The structure and function of kidney podocytes is not affected by decreased synaptopodin expression[87]. This can be explained by the fact that in the brain of Synaptopodin$^{-/-}$ mice α-actinin-2 is downregulated, resulting in a reduction in actin filament formation. In contrast, kidney podocytes of Synaptopodin$^{-/-}$ mice upregulate Synpo-T and therefore have normal levels of α-actinin-4, resulting in rescue of actin filament formation[85].
Myopodin is the second member of the synaptopodin gene family, and has actin binding activity as well[88]. It is expressed in adult heart, skeletal muscle and smooth muscle cells. Myopodin localizes at the Z-disc of skeletal muscle cells and cardiomyocytes and can translocate to the nucleus [88, 89]. Myopodin forms a protein complex with α-actinin, calcineurin, protein kinase A (PKA) and calmodulin-dependent kinase II (CaMKII). Activation of PKA and CaMKII or inhibition of calcineurin results in phosphorylation of myopodin and its

subsequent translocation to the nucleus[90].

*CHAP is a new member of the synaptopodin gene family*

Micro-array analysis of gene expression technique is a powerful tool to discover new genes associated with specific biological processes. Using an assay in which human embryonic stem cells (hESC) were differentiated to cardiomyocytes, we discovered a new cardiac enriched gene, which was homologous to synaptopodin and myopodin. This new gene was annotated as Synpatopodin-2-like (SYNPO2L)[91] and we renamed it later Cytoskeletal Heart-enriched Actin-associated Protein (CHAP). Mouse CHAP is located on chromosome 14 and exists as two isoforms: a long isoform CHAPa (978 aa) and a shorter isoform CHAPb (749 aa), produced by an alternative ATG site at the beginning of exon 4. The CHAPa and b isoforms are almost identical, with a nuclear localization signal (NLS) and actin binding sites. However, the N-terminal of CHAPa is longer and contains a PDZ domain.

During development, *ChapB* is first expressed at the cardiac crescent stage (E7.75), later in the linear heart tube and in the looped heart. Furthermore, from E10 onward expression is also detected in the somites. Expression of *ChapB* is downregulated in adult hearts, whereas *ChapA* is expressed adult heart and skeletal muscle (Figure 5)[92].

In cardiomyocytes, CHAP is detected in the Z-disc and co-stains with α-actinin-2, whereas

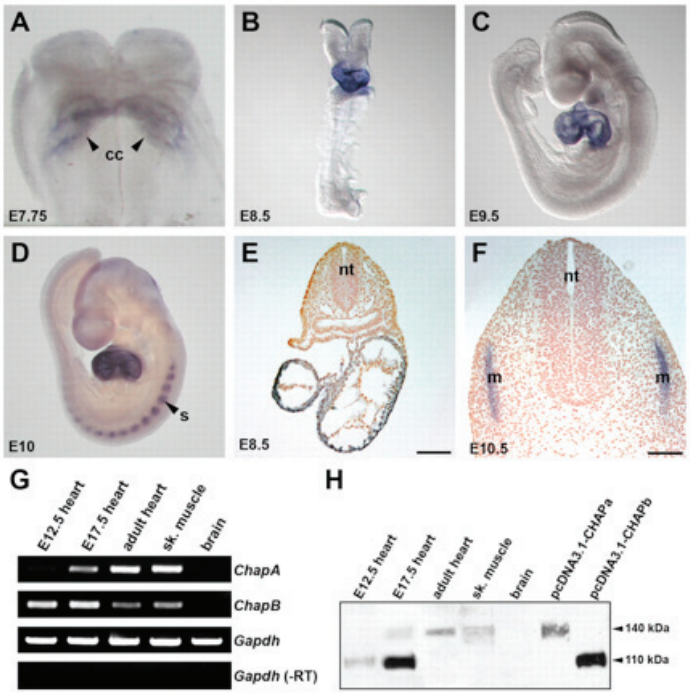


**Figure 5: Whole mount in situ hybridization (A-D) showing expression of *Chap* during mouse development. *Chap* is first expressed in the cardiac crescent (cc) at E7.75 (A). In later stages *Chap* expression is observed throughout the whole heart at E8.5 (B) and E9.5 (C). At E10 (D), besides expression of *Chap* in the heart, *Chap* expression observed in the somites. E: Section of an E8.5 mouse embryo showing *Chap* expression in cardiomyocytes of the heart. F: Section of an E10.5 mouse embryo showing *Chap* is expressed in the myotome part of the somites. G: RT-PCR analysis of showing expression of *ChapA* in adult heart and skeletal muscle, and expression of *ChapB* in the heart during embryonic development. H: western blot analysis of CHAPa and b expression during embryonic development and in adult heart and skeletal muscle. Adapted from[92].**

no co-staining is seen with the M-band marker myomesin. Furthermore, CHAP can interact directly with α-actinin-2. CHAP can also translocate to the nucleus, suggesting a function in transcription as a co-factor.
Morpholino mediated knockdown of *chap* in zebrafish resulted in defects in heart looping, cardiac edema and disturbed skeletal muscle development[92].
These initial data showed an essential function of CHAP in cardiac and skeletal muscle development. Given the homology between CHAP, synaptopodin and myopodin it is likely that CHAP also functions as an actin bundling protein and/or in the calcineurin pathway. Furthermore, the location of CHAP in the Z-disc and the binding to α-actinin-2 suggests a role for CHAP in the development of cardiomyopathy. To elucidate this, we investigated the role of CHAP during development and disease in this thesis.

## Aim and outline

In this thesis the function of CHAP during embryonic development and in adult tissues and disease was analyzed by making use of transgenic mouse models, expression analysis and *in vitro* experiments. We show that *CHAP* expression during development is conserved between species, which implies an important role during cardiac and skeletal muscle development. Furthermore, we show *in vivo* and *in vitro* that CHAPa and CHAPb have distinct functions in muscle development and function.
**Chapter 2** describes the sequence and expression analysis of the chick (Gallus gallus) homolog of human and mouse CHAPa. Furthermore, detailed expression analysis of mouse CHAP in embryonic and adult skeletal and smooth muscle is given. To investigate the function of CHAP during muscle development and disease in more detail, we attempted to generate a CHAP knockout mouse. As a first step, **chapter 3** gives a detailed description of generation of CHAP targeted mouse embryonic stem cells. These cells were used to investigate the consequences of CHAP knockdown on cardiac differentiation *in vitro*. Their use to generate chimeric mice is pending. In addition, we investigated te effect of morpholino mediated knockdown of *CHAP* in chick embyro's. In **chapter 4** we analyzed the role of both CHAP isoforms in the adult heart by generation of CHAPa- and b heart-specific transgenic mice. Whereas, in CHAPa Tg mice no phenotype is observed, CHAPb Tg mice develop cardiomyopathy with diastolic dysfunction. In addition, the CHAPb Tg mice show formation of actin stress fibers and upregulation actin signaling. To study the effect of CHAP overexpression more directly, we generated adenoviruses and in **chapter 5** used these to study the function of CHAP by in vitro overexpression of CHAPa- and b in a model of skeletal muscle development (C2C12 cells) and E17.5 mouse cardiomyocytes. We show that, as in the Tg mice, an actin bundling function *in vitro* for CHAPb and also show a function for CHAPa in the integrity of the Z-disc. However, unlike *in vivo* overexpression of CHAPb, the actin signaling pathway is not affected to the same extent by *in vitro* overexpression. In **chapter 6** a more detailed expression analysis of CHAP is given. In this chapter expression of CHAP in small intestine, kidney and brain is shown. CHAPb expression in these organs is related to the expression of F-actin and show again a function for this protein in actin bundling.
The results of this thesis are summarized and discussed in **chapter 7** and suggestions for future research are given.

# References


(1) Brand T. Heart development: molecular insights into cardiac specification and early morphogenesis. *Dev Biol* 2003 June 1;258(1):1-19.

(2) Gittenberger-de Groot AC, Bartelings MM, Deruiter MC, Poelmann RE. Basics of cardiac development for the understanding of congenital heart malformations. *Pediatr Res* 2005 February;57(2):169-76.

(3) Zaffran S, Frasch M. Early signals in cardiac development. *Circ Res* 2002 September 20;91(6):457-69.

(4) Bruneau BG. The developmental genetics of congenital heart disease. *Nature* 2008 February 21;451(7181):943-8.

(5) Rochais F, Mesbah K, Kelly RG. Signaling pathways controlling second heart field development. *Circ Res* 2009 April 24;104(8):933-42.

(6) Buckingham M, Bajard L, Chang T, Daubas P, Hadchouel J, Meilhac S, Montarras D, Rocancourt D, Relaix F. The formation of skeletal muscle: from somite to limb. *J Anat* 2003 January;202(1):59-68.

(7) Bryson-Richardson RJ, Currie PD. The genetics of vertebrate myogenesis. *Nat Rev Genet* 2008 August;9(8):632-46.

(8) Christ B, Brand-Saberi B. Limb muscle development. *Int J Dev Biol* 2002;46(7):905-14.

(9) Wang DZ, Olson EN. Control of smooth muscle development by the myocardin family of transcriptional coactivators. *Curr Opin Genet Dev* 2004 October;14(5):558-66.

(10) Majesky MW, Dong XR, Regan JN, Hoglund VJ. Vascular smooth muscle progenitor cells: building and repairing blood vessels. *Circ Res* 2011 February 4;108(3):365-77.

(11) Owens GK, Kumar MS, Wamhoff BR. Molecular regulation of vascular smooth muscle cell differentiation in development and disease. *Physiol Rev* 2004 July;84(3):767-801.

(12) Cox L, Umans L, Cornelis F, Huylebroeck D, Zwijsen A. A broken heart: a stretch too far: an overview of mouse models with mutations in stretch-sensor components. *Int J Cardiol* 2008 December 17;131(1):33-44.

(13) Lange S, Ehler E, Gautel M. From A to Z and back? Multicompartment proteins in the sarcomere. *Trends Cell Biol* 2006 January;16(1):11-8.

(14) Kruger M, Linke WA. Titin-based mechanical signalling in normal and failing myocardium. *J Mol Cell Cardiol* 2009 April;46(4):490-8.

(15) Granzier HL, Labeit S. The giant protein titin: a major player in myocardial mechanics, signaling, and disease. *Circ Res* 2004 February 20;94(3):284-95.

(16) Frank D, Kuhn C, Katus HA, Frey N. The sarcomeric Z-disc: a nodal point in signalling and disease. *J Mol Med* 2006 June;84(6):446-68.

(17) Sanoudou D, Vafiadaki E, Arvanitis DA, Kranias E, Kontrogianni-Konstantopoulos A. Array lessons from the heart: focus on the genome and transcriptome of cardiomyopathies. *Physiol Genomics* 2005 April 14;21(2):131-43.

(18) Wang L, Seidman JG, Seidman CE. Narrative review: harnessing molecular genetics for the diagnosis and management of hypertrophic cardiomyopathy. *Ann Intern Med* 2010 April 20;152(8):513-20, W181.

(19) McConnell BK, Fatkin D, Semsarian C, Jones KA, Georgakopoulos D, Maguire CT, Healey MJ, Mudd JO, Moskowitz IP, Conner DA, Giewat M, Wakimoto H, Berul CI, Schoen FJ, Kass DA, Seidman CE, Seidman JG. Comparison of two murine models of familial hypertrophic cardiomyopathy. *Circ Res* 2001 March 2;88(4):383-9.

(20) Geisterfer-Lowrance AA, Christe M, Conner DA, Ingwall JS, Schoen FJ, Seidman CE, Seidman JG. A mouse model of familial hypertrophic cardiomyopathy. *Science* 1996 May 3;272(5262):731-4.

(21) Georgakopoulos D, Christe ME, Giewat M, Seidman CM, Seidman JG, Kass DA. The pathogenesis of familial hypertrophic cardiomyopathy: early and evolving effects from an alpha-cardiac myosin heavy chain missense mutation. *Nat Med* 1999 March;5(3):327-30.

(22) Tardiff JC, Hewett TE, Palmer BM, Olsson C, Factor SM, Moore RL, Robbins J, Leinwand LA. Car diac troponin T mutations result in allele-specific phenotypes in a mouse model for hypertrophic car diomyopathy. *J Clin Invest* 1999 August;104(4):469-81.

(23) Du CK, Morimoto S, Nishii K, Minakami R, Ohta M, Tadano N, Lu QW, Wang YY, Zhan DY, Mochizuki M, Kita S, Miwa Y, Takahashi-Yanaga F, Iwamoto T, Ohtsuki I, Sasaguri T. Knock-in mouse model of dilated cardiomyopathy caused by troponin mutation. *Circ Res* 2007 July 20;101(2):185-94.

(24) Beqqali A, van Eldik W, Mummery C, Passier R. Human stem cells as a model for cardiac differentia-

tion and disease. *Cell Mol Life Sci* 2009 March;66(5):800-13.
(25) Fatkin D, McConnell BK, Mudd JO, Semsarian C, Moskowitz IG, Schoen FJ, Giewat M, Seidman CE, Seidman JG. An abnormal Ca(2+) response in mutant sarcomere protein-mediated familial hypertrophic cardiomyopathy. *J Clin Invest* 2000 December;106(11):1351-9.
(26) Marian AJ, Wu Y, Lim DS, McCluggage M, Youker K, Yu QT, Brugada R, DeMayo F, Quinones M, Roberts R. A transgenic rabbit model for human hypertrophic cardiomyopathy. *J Clin Invest* 1999 December;104(12):1683-92.
(27) McConnell BK, Jones KA, Fatkin D, Arroyo LH, Lee RT, Aristizabal O, Turnbull DH, Georga kopoulos D, Kass D, Bond M, Niimura H, Schoen FJ, Conner D, Fischman DA, Seidman CE, Seidman JG. Dilated cardiomyopathy in homozygous myosin-binding protein-C mutant mice. *J Clin Invest* 1999 November;104(9):1235-44.
(28) Witt CC, Gerull B, Davies MJ, Centner T, Linke WA, Thierfelder L. Hypercontractile properties of cardiac muscle fibers in a knock-in mouse model of cardiac myosin-binding protein-C. *J Biol Chem* 2001 February 16;276(7):5353-9.
(29) Harris SP, Bartley CR, Hacker TA, McDonald KS, Douglas PS, Greaser ML, Powers PA, Moss RL. Hypertrophic cardiomyopathy in cardiac myosin binding protein-C knockout mice. *Circ Res* 2002 March 22;90(5):594-601.
(30) Lutucuta S, Tsybouleva N, Ishiyama M, Defreitas G, Wei L, Carabello B, Marian AJ. Induction and reversal of cardiac phenotype of human hypertrophic cardiomyopathy mutation cardiac troponin T-Q92 in switch on-switch off bigenic mice. *J Am Coll Cardiol* 2004 December 7;44(11):2221-30.
(31) Lombardi R, Bell A, Senthil V, Sidhu J, Noseda M, Roberts R, Marian AJ. Differential interactions of thin filament proteins in two cardiac troponin T mouse models of hypertrophic and dilated cardiomyopathies. *Cardiovasc Res* 2008 July 1;79(1):109-17.
(32) Javadpour MM, Tardiff JC, Pinz I, Ingwall JS. Decreased energetics in murine hearts bearing the R92Q mutation in cardiac troponin T. *J Clin Invest* 2003 September;112(5):768-75.
(33) Maass AH, Ikeda K, Oberdorf-Maass S, Maier SK, Leinwand LA. Hypertrophy, fibrosis, and sudden cardiac death in response to pathological stimuli in mice with mutations in cardiac troponin T. *Circula tion* 2004 October 12;110(15):2102-9.
(34) Du CK, Morimoto S, Nishii K, Minakami R, Ohta M, Tadano N, Lu QW, Wang YY, Zhan DY, Mochizuki M, Kita S, Miwa Y, Takahashi-Yanaga F, Iwamoto T, Ohtsuki I, Sasaguri T. Knock-in mouse model of dilated cardiomyopathy caused by troponin mutation. *Circ Res* 2007 July 20;101(2):185-94.
(35) Juan F, Wei D, Xiongzhi Q, Ran D, Chunmei M, Lan H, Chuan Q, Lianfeng Z. The changes of the cardiac structure and function in cTnTR141W transgenic mice. *Int J Cardiol* 2008 August 1;128(1):83-90.
(36) Knoll R, Hoshijima M, Hoffman HM, Person V, Lorenzen-Schmidt I, Bang ML, Hayashi T, Shiga N, Yasukawa H, Schaper W, McKenna W, Yokoyama M, Schork NJ, Omens JH, McCulloch AD, Kimura A, Gregorio CC, Poller W, Schaper J, Schultheiss HP, Chien KR. The cardiac mechanical stretch sensor machinery involves a Z disc complex that is defective in a subset of human dilated cardiomyopathy. *Cell* 2002 December 27;111(7):943-55.
(37) Wilkins BJ, Molkentin JD. Calcium-calcineurin signaling in the regulation of cardiac hypertrophy. *Biochem Biophys Res Commun* 2004 October 1;322(4):1178-91.
(38) Molkentin JD, Lu JR, Antos CL, Markham B, Richardson J, Robbins J, Grant SR, Olson EN. A calcineurin-dependent transcriptional pathway for cardiac hypertrophy. *Cell* 1998 April 17;93(2):215-28.
(39) Bourajjaj M, Armand AS, da Costa Martins PA, Weijts B, van der NR, Heeneman S, Wehrens XH, De Windt LJ. NFATc2 is a necessary mediator of calcineurin-dependent cardiac hypertrophy and heart failure. *J Biol Chem* 2008 August 8;283(32):22295-303.
(40) Wilkins BJ, De Windt LJ, Bueno OF, Braz JC, Glascock BJ, Kimball TF, Molkentin JD. Targeted disruption of NFATc3, but not NFATc4, reveals an intrinsic defect in calcineurin-mediated cardiac hypertrophic growth. *Mol Cell Biol* 2002 November;22(21):7603-13.
(41) Frey N, Richardson JA, Olson EN. Calsarcins, a novel family of sarcomeric calcineurin-binding pro teins. *Proc Natl Acad Sci U S A* 2000 December 19;97(26):14632-7.
(42) Frank D, Kuhn C, van EM, Gehring D, Hanselmann C, Lippl S, Will R, Katus HA, Frey N. Calsar cin-1 protects against angiotensin-II induced cardiac hypertrophy. *Circulation* 2007 Novem ber 27;116(22):2587-96.

(43) Frey N, Barrientos T, Shelton JM, Frank D, Rutten H, Gehring D, Kuhn C, Lutz M, Rothermel B, Bassel-Duby R, Richardson JA, Katus HA, Hill JA, Olson EN. Mice lacking calsarcin-1 are sensitized to calcineurin signaling and show accelerated cardiomyopathy in response to pathological biomechanical stress. *Nat Med* 2004 December;10(12):1336-43.

(44) Zhou Q, Ruiz-Lozano P, Martone ME, Chen J. Cypher, a striated muscle-restricted PDZ and LIM domain-containing protein, binds to alpha-actinin-2 and protein kinase C. *J Biol Chem* 1999 July 9;274(28):19807-13.

(45) Passier R, Richardson JA, Olson EN. Oracle, a novel PDZ-LIM domain protein expressed in heart and skeletal muscle. *Mech Dev* 2000 April;92(2):277-84.

(46) van der Meer DL, Marques IJ, Leito JT, Besser J, Bakkers J, Schoonheere E, Bagowski CP. Zebrafish cypher is important for somite formation and heart development. *Dev Biol* 2006 November 15;299(2):356-72.

(47) Zheng M, Cheng H, Li X, Zhang J, Cui L, Ouyang K, Han L, Zhao T, Gu Y, Dalton ND, Bang ML, Peterson KL, Chen J. Cardiac-specific ablation of Cypher leads to a severe form of dilated cardiomyopathy with premature death. *Hum Mol Genet* 2009 February 15;18(4):701-13.

(48) Zhou Q, Chu PH, Huang C, Cheng CF, Martone ME, Knoll G, Shelton GD, Evans S, Chen J. Ablation of Cypher, a PDZ-LIM domain Z-line protein, causes a severe form of congenital myopathy. *J Cell Biol* 2001 November 12;155(4):605-12.

(49) Cheng H, Zheng M, Peter AK, Kimura K, Li X, Ouyang K, Shen T, Cui L, Frank D, Dalton ND, Gu Y, Frey N, Peterson KL, Evans SM, Knowlton KU, Sheikh F, Chen J. Selective deletion of long but not short Cypher isoforms leads to late-onset dilated cardiomyopathy. *Hum Mol Genet* 2011 May 1;20(9):1751-62.

(50) Vatta M, Mohapatra B, Jimenez S, Sanchez X, Faulkner G, Perles Z, Sinagra G, Lin JH, Vu TM, Zhou Q, Bowles KR, Di LA, Schimmenti L, Fox M, Chrisco MA, Murphy RT, McKenna W, Elliott P, Bowles NE, Chen J, Valle G, Towbin JA. Mutations in Cypher/ZASP in patients with dilated cardiomyopathy and left ventricular non-compaction. *J Am Coll Cardiol* 2003 December 3;42(11):2014-27.

(51) Nakagawa N, Hoshijima M, Oyasu M, Saito N, Tanizawa K, Kuroda S. ENH, containing PDZ and LIM domains, heart/skeletal muscle-specific protein, associates with cytoskeletal proteins through the PDZ domain. *Biochem Biophys Res Commun* 2000 June 7;272(2):505-12.

(52) Cheng H, Kimura K, Peter AK, Cui L, Ouyang K, Shen T, Liu Y, Gu Y, Dalton ND, Evans SM, Knowlton KU, Peterson KL, Chen J. Loss of enigma homolog protein results in dilated cardiomyopathy. *Circ Res* 2010 August 6;107(3):348-56.

(53) Olson EN, Nordheim A. Linking actin dynamics and gene transcription to drive cellular motile functions. *Nat Rev Mol Cell Biol* 2010 May;11(5):353-65.

(54) Maekawa M, Ishizaki T, Boku S, Watanabe N, Fujita A, Iwamatsu A, Obinata T, Ohashi K, Mizuno K, Narumiya S. Signaling from Rho to the actin cytoskeleton through protein kinases ROCK and LIM-kinase. *Science* 1999 August 6;285(5429):895-8.

(55) Zeidan A, Javadov S, Karmazyn M. Essential role of Rho/ROCK-dependent processes and actin dynamics in mediating leptin-induced hypertrophy in rat neonatal ventricular myocytes. *Cardiovasc Res* 2006 October 1;72(1):101-11.

(56) Brown JH, Del Re DP, Sussman MA. The Rac and Rho hall of fame: a decade of hypertrophic signal ing hits. *Circ Res* 2006 March 31;98(6):730-42.

(57) Lee JH, Katakai T, Hara T, Gonda H, Sugai M, Shimizu A. Roles of p-ERM and Rho-ROCK signal ing in lymphocyte polarity and uropod formation. *J Cell Biol* 2004 October 25;167(2):327-37.

(58) Ahuja P, Perriard E, Pedrazzini T, Satoh S, Perriard JC, Ehler E. Re-expression of proteins involved in cytokinesis during cardiac hypertrophy. *Exp Cell Res* 2007 April 1;313(6):1270-83.

(59) Sah VP, Minamisawa S, Tam SP, Wu TH, Dorn GW, Ross J, Jr., Chien KR, Brown JH. Cardiac-specific overexpression of RhoA results in sinus and atrioventricular nodal dysfunction and contractile failure. *J Clin Invest* 1999 June;103(12):1627-34.

(60) Phrommintikul A, Tran L, Kompa A, Wang B, Adrahtas A, Cantwell D, Kelly DJ, Krum H. Effects of a Rho kinase inhibitor on pressure overload induced cardiac hypertrophy and associated diastolic dysfunction. *Am J Physiol Heart Circ Physiol* 2008 April;294(4):H1804-H1814.

(61) Parmacek MS. Myocardin-related transcription factors: critical coactivators regulating cardiovascular development and adaptation. *Circ Res* 2007 March 16;100(5):633-44.

(62) Balza RO, Jr., Misra RP. Role of the serum response factor in regulating contractile apparatus gene expression and sarcomeric integrity in cardiomyocytes. *J Biol Chem* 2006 March 10;281(10):6498-510.

(63) Miano JM, Ramanan N, Georger MA, de Mesy Bentley KL, Emerson RL, Balza RO, Jr., Xiao Q, Weiler H, Ginty DD, Misra RP. Restricted inactivation of serum response factor to the cardiovascular system. *Proc Natl Acad Sci U S A* 2004 December 7;101(49):17132-7.

(64) Niu Z, Yu W, Zhang SX, Barron M, Belaguli NS, Schneider MD, Parmacek M, Nordheim A, Schwartz RJ. Conditional mutagenesis of the murine serum response factor gene blocks cardiogenesis and the transcription of downstream gene targets. *J Biol Chem* 2005 September 16;280(37):32531-8.

(65) Parlakian A, Charvet C, Escoubet B, Mericskay M, Molkentin JD, Gary-Bobo G, De Windt LJ, Ludosky MA, Paulin D, Daegelen D, Tuil D, Li Z. Temporally controlled onset of dilated cardiomyopathy through disruption of the SRF gene in adult heart. *Circulation* 2005 November 8;112(19):2930-9.

(66) Zhang X, Chai J, Azhar G, Sheridan P, Borras AM, Furr MC, Khrapko K, Lawitts J, Misra RP, Wei JY. Early postnatal cardiac changes and premature death in transgenic mice overexpressing a mutant form of serum response factor. *J Biol Chem* 2001 October 26;276(43):40033-40.

(67) Wang Z, Wang DZ, Pipes GC, Olson EN. Myocardin is a master regulator of smooth muscle gene expression. *Proc Natl Acad Sci U S A* 2003 June 10;100(12):7129-34.

(68) Long X, Creemers EE, Wang DZ, Olson EN, Miano JM. Myocardin is a bifunctional switch for smooth versus skeletal muscle differentiation. *Proc Natl Acad Sci U S A* 2007 October 16;104(42):16570-5.

(69) Li S, Wang DZ, Wang Z, Richardson JA, Olson EN. The serum response factor coactivator myocardin is required for vascular smooth muscle development. *Proc Natl Acad Sci U S A* 2003 August 5;100(16):9366-70.

(70) Huang J, Cheng L, Li J, Chen M, Zhou D, Lu MM, Proweller A, Epstein JA, Parmacek MS. Myocardin regulates expression of contractile genes in smooth muscle cells and is required for closure of the ductus arteriosus in mice. *J Clin Invest* 2008 February;118(2):515-25.

(71) Huang J, Min LM, Cheng L, Yuan LJ, Zhu X, Stout AL, Chen M, Li J, Parmacek MS. Myocardin is required for cardiomyocyte survival and maintenance of heart function. *Proc Natl Acad Sci U S A* 2009 November 3;106(44):18734-9.

(72) Xing W, Zhang TC, Cao D, Wang Z, Antos CL, Li S, Wang Y, Olson EN, Wang DZ. Myocardin induces cardiomyocyte hypertrophy. *Circ Res* 2006 April 28;98(8):1089-97.

(73) Li S, Chang S, Qi X, Richardson JA, Olson EN. Requirement of a myocardin-related transcription factor for development of mammary myoepithelial cells. *Mol Cell Biol* 2006 August;26(15):5797-808.

(74) Small EM, Thatcher JE, Sutherland LB, Kinoshita H, Gerard RD, Richardson JA, Dimaio JM, Sadek H, Kuwahara K, Olson EN. Myocardin-related transcription factor-a controls myofibroblast activation and fibrosis in response to myocardial infarction. *Circ Res* 2010 July 23;107(2):294-304.

(75) Oh J, Richardson JA, Olson EN. Requirement of myocardin-related transcription factor-B for remodeling of branchial arch arteries and smooth muscle differentiation. *Proc Natl Acad Sci U S A* 2005 October 18;102(42):15122-7.

(76) Li J, Zhu X, Chen M, Cheng L, Zhou D, Lu MM, Du K, Epstein JA, Parmacek MS. Myocardin-related transcription factor B is required in cardiac neural crest for smooth muscle differentia tion and cardiovascular development. *Proc Natl Acad Sci U S A* 2005 June 21;102(25):8916-21.

(77) Naya FJ, Black BL, Wu H, Bassel-Duby R, Richardson JA, Hill JA, Olson EN. Mitochondrial deficiency and cardiac sudden death in mice lacking the MEF2A transcription factor. *Nat Med* 2002 November;8(11):1303-9.

(78) Lin Q, Schwarz J, Bucana C, Olson EN. Control of mouse cardiac morphogenesis and myogenesis by transcription factor MEF2C. *Science* 1997 May 30;276(5317):1404-7.

(79) Kim Y, Phan D, van RE, Wang DZ, McAnally J, Qi X, Richardson JA, Hill JA, Bassel-Duby R, Olson EN. The MEF2D transcription factor mediates stress-dependent cardiac remodeling in mice. *J Clin Invest* 2008 January;118(1):124-32.

(80) Kim Y, Phan D, van RE, Wang DZ, McAnally J, Qi X, Richardson JA, Hill JA, Bassel-Duby R, Olson EN. The MEF2D transcription factor mediates stress-dependent cardiac remodeling in mice. *J Clin Invest* 2008 January;118(1):124-32.

(81) Xu J, Gong NL, Bodi I, Aronow BJ, Backx PH, Molkentin JD. Myocyte enhancer factors 2A and 2C induce dilated cardiomyopathy in transgenic mice. *J Biol Chem* 2006 April 7;281(14):9152-62.

(82) Arai A, Spencer JA, Olson EN. STARS, a striated muscle activator of Rho signaling and serum response factor-dependent transcription. *J Biol Chem* 2002 July 5;277(27):24453-9.

(83) Kuwahara K, Barrientos T, Pipes GC, Li S, Olson EN. Muscle-specific signaling mechanism that links

actin dynamics to serum response factor. *Mol Cell Biol* 2005 April;25(8):3173-81.

(84) Kuwahara K, Teg Pipes GC, McAnally J, Richardson JA, Hill JA, Bassel-Duby R, Olson EN. Modula tion of adverse cardiac remodeling by STARS, a mediator of MEF2 signaling and SRF activity. *J Clin Invest* 2007 May;117(5):1324-34.

(85) Asanuma K, Kim K, Oh J, Giardino L, Chabanis S, Faul C, Reiser J, Mundel P. Synaptopodin regulates the actin-bundling activity of alpha-actinin in an isoform-specific manner. *J Clin Invest* 2005 May;115(5):1188-98.

(86) Asanuma K, Yanagida-Asanuma E, Faul C, Tomino Y, Kim K, Mundel P. Synaptopodin orchestrates actin organization and cell motility via regulation of RhoA signalling. *Nat Cell Biol* 2006 May;8(5):485-91.

(87) Deller T, Korte M, Chabanis S, Drakew A, Schwegler H, Stefani GG, Zuniga A, Schwarz K, Bonhoeffer T, Zeller R, Frotscher M, Mundel P. Synaptopodin-deficient mice lack a spine apparatus and show deficits in synaptic plasticity. *Proc Natl Acad Sci U S A* 2003 September 2;100(18):10494-9.

(88) Weins A, Schwarz K, Faul C, Barisoni L, Linke WA, Mundel P. Differentiation- and stress-depend ent nuclear cytoplasmic redistribution of myopodin, a novel actin-bundling protein. *J Cell Biol* 2001 October 29;155(3):393-404.

(89) Faul C, Huttelmaier S, Oh J, Hachet V, Singer RH, Mundel P. Promotion of importin alpha-mediated nuclear import by the phosphorylation-dependent binding of cargo protein to 14-3-3. *J Cell Biol* 2005 May 9;169(3):415-24.

(90) Faul C, Dhume A, Schecter AD, Mundel P. Protein kinase A, Ca2+/calmodulin-dependent kinase II, and calcineurin regulate the intracellular trafficking of myopodin between the Z-disc and the nucleus of cardiac myocytes. *Mol Cell Biol* 2007 December;27(23):8215-27.

(91) Beqqali A, Kloots J, Ward-van OD, Mummery C, Passier R. Genome-wide transcriptional profiling of human embryonic stem cells differentiating to cardiomyocytes. *Stem Cells* 2006 August;24(8):1956-67.

(92) Beqqali A, Monshouwer-Kloots J, Monteiro R, Welling M, Bakkers J, Ehler E, Verkleij A, Mummery C, Passier R. CHAP is a newly identified Z-disc protein essential for heart and skeletal muscle function. *J Cell Sci* 2010 April 1;123(Pt 7):1141-50.

# Chapter 2

## CHAP is expressed in striated and smooth muscle cells in chick and mouse during embryonic and adult stages

Willemijn van Eldik, Abdelaziz Beqqali, Jantine Monshouwer-Kloots,
Christine Mummery, Robert Passier
International Journal of Developmental Biology 2011: 55(6) 649-655

# Abstract

We recently identified a new Z-disc protein, CHAP (Cytoskeletal Heart-enriched Actin-associated Protein), which is expressed in striated muscle and plays an important role during embryonic muscle development in mouse and zebrafish. Here, we confirm and further extend these findings by (i) the identification and characterization of the CHAP orthologue in chick and (ii) providing a detailed analysis of CHAP expression in mouse during embryonic and adult stages. Chick CHAP contains a PDZ domain and a nuclear localization signal, resembling the human and mouse CHAPa. *CHAP* is expressed in the developing heart and somites, as well as muscle precursors of the limb buds in mouse and chick embryos. CHAP expression in heart and skeletal muscle is maintained in adult mice, both in slow and fast muscle fibers. Moreover, besides expression in striated muscle, we demonstrate that CHAP is expressed in smooth muscle cells of aorta, carotid and coronary arteries in adult mice, but not during embryonic development.

# Introduction

The Z-disc delineates the borders of the sarcomere, the contractile unit of striated muscle and represents an anchoring plane for various proteins. In addition to their role in force transmission, Z-disc proteins may also be involved in signal transduction[1]. Recently, we indentified a novel Z-disc protein, which we named CHAP (Cytoskeletal Heart-enriched Actin-associated Protein) [2, 3]. We have shown that CHAP has two isoforms, CHAPa and CHAPb, in both humans and mice. CHAPa, the longest isoform (978 amino acids (aa)) contains an N-terminal PDZ domain, as well as a nuclear localization signal (NLS). The shorter CHAPb isoform (749 aa) lacks the PDZ domain, but still contains the NLS. CHAP interacts with α-actinin-2, another Z-disc protein, and is able to translocate to the nucleus [3]. Previously, we have shown that *ChapA* is predominantly expressed in adult heart and muscle tissues, whereas *ChapB* is expressed at higher levels in striated muscles during embryonic development. *ChapB* expression in mouse is evident from the cardiac crescent stage (E7.5) onwards. During later embryonic stages *ChapB* expression is maintained in the developing heart, but is also expressed in the somites (giving rise to skeletal muscle). In addition, we have identified the zebrafish *chap* orthologue and demonstrated by morpholino antisense oligonucleotide-mediated knockdown that *chap* is essential for zebrafish heart and muscle development. Knockdown of *chap* in the zebrafish resulted in aberrant muscle development, indicated by defects in cardiac looping, formation of pericardial oedema and disorganized sarcomeres [3].

Here, we identified the chick (Gallus gallus) orthologue of CHAP. We show that CHAP gene and protein resembles the human and mouse CHAPa isoform, with the predicted PDZ and NLS domains. A detailed analysis of *CHAP* mRNA and protein expression during development in chick and mouse embryos and in adult tissues is shown. Furthermore, we demonstrate that CHAP is not only expressed in cardiomyocytes, and slow and fast skeletal muscle, but interestingly also in smooth muscle cells of the cardiovascular lineage.

# Materials and methods

*Animals*

Swiss mice were intercrossed and females were sacrificed for collection of embryos at different time points (E12.5, 13.5 and 17.5). Fertilized eggs of White Leghorn chicken were incubated at 37 °C and 80% humidity. Chick embryos were staged according to the criteria of Hamburger and Hamilton (HH)[4]. Mouse (E12.5 and E13.5) and chick embryos (HH8-HH30) were collected and fixed in 4% paraformaldehyde (PFA; w/v) in phosphate buffered saline (PBS) overnight at 4 °C. Embryos were further processed for whole-mount or section *in situ* hybridization, or immunohistochemistry. Processing of mouse embryos for cryosections was adapted from [5]. In brief, E17.5 embryos were fixed in 0.2% PFA solution containing 4% sucrose, 0.12mM $CaCl_2.2H_2O$, 0.2M $Na_2HPO_4.2H_2O$, 0.2M $NaH_2PO_4.H_2O$ over night at 4 °C. Next, embryos were washed in the same solution without PFA during the day at 4 °C, followed by 0.24M phosphate buffer and 30% sucrose over night at 4 °C. The next day embryos were embedded in Tissue-Tek (Sakura Finetek) on dry ice and stored at -20 °C until sectioning. Organs of adult Swiss mice were isolated, rinsed in PBS and processed for RNA isolation and cryosectioning.

*RNA isolation and cDNA synthesis*

Total RNA from chick hearts of stage 19, 21 and 27 was isolated using Trizol reagent (Invitrogen), followed by chloroform extraction and ethanol precipitation. Subsequently mRNA was reverse transcribed into cDNA using Superscript II (Invitrogen) and random primers according to the suppliers' protocol.

For qPCR analysis, total RNA was isolated from gastrocnemius and soleus muscles of adult Swiss mice using Trizol reagent as describe above, followed by DNase-treatment (DNA-free, Ambion) and conversion to cDNA using iScript cDNA synthesis kit according to the suppliers' protocol (Bio-Rad). qPCR was performed using the CFX96 Real-Time PCR detection system (Bio-Rad). The following primers were used: C*hapA* (sense: 5'-GAGGAGGTGCAGGTCACATT-3'; antisense: 5'-CTGAAGAGCCTGGGAAACAG-3'), *ChapB* (sense: 5'-CCGCCGCTTCTTAAACATAA-3 antisense: 5'-GGCTTTAAAGGGCCTTGG-3') and as reference gene *Gapdh* (sense: 5'-GTTTGTGATGGGTGTGAACCAC-3', antisense: 5'-CTGGTCCTCAGTGTAGCCCAA-3'). Data were analyzed with Bio-Rad CFX Manager.

*Cloning of full-length chick CHAP*

Using the mouse and human CHAP coding sequences, a chick *CHAP* orthologue (XM_421618) was identified after BLAST search. Full-length cDNA of chick *CHAP* was amplified by PCR (multiple clones) from chicken HH19-27 hearts and subsequently cloned into the pCRII-TOPO vector (Invitrogen). The full-length coding sequence of chick *CHAP* was confirmed by sequencing.

*Whole- mount and section in situ hybridization*

RNA probes were generated from PCR products cloned into pCRII-TOPO using T7 or SP6 primers. For generation of a chick *CHAP* probe template, the following primers were used: sense 5'- GGTCTCCCCTTTCTCACCTC-3' and antisense 5'-CACCACAAACTTGTCCATGC-3' (PCR product: 810 bp). Probes for detection of mouse *Chap* were generated as described previously [3]. Probes were digoxigenin-labeled according to the suppliers' protocol (Roche

Applied Science). For *in situ* hybridization 10 μm sections of chick or mouse embryos were mounted on superfrost slides (Menzel). *In situ* hybridization was performed as previously described [6]. Whole-mount *in situ* hybridization was performed as previously described [7].

*Immunofluorescence*
Mouse embryos and adult tissues were sectioned (5 μM) and mounted on starfrost slides (Knittel). Antibody staining on cryo-sections was performed as previously described [8]. Primary antibodies were as follows: anti-CHAP (rabbit, 1:50, custom made by Eurogentec), anti-myosin (mouse, 1:1000, NOQ7.5.4D, Sigma-Aldrich Chemie) and anti-α-smooth muscle actin (mouse, 1:500, 1A4, Sigma-Aldrich Chemie). Secondary antibodies were as follows: Cy-3 conjugated anti-mouse (1:250, Jackson Immunoresearch Laboratories) and Alexa488 conjugated anti-rabbit (1:200, Invitrogen). Cell nuclei were stained with DAPI (Molecular Probes)

*Immunohistochemistry*
Mouse embryos (E12.5) were sectioned (5 μM) and mounted on starfrost slides (Knittel). Antigen retrieval was performed by microwave heating of tissue sections in citrate buffer (pH 6). Endogenous peroxidase was blocked by incubating the slides in 0.3% $H_2O_2$ in PBS. Sections were incubated overnight with CHAP antibody (1:2000) at room temperature. Biotin-conjugated goat anti-rabbit (BA-1000, Vector Labs) was used as secondary antibody. Subsequently, the sections were incubated with Vectastain ABC staining kit (PK-6100, Vector Labs) for 45 min. Slides were rinsed in PBS and Tris/Maleate (pH 7.6). 3-3′diaminobenzidine tetrahydrochloride (D5637, Sigma-Aldrich) was used as chromogen and Mayer's hematoxylin as counterstaining. Finally, all slides were dehydrated and mounted with Entellan (Merck).

# Results and discussion

After BLAST search using full-length sequences of the previously identified *CHAP* orthologues (zebrafish, mouse, and human) [3], we identified the chick (Gallus gallus, Gg) orthologue of *CHAP* (GenBank accession no. XM_421618). For amplification, cloning and sequencing of chick *CHAP* we amplified the predicted full-length open reading frame (ORF) from hearts of chick embryos (HH19, 23 and 27), which resulted in a 3243 bp PCR product. After sequencing we found that the 1081 aa predicted chick CHAP protein (Fig. 1C) had a 48% and 47% homology with human (Hs) and mouse (Mm) CHAPa, respectively (Fig. 1A). Furthermore, there was a 43% and 40% homology with zebrafish Chap-1 (DrChap-1) and Chap-2 (DrChap-2), respectively (Fig. 1A). The NLS and PDZ domain are conserved between the different species. The chick PDZ domain of CHAP showed 63% and 61% homology with the PDZ domains of human and mouse, respectively. The *CHAP* gene is mapped on chromosome 6 and consists of four exons (Fig. 1B). Similar to zebrafish *chap*, no chick CHAPb (lacking the PDZ-domain) was identified. In addition to homology of sequence between different species, we also observed conserved syntenic organization. For instance, *myozenin-1*, another z-disc protein, is located immediately downstream of the mouse *Chap* gene [3]. A similar genomic organization was found in the chick genome.

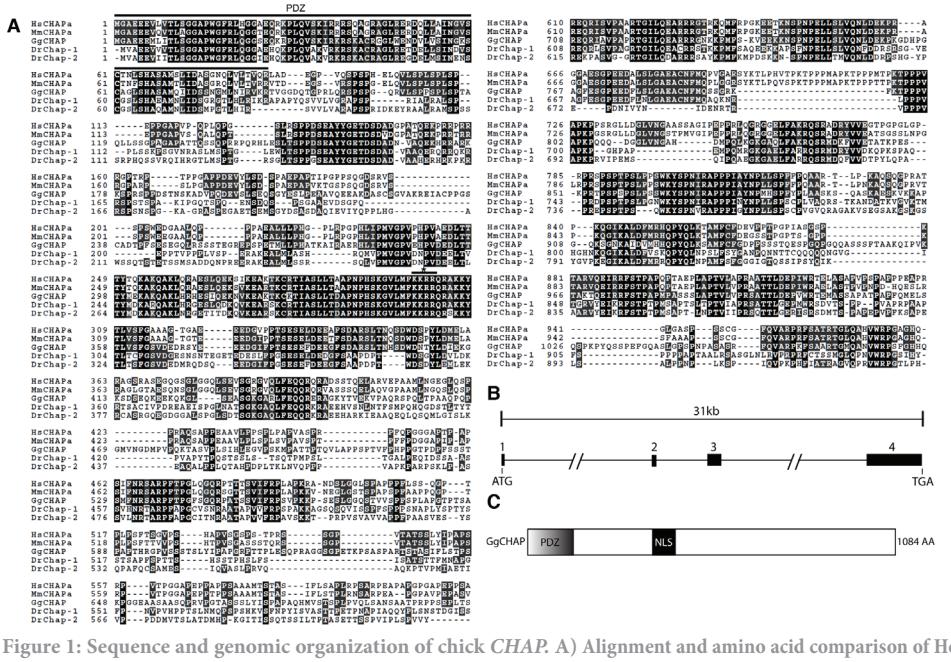


**Figure 1: Sequence and genomic organization of chick *CHAP*. A) Alignment and amino acid comparison of Homo sapiens (Hs), Mus musculus (Mm) CHAPa, Gallus gallus (Gg) and Danio rerio (Dr) CHAP. Identical amino acids are shown in black, similar amino acids are gray and gaps are represented by a dash. PDZ and NLS (*) domains are indicated. B) Genomic organization of chick CHAP gene. ATG represents start codon, TGA represents stop codon and exons (black boxes) are numbered. C) Schematic representation of chick (Gg) CHAP protein showing the location of the PDZ and NLS domains.**

*Expression of CHAP during development in chick and mouse embryos*

To investigate the expression pattern of chick *CHAP* during development we performed whole-mount *in situ* hybridization. Expression of *CHAP* could first be detected at stage HH8 in the cardiac crescent (Fig. 2A). At HH10 and HH11 *CHAP* was expressed in the linear and looping heart tube (Fig. 2B and C). *CHAP* could be detected in the ventricle and outflow tract (OFT), but not in the sinus venosus. At stage HH13, *CHAP* was strongly expressed in the looping heart (Fig. 2D). From HH15 onward *CHAP* was expressed in the heart and somites (Fig. 2E), with higher expression in the anterior somites, which are more mature than the posterior somites. At HH17 (Fig. 2F) *CHAP* was also expressed in the more posterior somites, suggesting that the expression increases as the somites mature. At stage HH17 (Fig. 2F) and stage HH21 (Fig. 2G and H) *CHAP* expression was maintained in the heart and somites. At stage HH25 *CHAP* was expressed in the muscle precursors of the limb buds, heart and somites (Fig. 2I and J). The expression of *CHAP* in muscle precursors of the limb buds of the developing legs and wings was more pronounced in embryos in stages HH28-30 (Fig. 2K, N and O). Hearts of HH30 showed a high expression of *CHAP* in both atria and ventricles, but not in the OFT (Fig. 2L and M). Comparison of expression pattern of *CHAP* during early embryonic development with that of mouse and zebrafish, demonstrate that the *CHAP* expression pattern is conserved between these species [3].

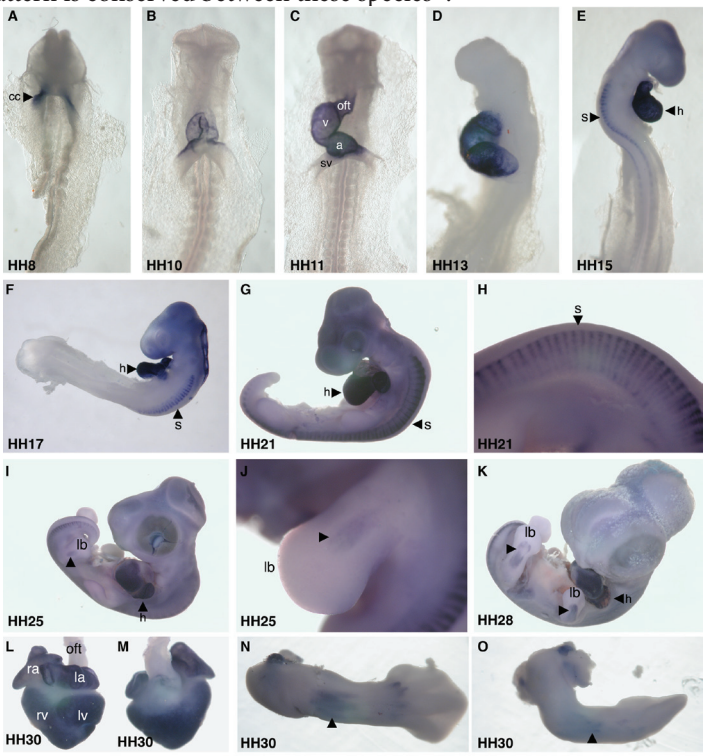


**Figure 2: Whole mount in situ hybridization of chick *CHAP* during development. A-O) Whole mount in situ hybridization with digoxigenin-UTP labeled chick *CHAP* riboprobe on different developmental stages of chick embryos: HH8 (A), HH10 (B), HH11 (C), HH13 (D), HH15 (E), HH17 (F), HH21 (G-H), HH25 (I-J), HH28 (K), HH30 heart (L-M), HH30 leg (N) and HH30 wing (O). Cardiac crescent (cc), ventricle (v), atrium (a) and outflow tract (oft), sinus venosus (sv), heart (h), somites (s), muscle precursors (arrow head) of the limb buds (lb) , left ventricle (lv), right ventricle (rv), left atrium (la), right atrium (ra).**

To study *CHAP* expression during chick development in more detail, we performed section *in situ* hybridization at different stages. At stage HH18 and HH26 *CHAP* was expressed in heart muscle cells and the myotome part of the somites (Fig. 3A-C), confirming the results of whole-mount *in situ* hybridization. Occasionally, higher levels of *CHAP* could be identified at the border with the dermatome, suggesting that *CHAP* is expressed in more mature cells of the somites, which is also in agreement with the higher expression of *CHAP* in more anterior somites. At stage HH30 expression of *CHAP* was localized in ventricles and atria, whereas endocardial cushions are negative for *CHAP* (Fig. 3D and G). Furthermore, trunk muscle masses (Fig. 3E and H), muscle groups from the limb buds of the developing wings (Fig. 3F), tongue, eyes and jaws show *CHAP* expression (Fig. 3I).

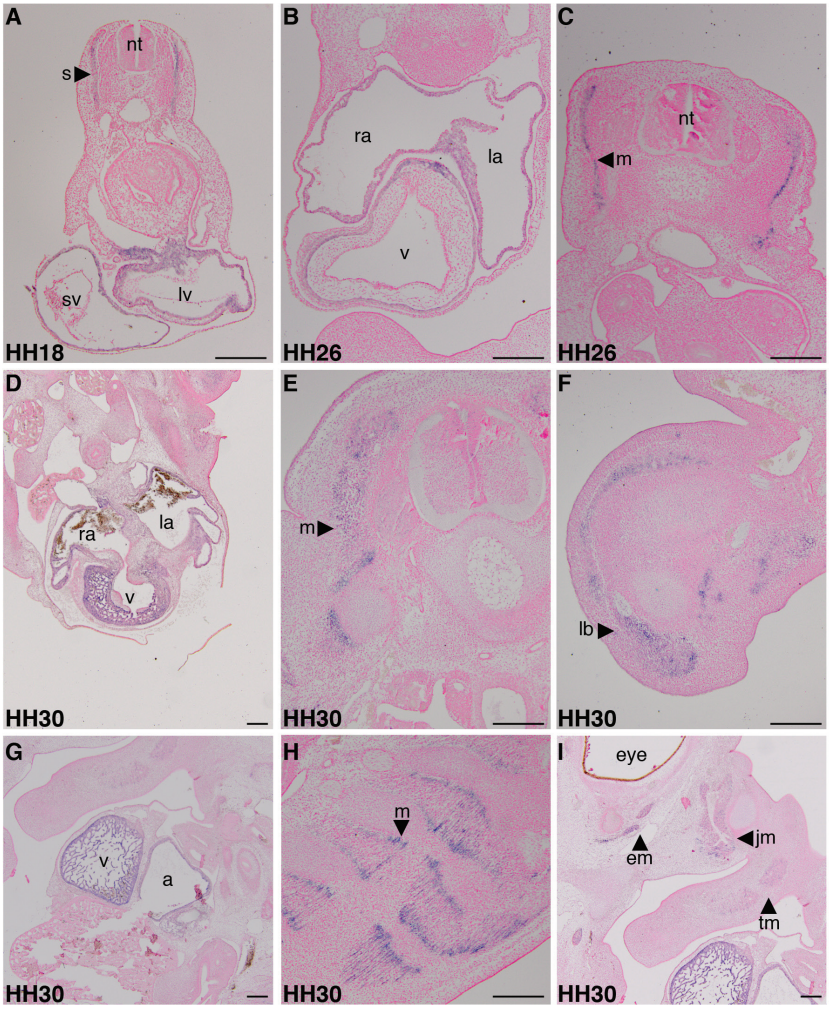


**Figure 3: In situ hybridization of *CHAP* chick on sections. A-I: In situ hybridization with digoxigenin-UTP labeled *CHAP* riboprobe was performed on sections of chick embryos on stages HH18 (A), HH26 (B-C) and HH30 (D-I). Somites (s), myotome (m), limb buds (lb), eye muscles (em), jaw muscles (jm) and tongue muscles (tm), sinus venosus (sv), left ventricle (lv), ventricle (v), left atrium (la), right atrium (ra), atrium (a), neural tube (nt). Scale bars: 250 µm.**

To compare CHAP expression in chick and mouse embryos, we performed *in situ* hybridization on sagittal sections of E13.5 mouse embryos, using a probe that recognizes both *ChapA* and *ChapB* isoforms. As expected, expression of *Chap* was pronounced in the ventricles and atria of the heart (Fig. 4A and B). Furthermore *Chap* was also expressed in the developing muscles of the tongue, jaw, limb buds and tail (Fig. 4A). Detection of *Chap* was considered to be expression of *ChapB*, since we have previously demonstrated that *ChapB* is the predominant isoform in embryonic and fetal stages [3]. In order to determine whether *Chap* mRNA expression was comparable with protein expression, we performed immunohistochemistry with an antibody that specifically recognizes CHAP (both a and b isoforms). In E12.5 embryos, CHAP protein was detected in heart, trunk muscle masses and muscles of the tongue, eyes and jaws, which was comparable to *Chap* mRNA expression (Fig. 4C and D). Furthermore, a striated expression pattern for CHAP, as expected for Z-disc proteins, was observed in muscle cells (Fig. 4E), confirming the specificity of the antibody staining.

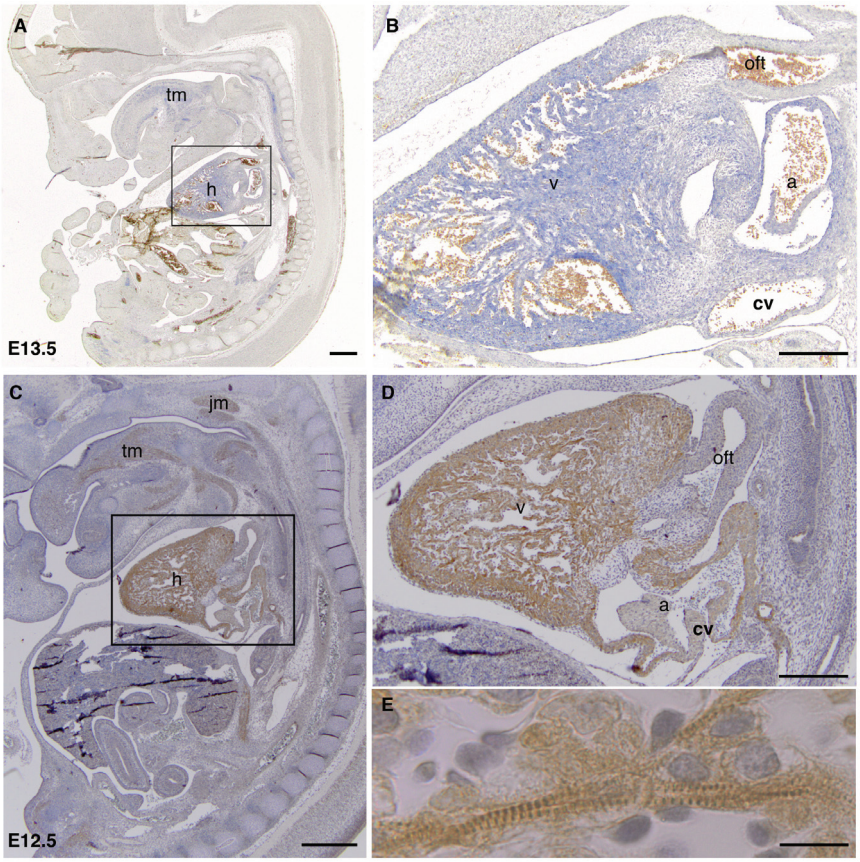


**Figure 4: Expression and localization of CHAP in mouse embryos. A-B) Section in situ hybridization with digoxigenin-UTP labeled mouse *Chap* riboprobe was performed on sagittal sections of E13.5 mouse embryos. A higher magnification of *Chap* expression in the heart (box in A) is shown in (B). C-E: Immunostaining for CHAP on sagittal sections of E12.5 mouse embryos (C). Magnification of C (box) is shown in (D). A higher magnification (E) of heart shown in (D) displays a sarcomeric pattern for CHAP. Heart (h), jaw muscle (jm), tongue muscle (tm), ventricle (v), atrium (a), cardinal vein (cv), and outflow tract (oft). Scale bars in A/C 500 µm, in B/D 250 µm and in E 10 µm.**

*Expression of CHAP in adult skeletal muscle*

We have previously shown that both CHAPa and CHAPb are expressed in adult mouse heart and skeletal muscle [3]. Here, we investigated the expression of CHAP in adult skeletal muscles in more detail. Skeletal muscle can be divided into slow (type I) and fast (type II) twitch fibers. To determine the expression levels of both *Chap* isoforms, we isolated slow (soleus) and fast (gastrocnemius) muscles of adult mice. qPCR analysis of these tissues showed that both *ChapA* (Fig. 5, black bars) and *ChapB* (Fig. 5, white bars) were expressed higher in soleus than in gastrocnemius. Expression of *ChapA* was approximately 10-fold higher than

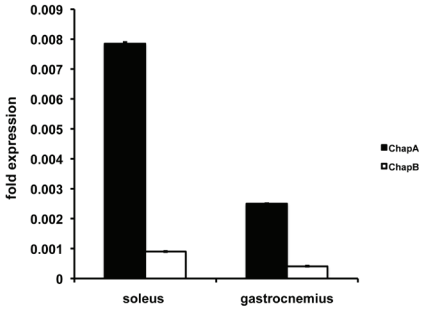


**Figure 5: ChapA and ChapB expression in adult skeletal muscle. Quantitative real-time PCR expression of *ChapA* and *ChapB* mRNA in soleus (slow) and gastrocnemius (fast) muscles. *Gapdh* used as internal control.**

*ChapB* expression in both soleus and gastrocnemius. To confirm expression at the protein level, we performed CHAP antibody staining in combination with myosin, a slow muscle fiber marker, on sections of mouse soleus and gastrocnemius. Indeed, CHAP protein was expressed in both soleus and gastrocnemius muscle cells (Fig. 6), confirming the results of the qPCR. Although *Chap* mRNA levels were approximately 3-fold higher in soleus muscle, immunofluorescence did not show obvious differences for CHAP protein expression between soleus and gastrocnemius muscles. However, more quantitative proteins assays would be necessary to confirm this.

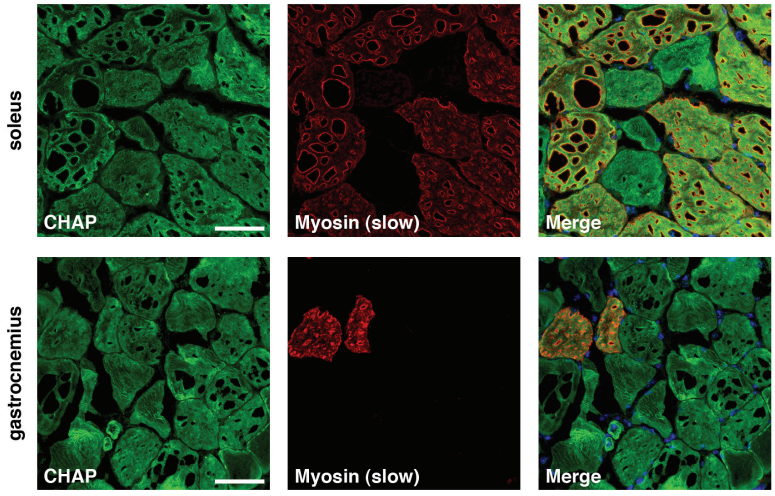


**Figure 6: Expression and localization of CHAP in adult fast and slow muscle. Immunostaining on cross-sections of mouse soleus (slow, upper panel) and gastrocnemius (fast, lower panel) using anti-CHAP (green) and anti-myosin (red) antibodies. Myosin staining (red) was used as a marker for slow muscle fibers, and DAPI was used to stain nuclei (blue). Scale bars: 50 µm.**

*CHAP is expressed in smooth muscle cells*

We have previously observed CHAP expression at the Z-disc in cardiomyocytes of adult mice. More detailed examination indicated CHAP expression in smooth muscle cells. To confirm this observation we performed immunostainings for CHAP and α-smooth muscle actin (ASMA), a smooth muscle marker (but also expressed in cardiomyocytes during early cardiac development), on sections of embryonic (E17.5), adult mouse heart, carotid arteries and aorta. We observed that besides expression in cardiomyocytes in E17.5 mouse embryos CHAP was also expressed in the vena cava, but not in the aorta (data not shown), carotid arteries (Fig. 7A) and subclavian artery (Fig. 7B and C). A higher magnification (Fig. 7B and C) showed that CHAP is expressed in a striated pattern and co-localized with ASMA-positive cells, suggesting that CHAP is expressed in cardiomyocytes from the vena cava. It has been demonstrated previously that cardiomyocytes are present in the tunica media of the vena cava during embryonic development [9, 10]. However, in adult tissues CHAP expression was also observed in smooth muscle cells of aorta, carotid arteries and coronary arteries (Fig. 8). Although CHAP and ASMA are expressed in the same cells, the subcellular localization of both proteins is clearly different.

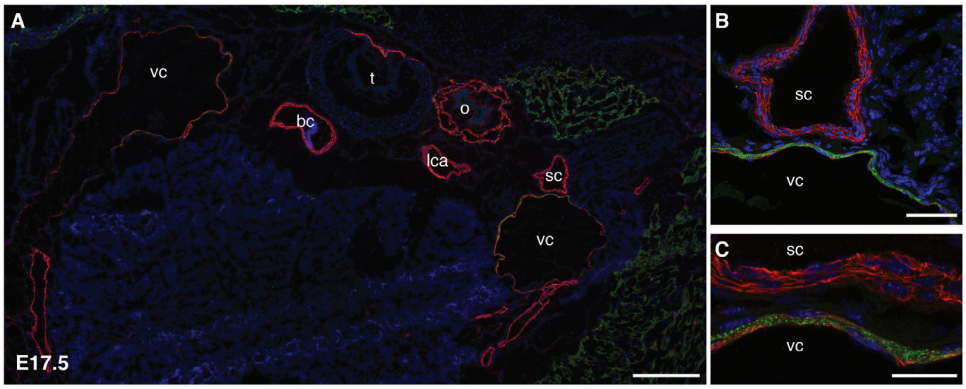


**Figure 7: Co-localization of CHAP with α-smooth muscle actin (ASMA) in cardiomyocytes of the vena cava. Immunostaining for CHAP (green) and α-smooth muscle actin (red) on cross-sections of E17.5 mouse embryos (A-C). DAPI was used to stain nuclei (blue). Vena cava (vc), brachiocephalic artery (bc), left carotid artery (lca), subclavian artery (sc) trachea (t), and oesophagus (o). Scale bars: in A 250 µm, B 50 µm and C 20 µm.**

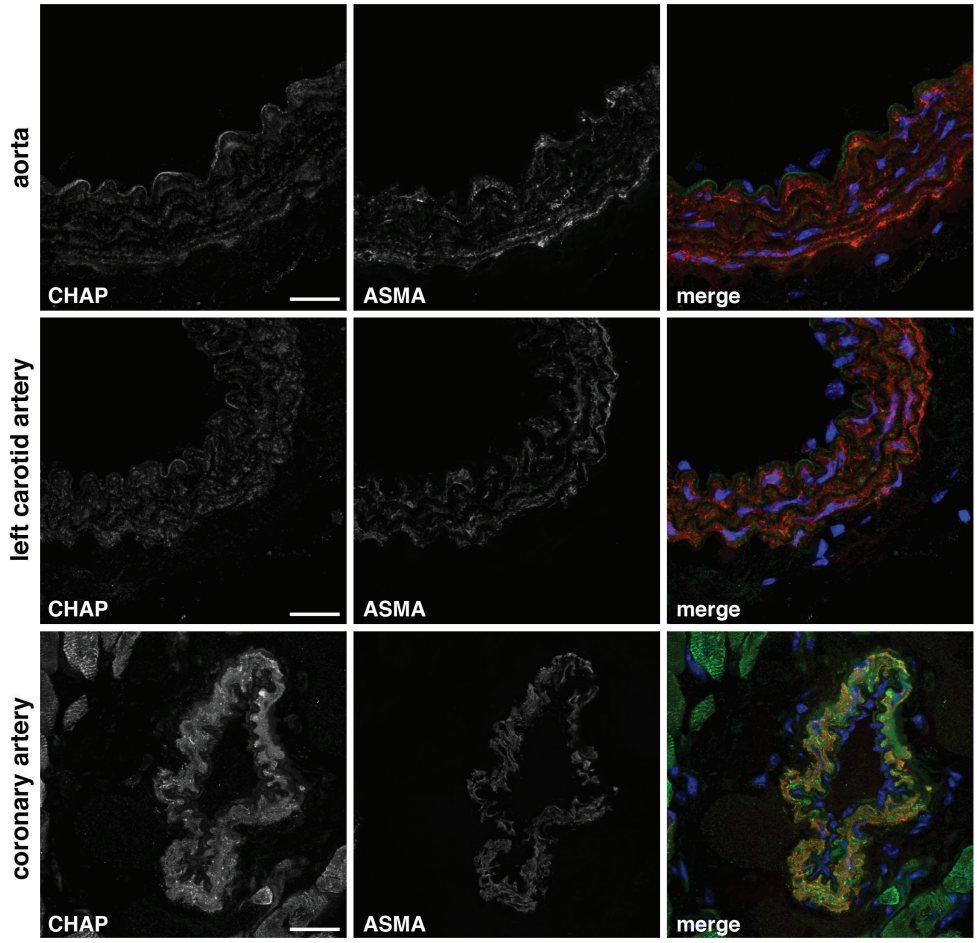


**Figure 8: Expression and localization of CHAP in adult smooth muscle cells. Immunostaining for CHAP (green) and α-smooth muscle actin (ASMA; red) on cross-sections of adult mouse aorta, left carotid artery and coronary artery. DAPI was used to stain nuclei (blue). Scale bars: 20 μm.**

*Conclusion*

In the present study we identified and characterized chick CHAP which has significant homology to the human and mouse CHAPa isoform and zebrafish Chap-1 and -2, and contains highly conserved motifs such as the N-terminal PDZ domain and the NLS. Expression of both chick *CHAP* and mouse *Chap* mRNA and protein were detected in heart and skeletal muscle (such as limbs, jaw, eye and tongue) throughout embryonic development. Furthermore, we demonstrate in the present study that CHAP is also expressed in cardiomyocytes from the vena cava during mouse embryonic development and in smooth muscle cells of aorta, and coronary and carotid arteries of adult mice. It has been shown previously that multipotent cardiovascular progenitor cells, marked by transcription factors Isl-1 and Nkx2.5, have the capacity to differentiate to vascular smooth muscle cells and cardiomyocytes. [11, 12]. Since cardiomyocytes and smooth muscle cells are derived from different origins during development, this suggests that CHAP is expressed in different cardiovascular progenitor cells.

Conserved predicted motifs, syntenic organization and developmental expression patterns, suggest that CHAP may play an important role during muscle development. Indeed, knockdown of *chap* by antisense oligonucleotides in zebrafish had shown previously decreased cardiac contractility, defects in cardiac looping and myofibrillar disarray in muscle cells during embryonic development [3]. CHAP displays homology to synaptopodin and myopodin, which have both been shown to function in actin/α-actinin binding and /or signaling [13-15]. Whereas synaptopodin is expressed in kidney and brain in an isoform specific manner [15], expression of myopodin can be found in smooth, skeletal and heart muscle cells, which is comparable to that of CHAP. Like CHAP, myopodin is localized at the Z-disc of striated muscles and is able to translocate to the nucleus [16, 17]. It has been shown for myopodin that trafficking between the Z-disc and the nucleus is dependent on PKA and CamKII kinase and calcineurin phosphatase activities [18]. Future studies will elucidate whether similar pathways control CHAP trafficking in muscle cells. Furthermore, it would be of interest to study the function and mechanism of action of CHAP in physiological and healthy and pathophysiological situations related to striated and smooth muscle cells. In humans, hypertrophic cardiomyopathy (HCM) and dilated cardiomyopathy (DCM) have been associated with mutations in cytoskeletal and sarcomeric proteins [19, 20]. In addition, it has been shown in different mouse models that mutations in sarcomeric proteins such as α-myosin heavy chain [21, 22], myosin binding protein C [23, 24] and cardiac troponin T [25] can cause HCM-like phenotypes. The sarcomeric protein CHAP may represent a novel candidate gene for screening mutations in DCM and HCM patients.

# Acknowledgements

We thank C. van Munsteren and L. Wisse for technical assistance. This study was supported by the Netherlands Heart Foundation grant 2006B209 (W.E.), and by European Community's Sixth Framework Programme contract ('HeartRepair') LSHM-CT-2005-018630 (A.B.).

# References


(1) Lange S, Ehler E, Gautel M. From A to Z and back? Multicompartment proteins in the sarcomere. *Trends Cell Biol* 2006 January;16(1):11-8.

(2) Beqqali A, Kloots J, Ward-van Oostwaard D, Mummery C, Passier R. Genome-wide transcriptional profiling of human embryonic stem cells differentiating to cardiomyocytes. *Stem Cells* 2006 August;24(8):1956-67.

(3) Beqqali A, Monshouwer-Kloots J, Monteiro R, Welling M, Bakkers J, Ehler E, Verkleij A, Mummery C, Passier R. CHAP is a newly identified Z-disc protein essential for heart and skeletal muscle function. *J Cell Sci* 2010 April 1;123(Pt 7):1141-50.

(4) Hamburger V, Hamilton HL. A series of normal stages in the development of the chick embryo. 1951. *Dev Dyn* 1992 December;195(4):231-72.

(5) Bajanca F, Luz M, Duxson MJ, Thorsteinsdottir S. Integrins in the mouse myotome: developmental changes and differences between the epaxial and hypaxial lineage. *Dev Dyn* 2004 October;231(2):402-15.

(6) Moorman AF, Houweling AC, de Boer PA, Christoffels VM. Sensitive nonradioactive detection of mRNA in tissue sections: novel application of the whole-mount in situ hybridization protocol. *J Histochem Cytochem* 2001 January;49(1):1-8.

(7) Nieto MA, Bennett MF, Sargent MG, Wilkinson DG. Cloning and developmental expression of Sna, a murine homologue of the Drosophila snail gene. *Development* 1992 September;116(1):227-37.

(8) van Laake LW, Passier R, Monshouwer-Kloots J, Nederhoff MG, Ward-van OD, Field LJ, van Echteld CJ, Doevendans PA, Mummery CL. Monitoring of cell therapy and assessment of cardiac function using magnetic resonance imaging in a mouse model of myocardial infarction. *Nat Protoc* 2007;2(10):2551-67.

(9) Vrancken Peeters MP, Gittenberger-de Groot AC, Mentink MM, Hungerford JE, Little CD, Poelmann RE. Differences in development of coronary arteries and veins. *Cardiovasc Res* 1997 October;36(1):101-10.

(10) Endo H, Ogawa K, Kurohmaru M, Hayashi Y. Development of cardiac musculature in the cranial vena cava of rat embryos. *Anat Embryol (Berl)* 1996 May;193(5):501-4.

(11) Moretti A, Caron L, Nakano A, Lam JT, Bernshausen A, Chen Y, Qyang Y, Bu L, Sasaki M, Martin-Puig S, Sun Y, Evans SM, Laugwitz KL, Chien KR. Multipotent embryonic isl1+ progenitor cells lead to cardiac, smooth muscle, and endothelial cell diversification. *Cell* 2006 December 15;127(6):1151-65.

(12) Sun Y, Liang X, Najafi N, Cass M, Lin L, Cai CL, Chen J, Evans SM. Islet 1 is expressed in distinct cardiovascular lineages, including pacemaker and coronary vascular cells. *Dev Biol* 2007 April 1;304(1):286-96.

(13) Asanuma K, Yanagida-Asanuma E, Faul C, Tomino Y, Kim K, Mundel P. Synaptopodin orchestrates actin organization and cell motility via regulation of RhoA signalling. *Nat Cell Biol* 2006 May;8(5):485-91.

(14) Weins A, Schwarz K, Faul C, Barisoni L, Linke WA, Mundel P. Differentiation- and stress-dependent nuclear cytoplasmic redistribution of myopodin, a novel actin-bundling protein. *J Cell Biol* 2001 October 29;155(3):393-404.

(15) Asanuma K, Kim K, Oh J, Giardino L, Chabanis S, Faul C, Reiser J, Mundel P. Synaptopodin regulates the actin-bundling activity of alpha-actinin in an isoform-specific manner. *J Clin Invest* 2005 May;115(5):1188-98.

(16) Faul C, Dhume A, Schecter AD, Mundel P. Protein kinase A, Ca2+/calmodulin-dependent kinase II, and calcineurin regulate the intracellular trafficking of myopodin between the Z-disc and the nucleus of cardiac myocytes. *Mol Cell Biol* 2007 December;27(23):8215-27.

(17) De Gank A, Hubert T, Van IK, Geelen D, Vandekerckhove J, De C, V, Gettemans J. A monopartite nuclear localization sequence regulates nuclear targeting of the actin binding protein myopodin. *FEBS Lett* 2005 December 5;579(29):6673-80.

(18) Faul C, Dhume A, Schecter AD, Mundel P. Protein kinase A, Ca2+/calmodulin-dependent kinase II, and calcineurin regulate the intracellular trafficking of myopodin between the Z-disc and the nucleus of cardiac myocytes. *Mol Cell Biol* 2007 December;27(23):8215-27.

(19) Sanoudou D, Vafiadaki E, Arvanitis DA, Kranias E, Kontrogianni-Konstantopoulos A. Array lessons from the heart: focus on the genome and transcriptome of cardiomyopathies. *Physiol Genomics* 2005 April 14;21(2):131-43.

(20) Beqqali A, van Eldik W, Mummery C, Passier R. Human stem cells as a model for cardiac differentia-

tion and disease. *Cell Mol Life Sci* 2009 March;66(5):800-13.
(21) Georgakopoulos D, Christe ME, Giewat M, Seidman CM, Seidman JG, Kass DA. The pathogenesis of familial hypertrophic cardiomyopathy: early and evolving effects from an alpha-cardiac myosin heavy chain missense mutation. *Nat Med* 1999 March;5(3):327-30.
(22) Geisterfer-Lowrance AA, Christe M, Conner DA, Ingwall JS, Schoen FJ, Seidman CE, Seidman JG. A mouse model of familial hypertrophic cardiomyopathy. *Science* 1996 May 3;272(5262):731-4.
(23) Witt CC, Gerull B, Davies MJ, Centner T, Linke WA, Thierfelder L. Hypercontractile properties of cardiac muscle fibers in a knock-in mouse model of cardiac myosin-binding protein-C. *J Biol Chem* 2001 February 16;276(7):5353-9.
(24) Harris SP, Bartley CR, Hacker TA, McDonald KS, Douglas PS, Greaser ML, Powers PA, Moss RL. Hypertrophic cardiomyopathy in cardiac myosin binding protein-C knockout mice. *Circ Res* 2002 March 22;90(5):594-601.
(25) Tardiff JC, Hewett TE, Palmer BM, Olsson C, Factor SM, Moore RL, Robbins J, Leinwand LA. Cardiac troponin T mutations result in allele-specific phenotypes in a mouse model for hypertrophic cardiomyopathy. *J Clin Invest* 1999 August;104(4):469-81.

# Chapter 3

## The role of CHAP during heart development: *in vivo* and *in vitro* knockdown in mouse and chick

Willemijn van Eldik, Abdelaziz Beqqali, Jantine Monshouwer-Kloots, Siobhan Loughna, Stieneke van den Brink, Christine Mummery, Robert Passier

# Abstract

We have previously shown that Cytoskeletal Heart-enriched Actin-associated Protein (CHAP) plays an important role during skeletal and heart muscle development in zebrafish by a gene knockdown approach. In order to study the role of CHAP more specifically during muscle development and disease we targeted the CHAP genomic locus in mouse embryonic stem cells (mESC) for creating both straight and conditional knockout mice for CHAP. High percentage chimeric mice were obtained for both approaches and were further bred for germline transmission. At the present time, no germ knockout lines were generated for both targeted constructs. Besides the opportunity to study the loss of CHAP during development and disease at specific times and organs, another advantage is to study the role of CHAP during cardiomyocyte differentiation in these targeted ESC lines.

To investigate the cardiac differentiation potential of the heterozygous CHAP LacZ mESC in vitro, we differentiated these cells to cardiomyocytes by formation of embryoid bodies (EBs). qPCR analysis showed that *ChapB* was significantly downregulated in these EBs in comparison to wild type cells. Although, expression levels of *ChapA* were not significantly different, a trend towards reduced mRNA levels in the heterozygous cells could be observed. Despite decreased levels of CHAPb, both sarcomeric organization and beating frequency were not affected in CHAP heterozygous mESC lines, indicating that mutation of one single copy of CHAP does not lead to haploinsufficiency based on cellular and functional in vitro readouts.

Since CHAP is also expressed during muscle development in chick, which only has one isoform of CHAP and does not contain a duplicated genome (as in the zebrafish), we knocked down *CHAP* expression in chick during embryonic development. With increasing concentrations of *CHAP* morpholino's a higher percentage of embryo's with an aberrant cardiac looping phenotype was observed, although this was not statistically significant. These results from both mouse and chicken experiments show that reduced levels of CHAP are sufficient to maintain cardiomyocyte integrity and functionality with minimal effects on cardiac development.

# Introduction

Cytoskeletal Heart-enriched Actin-associated Protein (CHAP) is highly conserved in different species such as human, mouse, zebrafish and chicken. Whereas two isoforms of CHAP exist in human and mouse, only one isoform is present in zebrafish and chicken. In previous experiments in mice we identified that the shorter isoform CHAPb is expressed during embryonic development, whereas the longer isoform CHAPa is expressed in adult heart and skeletal muscle. The longer isoform consists of a PDZ domain, important for protein-protein interactions and a nuclear localization signal (NLS), whereas the shorter isoform lacks the PDZ domain. In both zebrafish and chick only one isoform can be identified with highest homology to the longer isoform CHAPa. We have previously shown by antisense morpholino knockdown of CHAP in zebrafish resulted in cardiac defects and impaired muscle formation, suggesting an important role for CHAP during development[1].

To elucidate the function of CHAP in specific organs and at specific times during mouse development and disease we developed different strategies for generating CHAP knockout lines in mouse embryonic stem cells (mESC). First, a CHAP LacZ knockin (CHAP $LacZ^{+/-}$) mouse embryonic stem cell line was generated, which replaces the complete CHAP gene for a LacZ gene. This line was used to study the effect of CHAP knockdown on the differentiation of mESC-derived cardiomyocytes *in vitro*. Second, a conditional knockout mESC line was generated in which the CHAP exon 5 was flanked by loxP sites. Both lines can be used to generate CHAP knockout ($CHAP^{f/+}$) lines, which can be used to study the effect of CHAP knockdown in mouse *in vivo*.

In addition, we investigated the effects of *CHAP* knockdown on heart development in chick embryos. In contrast to human and mice, the chick genome contains only one *CHAP* isoform (see chapter 2) and in contrast to the zebrafish, there is no duplication of the genome. Furthermore, the four-chambered chick heart represents a convenient model for studying human heart development[2, 3]. Comparable to the zebrafish it is possible to achieve knockdown of the gene of interest. Following an antisense morpholino-mediated knockdown in chick embryos we studied the role of *CHAP* on heart development.

# Materials and methods

*Cell culture*

Wild type (IB10) and targeted CHAP LacZ$^{+/-}$ and CHAP$^{f/+}$ mESC were grown on feeders in complete medium (CM: 1x GMEM (Invitrogen), 2 mM L-glutamin (Invitrogen), 1 mM Sodium Pyruvate (Invitrogen), non-essential amino acids (1:100, Invitrogen)), 8.8% fetal calf serum (FCS; Sigma-Aldrich Chemie). To keep the cells undifferentiated β-mercaptoethanol (1000x) and leukemia inhibitory factor ($10^6$ units/ml LIF, ESGRO, Millipore) were added to the CM (CM$^{++}$). For long-term feeder free growth of mESCs, cells were plated on gelatine coated dishes and grown in 60% BRL medium with β-mercaptoethanol and LIF added. 100% BRL medium was made by conditioning CM on Buffalo Rat Liver (BRL) cells. 60% BRL medium was made by mixing 100% BRL and CM to a 60/40 ratio.

*Generation of CHAP lacZ knockin and CHAP conditional mESC lines*

For generating CHAP LacZ$^{+/-}$ mESC the pNeo-LacZ-TK2 targeting vector (kindly provided by Dr. E. Olson) was used. A 5.3 kb long arm (primers: 5'- GTCGACTCAGTTTTTT-GAGACTGGAT-3' and 5'- GTCGACCGCACAGCTTAGCCTGTGG-3') was designed, amplified by PCR from a BAC-clone, subcloned into pGEM-T easy (Promega) and sequencing. The long arm was designed as such that the ATG starting codon of the CHAP gene was replaced by the coding sequence of LacZ gene (starting with ATG). A 2.5 kb short arm (primers: 5'-GGTACCCTCCTCAGCTCTCTGCTGGT-3' and 5'- ATGGTTGC-AGGTCAACACAA-3') was amplified and subcloned in a similar way as described for the long arm and was positioned at the 5' end of LacZ (see figure 1A).

For generating CHAP conditional knockout (CHAP$^{f/+}$) mESC line the pl451 targeting vector (kindly provided by J. van Es) was used. The following products were amplified and subcloned in pGEM-T easy vector and verified by sequence analysis: CHAP exon 5 (primers: 5'-CGGGATCCGCCAGCCTGGTCTACATAGC-3' and 5'-CGGGATCCAGCCTTG-TTCCTGGCTTTTG-3'), a 5.8 kb long arm (primers: 5'-CCATCGATCTTTCAAT-GACCGTGGCAAA-3' and 5'-CCATCGATGTCGGCCTTGAACTCACAGA-3') and a 2.5 kb short arm (same primers were used as for the CHAP LacZ$^{+/-}$). The products were subcloned into the pl451 targeting vector: the CHAP exon 5 product was flanked by loxP sites and the long arm and short arm were upstream and downstream of exon 5, respectively. Following correct targeting by homologous recombination exon 5 of CHAP will be flanked by LoxP sites (see figure 2A). Both targeting vectors contained a neomycin cassette for positive selection and a thymidine kinase (TK) cassette for negative selection.

The targeting constructs were linearized, purified and dissolved in sterile PBS (Invitrogen). 75-100 ug DNA was electroporated in mESC (IB10) with a 129Sv background. Cells were plated on gelatin-coated dishes and put overnight in the incubator. After 1 day medium was replaced by medium containing G418 and gancyclovir for positive and negative selection, respectively. The medium was replaced every other day. After approximately one week colonies were picked and transferred to 96 well plates on feeders. These plates were split into three other 96 well plates (two with feeders, one feeder-free). The two plates on feeders were frozen by dissolving cells in freezing medium (44.3% CM$^{++}$, 44.3% FCS and 11.4% DMSO) and stored at -80 $^{o}$C. The feeder-free plate was used to isolate DNA to screen resistant colonies for correct homologous recombination by Southern blot (see below). Correct recombined colonies were thawed, scaled-up and frozen again in multiple aliquots in liquid nitrogen.

*Southern blot*
Genomic DNA of resistant ES cell colonies was extracted by adding lysisbuffer (10 mM Tris pH 7.5, 10 mM EDTA, 10mM NaCl, 0.5% sarkosyl and 2 mg/ml protK) at 60 °C overnight. DNA was precipitated and digested by BamHI (5'targeting of $CHAP^{f/+}$), NcoI (5'targeting of CHAP $LacZ^{+/-}$) or KpnI (3'targeting of $CHAP^{f/+}$and CHAP $LacZ^{+/-}$) overnight and run on a 1% v/w agarose gel. Three probes were generated using the following primers: BamHI (329 bp) 5'-GGAGAGCCAGATGCTTTTTG-3' and 5'- CCACTCTTCTGCCCAGCTAC-3', NcoI (1 kb) 5'-GTCCTTCCAAACGCTAAACG-3' and 5'-CTACCGTAGGGAC-GCAAATC-3', KpnI (416 bp) 5'-CCACTATCTGCTCCCTCTCG-3' and 5'-CTCAGAA-GAGTGGGCTCCAG-3. The PCR products were cloned into pCRII (Invitrogen) and products were excised. The products were then radioactively labelled using α-[p32]dATP (PerkinElmer) by random priming (RadPrime, Invitrogen). DNA blots (Hybond-N+, GE Healthcare) were hybridized with the radioactive probe in ExpressHyb Hybridization buffer (Clontech) and visualized by using phosphor-imager (location of probes are indicated in schematic drawings of figure 1A and 2A).

*Generation of chimeric mice*
Recombinant ESC clones were injected in blastocysts obtained from C57BL6 (conditional knockout) or CD1 females (LacZ knockin). Chimeric male mice were crossed with C57BL6 or CD1 females to derive germline F1 progeny.

*Differentiation assays*
Wild type (IB10) and CHAP $LacZ^{+/-}$ mESC were differentiated using the hanging drop method. Before the procedure, cells were plated on gelatine-coated dishes for feeder depletion and grown in CM medium with β-mercaptoethanol and LIF. Cells were then washed with PBS, trypsinised and counted. 20 µl drops containing 1500 cells in differentiation medium (Iscove's Modified Dulbecco's Medium, Invitrogen), 15% FCS (Greiner), 5% Protein free Hybridoma medium (PFHMII, Invitrogen), 2 mM L-glutamine (Invitrogen), 50 µg/ml asorbic acid, 0.3% α-MTG and 0.5% Pen/Strep (Invitrogen)) were put on the lids of bacterial dishes with PBS and left for 7 days. Then embryoid bodies (EBs) were plated on gelatine-coated dishes in differentiation medium. After 7 days cells we either fixed EBs for 30 minutes in 2% paraformaldehyde (PFA) or dissolved them in Trizol (Invitrogen) and stored at -80 °C.

*RNA isolation and quantitative PCR*
EBs were dissolved in Trizol (Invitrogen) and RNA was isolated. RNA was treated with DNase (DNA-free, Ambion) and cDNA was made with the iScript kit (BioRad). qPCR was performed using the CFX96 Real-Time PCR detection system (Bio-Rad). The following primers were used *ChapA* (sense: 5'-GAGGAGGTGCAGGTCACATT-3'; antisense: 5'-CTGAAGAGCCTGGGAAACAG-3'), *ChapB* (sense: 5'-CCGCCGCTTCTTAAACATAA-3 antisense: 5'-GGCTTTAAAGGGCCTTGG-3') and as reference gene *Gapdh* (sense: 5'-GTTTGTGATGGGTGTGAACCAC-3', antisense: 5'-CTGGTCCTCAGTGTAGCCCAA-3). Data were analyzed with Bio-Rad CFX Manager.

*Immunofluorescence*
EBs were grown on gelatine-coated coverslips and fixed in 2% PFA for 30 minutes. Cells were permeabilized in 0.1% Triton-x-100 in PBS for 8 minutes. Subsequently, cells were incubated

with primary antibodies (CHAP 1:50 (rabbit, custommade by Eurogentec), myomesin (mouse, kindly provided by E. Ehler) 1:50 and α-actinin (mouse, Sigma) 1:800) in 4% normal goat serum overnight at 4 °C. Secondary antibodies used were goat-anti-mouse cy3 (1:250, Jackson Immuno research) and goat-anti-rabbit Alexa Fluor 488 (1:200, Invitrogen) for 1 hour at room temperature. Cells were counterstained by DAPI. Stainings were analysed with SP5 confocal microscope (Leica).

*Morpholino knockdown of CHAP in chick embryos*

Morpholino knockdown of *CHAP* was done as described by Cing et al[2]. In brief White Leghorn eggs were incubated at 38 °C. At Hamburger and Hamilton stage 11 a window was created and the extra-embryonic membranes overlying the heart were removed. Embryos were treated with control morpholino's (mutated human β-globin; sequence: 5'-CCTCTTACCTCAGTTACAATTTATA-3'), two concentrations of *CHAP*-specific morpholino's (sequence: 5'-TGAGCATTTCTTCTTCGGCTCCCAT-3') or left untreated (wild type). After 29 hours (stage 20) embryos were harvested, washed in PBS and fixated in 4% paraformaldehyde. Embryos were dehydrated by ethanol and xylene series and embedded in paraffin. Embryos (E12.5) were sectioned (5 μM) and mounted on starfrost slides (Knittel). Antigen retrieval was performed by microwave heating of tissue sections in citrate buffer (pH 6). Endogenous peroxidase was blocked by incubating the slides in 0.3% $H_2O_2$ in PBS. Sections were incubated overnight with Troponin I antibody (1:400; TnI; Santa Cruz) at room temperature. Biotin-conjugated goat anti-rabbit (BA-1000, Vector Labs) was used as secondary antibody. Subsequently, the sections were incubated with Vectastain ABC staining kit (PK-6100, Vector Labs) for 45 min. Slides were rinsed in PBS and Tris/Maleate (pH 7.6). 3-3diaminobenzidine tetrahydrochloride (D5637, Sigma-Aldrich) was used as chromogen and Mayer's hematoxylin as counterstaining. Finally, all slides were dehydrated and mounted with Entellan (Merck).

Reconstructions were made as follows: a picture was taken of every TnI positive stained slide, which were adapted in Photoshop (Adobe) and the program Amira 5.3 was used to make the reconstructions.

*In situ hybridization*

*CHAP* in situ hybridization were performed as described before (van Eldik et al.; Chapter 2) and was performed on *CHAP* morpholino treated, control morpholino treated and wild type embryo's.

*Statistical analysis*

Data were analysed with GraphPad Prism. All data are expressed as mean + the standard error of the mean (SEM). Statistical analysis was performed using students unpaired t-test. $P < 0.05$ was considered to be statistically different.

# Results

*Generation of CHAP knockout mouse ESC lines*

To investigate the consequences of CHAP knockdown *in vivo*, we knocked out CHAP in mESC. We used two approaches for this, a straight knockdown (CHAP LacZ$^{+/-}$), and a conditional knockdown (CHAP$^{f/+}$). In figure 1A a schematic overview for the CHAP LacZ$^{+/-}$ targeting is shown. The targeting construct was linearized and electroporated in mESC (IB10) with a 129Sv background. Screening of 200 colonies yielded two correctly recombined lines (Figure 1B). These lines were used to generate chimeric mice, by injecting mESC in blastocysts with CD1 background. Chimeric mice were obtained (Figure 1C) and high-percentage chimeric mice were crossed with CD1 mice in order to achieve germline transmission. CD1 mice have a white coat colour, whereas mice with a 129Sv background have an agouti coat colour. Germline transmission is achieved when the agouti coat colour of the 129Sv background is observed in progeny. Unfortunately, after several rounds of offspring, no germline transmission was achieved.

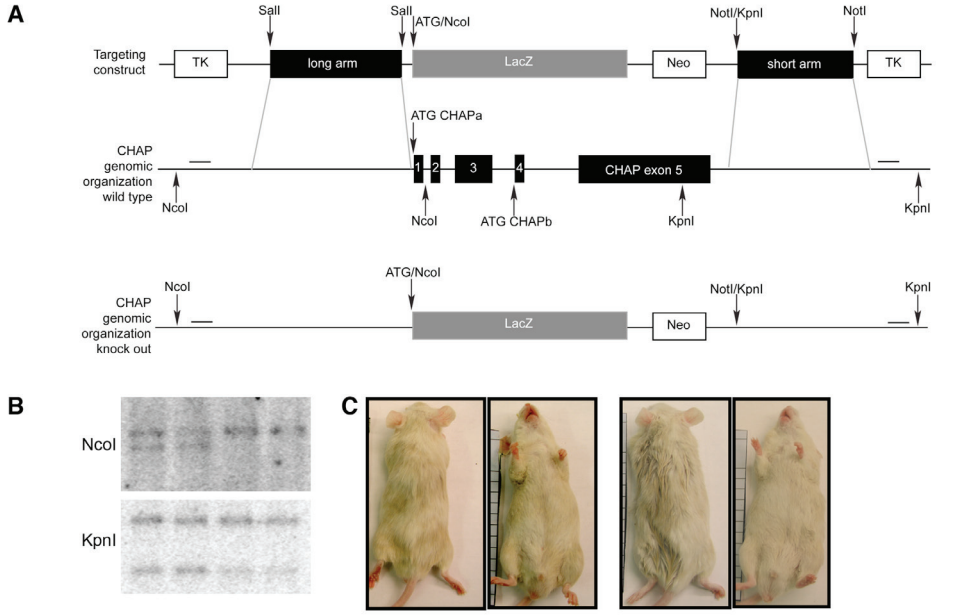


**Figure 1: Targeting strategy for CHAP LacZ mouse embryonic stem cells. A) Schematic overview of CHAP LacZ targeting. First panel shows the targeting construct. The construct replaces the wild type CHAP gene (second panel) for a LacZ gene starting at the ATG site of the CHAPa gene (third panel). Neomycine and thymidine kinase cassettes can be used for positve and negative selection respectively. Probes which can be used for testing for recombination are shown (lines in second and third panel). For 5' targeting NcoI gives a 8.3 kB band (wild type) and 7 kB band (targeted). For 3' targeting KpnI gives a 5.5 kB band (wild type) and 3.9 kB band (targeted). B) Southern blot showing the results of the targeting. Two positive clones were obtained which showed recombination of both 5' and '3 arm. C) Chimeric mice obtained after blastocyst injections.**

In figure 2A a schematic overview for the CHAP$^{f/+}$ is shown. In order to avoid interference of the neomycine-casette with endogenous expression of CHAP, the CHAP$^{f/+}$ line can be crossed with a mouse line expressing FLPe, leading to excision of this cassette (Figure 2A panel 3). The construct was linearized and electroporated in mESC (IB10) with a 129Sv background. Screening of 100 colonies yielded 7 correctly recombined lines (figure 2B). Two lines were used to generate chimeric mice, by injecting mESC in blastocysts with C57BL6 background. Male chimeric mice were crossed back to mice with a C57BL6 background. We obtained progeny with the agouti coat colour of the 129Sv background from one chimeric mouse, however after PCR and southern blot analysis (data not shown) these were found to be all wild type.

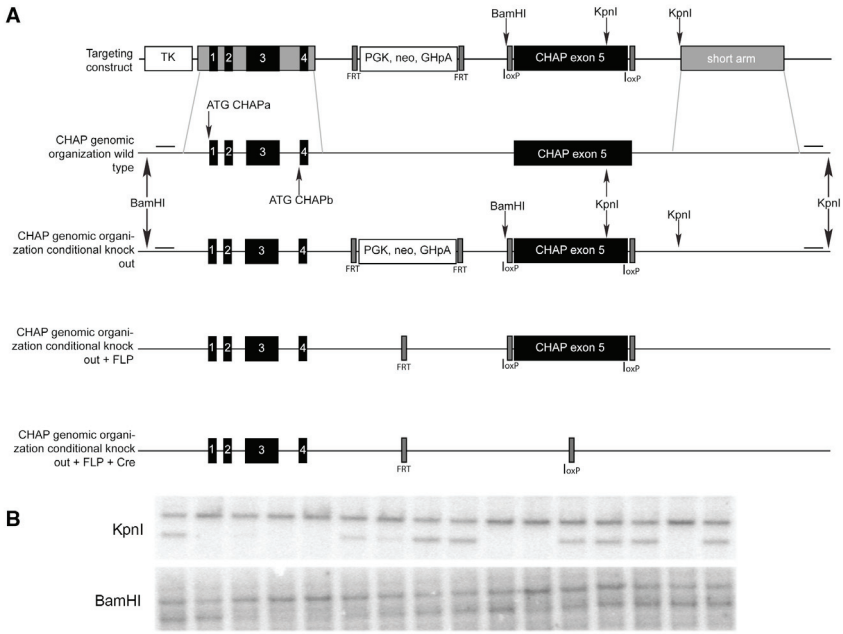


**Figure 2: Targeting strategy for CHAP$^{f/+}$ mouse embryonic stem cells. A) Schematic overview of CHAP$^{f/+}$ targeting. First panel shows the targeting construct. The construct replaces the wild type CHAP gene (second panel) for a CHAP gene with a LoxP flanked exon 5 (third panel). Neomycine and thymidine kinase cassettes can be used for positve and negative selection respectively. Probes which can be used for testing for recombination are shown (lines in second and third panel). For 5' targeting BamHI gives a 15 kB band (wild type) and 11.7 kB band (targeted). For 3' targeting KpnI gives a 5.5 kB band (wild type) and 3.9 kB band (targeted). The neomycine cassette is flanked by FRT sites and can be removed by crossing CHAP$^{f/+}$ mouse with a mouse that expresses FLPe (fourth panel). A heart specific CHAP knockout mouse can be obtained by crossing this mouse with a mouse that expresses Cre B) Southern blot showing the results of the targeting. Seven positive clones were obtained which showed recombination of both 5' and '3 arm.**

*Cardiac differentiation of wild type and CHAP LacZ$^{+/-}$ mESC*

To investigate the effect of CHAP knockdown in mESC *in vitro*, we differentiated wild type IB10 and CHAP LacZ$^{+/-}$ mESC to cardiomyocytes by using the hanging drop method. First, we investigated the expression of *ChapA* and *ChapB* in differentiated EBs. As expected qPCR analysis showed that expression of *ChapA* and *ChapB* in CHAP LacZ$^{+/-}$ EBs was approximately half of expression of wild type EBs, although this was not statistically significant for *ChapA* in three independent experiments (Figure 3).

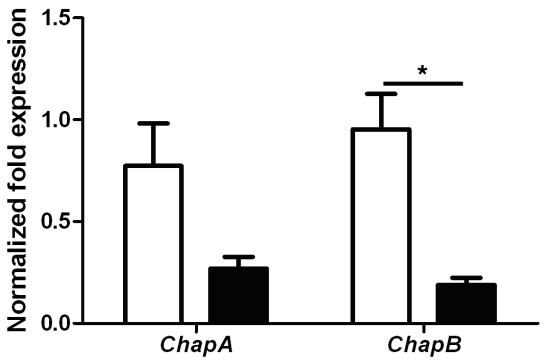


**Figure 3: qPCR analysis of expression of *ChapA* and *ChapB* in wild type (white bars) and CHAP LacZ$^{+/-}$ (black bars) embryoid bodies.**

Next, we investigated the functional properties of wild type and CHAP LacZ$^{+/-}$ EBs . For this we investigated if the number of beating EBs and the beating frequency (beats per minute) was different for wild type and CHAP LacZ$^{+/-}$ EBs. We did not observe a difference in the cardiac differentiation potential indicated by a similar percentage of beating EBs (Figure 4A), although we cannot exclude that the percentage of cardiomyocytes per EB is different between groups. Similarly, beating frequency also did not differ between groups (Figure 4B). In order to determine whether structural properties of wild type and CHAP LacZ$^{+/-}$ EBs were affected, we performed immunofluorescent analysis. Wild type and CHAP LacZ$^{+/-}$ EBs were co-stained for CHAP and α-actinin (Figure 5A), a Z-disc marker, and CHAP and myomesin (Figure 5B), an m-band marker. Staining of wild type and CHAP LacZ$^{+/-}$ EBs showed that there was no difference in sarcomeric organization and subcellular localization for α-actinin and myomesin between wild type and CHAP LacZ$^{+/-}$ EBs.

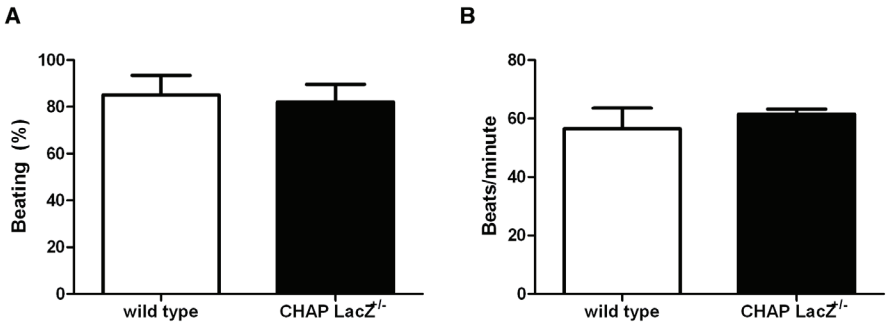


**Figure 4: Differentiation potential of wild type and CHAP LacZ$^{+/-}$ mouse embryonic stem cells (mESCs). A) Percentage beating areas obtained after differentiation of wild type (white bars) and CHAP LacZ$^{+/-}$ (black bars) mESCs. B) Beating frequency of wild type (white bars) and CHAP LacZ$^{+/-}$ (black bars).**

*Knockdown of CHAP in developing chick embryos*

In addition to analysing the function of CHAP by knockdown in mice, we also investigated the function of CHAP during chick heart development. In chapter 2 we showed that in chick only one CHAP isoform (homologous to human and mouse CHAPa) is expressed and that this isoform is expressed from the cardiac crescent stage onwards, and in later stages in somites

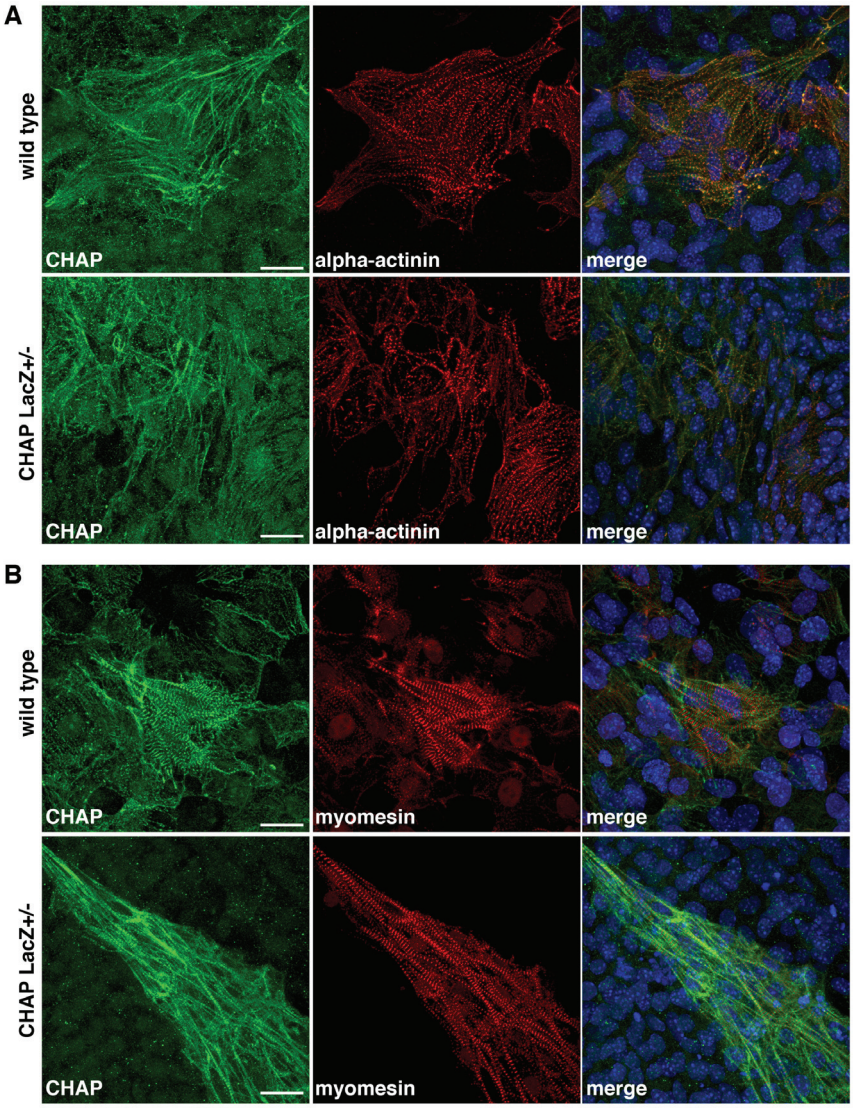


**Figure 5: sarcomeric organization of wild type and CHAP LacZ$^{+/-}$ embryoid bodies. A) Wild type and CHAP LacZ$^{+/-}$ EBs stained for CHAP (green) and α-actinin (red). Merge images are shown. B) Wild type and CHAP LacZ$^{+/-}$ EBs stained for CHAP (green) and myomesin (red). Merge images are shown. Scale bars: 20 µM.**

and developing muscles as well. To knockdown chick *CHAP* during development we treated embryos of stage 11 with two concentrations *CHAP* morpholinos, control morpholinos or untreated (wild type). Embryos were harvested at stage 20. Although cardiac defects, such as a cardiac looping defect, could occasionally be observed in the *CHAP* morpholino group, no consistent significant cardiac malformations were evident (Figure 6). Next, we investigated the expression of *CHAP* by in situ hybridisation. No difference was detected between the different groups (data not shown). This is not unexpected since morpholino antisense oligonucleotides block translation of RNA to protein. In addition, we also used our custommade antibody

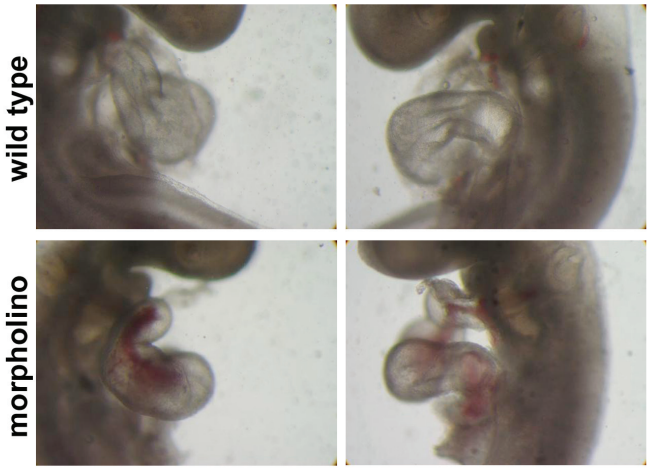


**Figure 6: *CHAP* morpholino knockdown in chick embryos. Examples of wild type and *CHAP*-morpholino treated chick embryos of stage HH19 are shown. The *CHAP* morpholino treated embryo shows a looping defect.**

against mouse CHAP, but unfortunately did not reveal specific staining.
To study changes in cardiac development in detail we decided to perform immunohistochemical stainings for TnI, which marks cardiomyocytes, for cardiac reconstructions. Because we found impaired looping in zebrafish embryos after *chap* morpholino treatment[1], we investigated the cardiac looping in these embryos as well. Cardiac looping varied among all embryos in the different groups, including in the control groups and therefore we cannot conclude at the present time that chick CHAP affects cardiac looping (Figure 7). To reach a possible statistical significant finding, these experiments should be extended (see discussion).

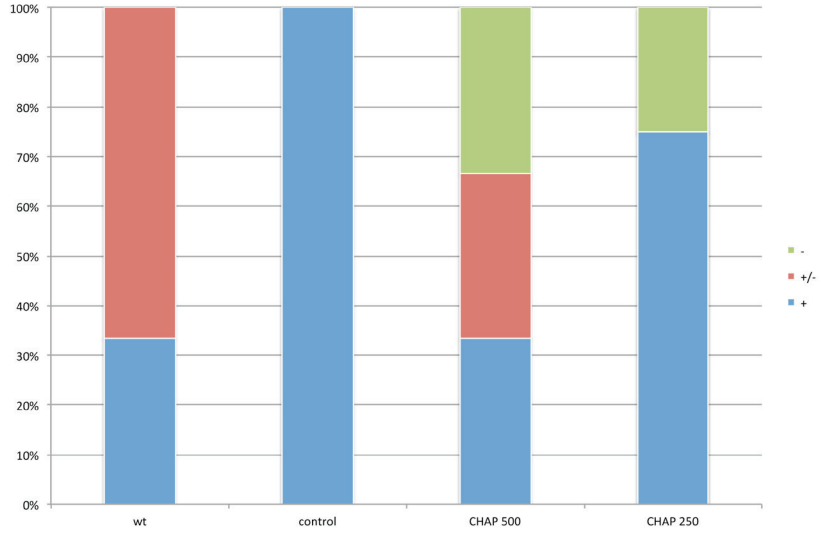


**Figure 7: Summary of cardiac looping (classified as not looped -, not completely looped +/- and looped +) of wild type (wt), control morpholino and *CHAP* morpholino (concentrations 500 and 250)**

# Discussion and future directions

Here, we generated CHAP LacZ$^{+/-}$ and CHAP$^{f/+}$ mESC lines. Control experiments show successful targeting leading to high-percentage chimeric mice. However, several attempts (more than 6 offspring litters for each chimeric mouse) did not yield germline transmission at the present time. In addition, we used the CHAP LacZ$^{+/-}$ mESC to study the effect of CHAP knockdown on cardiac differentiation *in vitro*. Although we found downregulation of *ChapA* and *ChapB*, no effect on differentiation was found. We found no difference in the number of beating areas, beating frequency and sarcomeric organization. From this we conclude that mutation of one allele of CHAP does not lead to haploinsufficiency. Alternatively, *in vitro* experiments using CHAP siRNA in hESC-derived cardiomyocytes could be used to investigate the effect on sarcomere structure and cardiomyocyte function. Preliminary data show that siRNA knockdown of CHAP results in disruption of the sarcomeric structure. However, we were not able to investigate down regulation of CHAP protein expression. Additional future experiments using proper controls (control siRNA) and investigating the effect on RNA and protein expression will give more information about the function of CHAP in human cardiomyocytes.

New techniques for efficient generation of knockout mice have been developed. Chimeric mice with more than 90% ES cell contribution can still be inefficient germ line transmitters. Therefore, a new technique in generating chimeric mice was developed. In this approach 8 cell embryos are laser injected with mESCs. Where in the conventional blastocyst injection method the injected ESC compete with host to create the inner cell mass (ICM), which results in F0 chimeric mice, in the 8 cell stage injected ESC seem to have an advantage over the host cells, which results in an ICM that consist completely of injected cells and thus fully ES cell derived F0 mice[4]. Using this technique it would be possible to obtain CHAP LacZ$^{+/-}$ and CHAP$^{f/+}$ mice.

Morpholino mediated knockdown of *chap* in zebrafish has shown that CHAP is essential for cardiac looping[1]. In vertebrates defects in cardiac looping result in cardiac malformations like double-outlet right ventricle, double-inlet left ventricle and transpositions of the great arteries[5]. If replacement of CHAP by a LacZ gene leads to embryonic lethality, a conditional knockdown approach may be used to overcome this problem. For example, crossing the CHAP$^{f/f}$ with a mouse that expresses Cre in the cardiac (α-MHC or Nkx2.5) lineage or skeletal muscle (MyoD) will elucidate more about the specific function of CHAP in these cells. Furthermore, using a tamoxifen inducible Cre approach, CHAP can be knocked down at a specific moment in adult mice.

In addition to investigating the role of CHAP during development, the knockout models can be used to investigate the role of CHAP in disease. For example, we have shown *in vitro* that CHAP mediates calcineurin signalling. Crossing a mouse with a constitutively active calcineurin in the heart[6] with CHAP knockout mice will give more evidence about the role of CHAP in calcineurin signalling *in vivo*.

In addition to using mouse as a model organism for heart development, chick embryos can also be used as model organism. The chick has the advantage to manipulate embryos in ovo by morpholino treatment[2, 3, 7] or RNAi electroporation[8-11]. In this experiment we chose to knockdown chick *CHAP* by morpholino treatment. Unfortunately, lack of CHAP-specific chick antibody prevented us to study CHAP protein expression in these embryos. We investigated the cardiac looping in these embryos, but found no consistent abnormality

in *CHAP* morpholino treated embryos compared to controls. These experiments need to be repeated in order to make solid conclusions on whether *CHAP* affects cardiac development in chick. In summary, future experiments including knockdown of CHAP in different species (mouse, chick and human) *in vivo* (mouse and chick) or *in vitro* (human, mouse, chick) will reveal more about the putative function of CHAP isoforms during cardiac and skeletal muscle development and disease.

# References


(1) Beqqali A, Monshouwer-Kloots J, Monteiro R, Welling M, Bakkers J, Ehler E, Verkleij A, Mummery C, Passier R. CHAP is a newly identified Z-disc protein essential for heart and skeletal muscle function. *J Cell Sci* 2010 April 1;123(Pt 7):1141-50.

(2) Ching YH, Ghosh TK, Cross SJ, Packham EA, Honeyman L, Loughna S, Robinson TE, Dearlove AM, Ribas G, Bonser AJ, Thomas NR, Scotter AJ, Caves LS, Tyrrell GP, Newbury-Ecob RA, Munnich A, Bonnet D, Brook JD. Mutation in myosin heavy chain 6 causes atrial septal defect. *Nat Genet* 2005 April;37(4):423-8.

(3) Matsson H, Eason J, Bookwalter CS, Klar J, Gustavsson P, Sunnegardh J, Enell H, Jonzon A, Vikkula M, Gutierrez I, Granados-Riveron J, Pope M, Bu'Lock F, Cox J, Robinson TE, Song F, Brook DJ, Marston S, Trybus KM, Dahl N. Alpha-cardiac actin mutations produce atrial septal defects. *Hum Mol Genet* 2008 January 15;17(2):256-65.

(4) Poueymirou WT, Auerbach W, Frendewey D, Hickey JF, Escaravage JM, Esau L, Dore AT, Stevens S, Adams NC, Dominguez MG, Gale NW, Yancopoulos GD, DeChiara TM, Valenzuela DM. F0 generation mice fully derived from gene-targeted embryonic stem cells allowing immediate phenotypic analyses. *Nat Biotechnol* 2007 January;25(1):91-9.

(5) Kathiriya IS, Srivastava D. Left-right asymmetry and cardiac looping: implications for cardiac development and congenital heart disease. *Am J Med Genet* 2000;97(4):271-9.

(6) Molkentin JD, Lu JR, Antos CL, Markham B, Richardson J, Robbins J, Grant SR, Olson EN. A calcineurin-dependent transcriptional pathway for cardiac hypertrophy. *Cell* 1998 April 17;93(2):215-28.

(7) Kos R, Tucker RP, Hall R, Duong TD, Erickson CA. Methods for introducing morpholinos into the chicken embryo. *Dev Dyn* 2003 March;226(3):470-7.

(8) Voiculescu O, Papanayotou C, Stern CD. Spatially and temporally controlled electroporation of early chick embryos. *Nat Protoc* 2008;3(3):419-26.

(9) Pekarik V, Bourikas D, Miglino N, Joset P, Preiswerk S, Stoeckli ET. Screening for gene function in chicken embryo using RNAi and electroporation. *Nat Biotechnol* 2003 January;21(1):93-6.

(10) Dai F, Yusuf F, Farjah GH, Brand-Saberi B. RNAi-induced targeted silencing of developmental control genes during chicken embryogenesis. *Dev Biol* 2005 September 1;285(1):80-90.

(11) Nakamura H, Katahira T, Sato T, Watanabe Y, Funahashi J. Gain- and loss-of-function in chick embryos by electroporation. *Mech Dev* 2004 September;121(9):1137-43.

# Chapter 4

## Z-disc protein CHAPb induces cardiomyopathy and diastolic dysfunction

Willemijn van Eldik, Abdelaziz Beqqali, Brigit den Adel, Jantine Monshouwer-Kloots, Daniela Salvatori, Saskia Maas, Nicky Boontje, Jolanda van der Velden, Paul Steendijk, Christine Mummery and Robert Passier

# Abstract

Cytoskeletal Heart-enriched Actin-associated Protein (CHAP) is a recently discovered Z-disc protein, which we found to be important for cardiac development. Here we studied the function of its two isoforms, resulting from alternative splicing of the *Chap* gene, in adult mouse hearts.

To determine the function of the "adult" CHAPa and "fetal" CHAPb isoforms through transgenic (Tg) overexpression specifically in mouse heart.

Two CHAPa and three CHAPb Tg founder lines were generated in which CHAP was driven by the myosin heavy chain (MHC) promoter. CHAPa Tg mice displayed normal cardiac function and phenotype, whereas CHAPb Tg mice showed mild cardiac hypertrophy, interstitial fibrosis and enlargement of the left atrium at 3 months of age, which was more pronounced by 6 months. Morphological cardiac hypertrophy and fibrosis were confirmed by evidence of activation of the hypertrophic gene program (*Nppa, Nppb, Myh7*) and increased expression of several collagens, respectively. Connexin40 and 43 were also downregulated in the left atrium, which was associated with delayed atrial conduction. CHAPb Tg hearts displayed both systolic and diastolic dysfunction partly caused by impaired sarcomere function evident from a reduced force generating capacity of single cardiomyocytes. Impaired cardiac function of CHAPb Tg mice coincided with activation of the actin-signaling pathway leading to the formation of stress fibers.

This study demonstrated that the fetal isoform CHAPb can initiate progression towards cardiac hypertrophy, which is accompanied by delayed atrial conduction and diastolic dysfunction. CHAP may thus be a novel candidate gene for familial cardiomyopathy.

# Introduction

Cardiac hypertrophy is an important determinant of cardiac disease. In pathological cardiac hypertrophy the increase in heart size is initially a compensatory mechanism, which eventually leads to impaired cardiac function and progression to heart failure[1-3]. Cardiac hypertrophy has various causes, which include responses to local environmental changes, such as myocardial infarction, pressure or volume overload and valvular defects, or by an intrinsic genetic defect that affects the cardiomyocyte directly and is referred to as familial hypertrophic and dilated cardiomyopathy (HCM and DCM, respectively). Besides cardiac hypertrophy, familial cardiomyopathy is also characterized by systolic and/or diastolic dysfunction, myofibrillar disarray and interstitial fibrosis. Several mutations in a relatively small group of genes have been associated with HCM and DCM. Whereas in HCM mutations predominantly interfere with proteins that are crucial for force generation, in DCM mutations affect proteins that play a role in force transmission from the sarcomere to the cytoskeleton[4]. Despite the increase in genetic associations with familial cardiomyopathies, our understanding of molecular regulation and signal pathways involved in familial cardiomyopathy (FCM) is still limited.

Recently, we discovered a novel protein that we called Cytoskeletal Heart-enriched Actin-associated Protein (CHAP)[5, 6], which is predominantly expressed in mouse striated muscle and localized at the Z-disc of sarcomeres. CHAP interacts with other Z-disc proteins, including α-actinin-2, the major component of the Z-disc[6]. Two CHAP isoforms have been identified as a result of alternative splicing: CHAPa, expressed in adult mouse striated muscles, is the longer isoform, containing an N-terminal PDZ and a nuclear localization signal (NLS), whilst CHAPb is shorter and lacks the PDZ domain. CHAPb is predominantly expressed during early cardiac and skeletal muscle development and is downregulated in adult mouse tissues. Interestingly, we observed a perinatal switch in splice variant expression from the fetal CHAPb to the adult CHAPa isoform[6]. Zebrafish and chick orthologues of CHAP, both of which only express the CHAPa isoform, are present in the heart during embryonic development from the cardiac crescent stage onwards, but at later stages can be detected in somites and smooth muscle cells[7]. Morpholino-mediated knockdown of *chap* in the zebrafish resulted in impaired heart looping, cardiac oedema, decreased cardiac contractility and impaired skeletal muscle formation, demonstrating the importance of *chap* during muscle development [6, 7].

CHAP displays highest homology to myopodin and synaptopodin. Whilst synaptopodin is expressed in the brain and kidney, myopodin, like CHAP, is expressed in skeletal muscle, smooth muscle and heart[8, 9]. Both synaptopodin and myopodin bind to α-actinin and are involved in actin signalling. Synaptopodin induces filamentous actin (F-actin) formation via α-actinin in an isoform dependent manner in neurons and kidney podocytes[9]. In podocytes, stress fiber formation by synaptopodin is regulated by preventing proteasomal breakdown of RhoA[10]. Myopodin on the other hand, is localized at the Z-disc through binding to α-actinin; its phosphorylation leads to detachment from the Z-disc and subsequent translocation to the nucleus[11], suggesting a role in molecular regulation by converting signaling pathways to downstream nuclear events.

Here, we demonstrate that CHAP initiates hypertrophic cardiomyopathy in transgenic mice if, specifically over-expressed in the heart. This was specific for CHAPb since the hearts of CHAPa Tg mice appeared normal up to one year of age. CHAPb Tg mice developed cardiac hypertrophy, fibrosis, left atrial enlargement as well as delayed atrial conduction, cardiac diastolic dysfunction and impaired calcium handling. Furthermore, activation of actin

signaling in these transgenic mice led to the formation of stress fibers. Together the results indicate that the fetal isoform CHAPb may be a novel candidate gene for cardiac hypertrophy and familial cardiomyopathies.

# Material and methods

*Generation of CHAP Tg mice*
Full length cDNA of mouse CHAPa or b cDNA, preceded by a N-terminal Flag and Kozak consensus sequence, was fused to the heart-specific murine α-myosin heavy chain (α-MHC) promoter. At the 3'end of CHAP a poly-A-signal of the human growth hormone (hGH) was included. Plasmid DNA was linearized by digestion with NotI, gel purified and dialyzed against Tris-EDTA (TE) buffer. DNA was injected into pronuclei from mice with a C57BL/6-CBA background. Transgenic (Tg) founder mice were crossed back (5 generations) to C57BL/6 mice to obtain a pure background. For genotyping genomic DNA was isolated from mice tail biopsies and analysed by PCR with a forward primer recognizing the C-terminus of CHAP (5'-TGGTGAAACCCCGTCTCTAC-3') and a reverse primer recognizing the hGH polyA signal (5'-CAGATTTTCCACTCCTGCAC-3'). All animal experiments were performed according to the regulations of the Leiden University Medical Center.

*Protein isolation and western blot analysis*
CHAP Tg mice and wild type littermates were sacrificed by cervical dislocation. Hearts were harvested, rinsed in PBS, snap frozen in liquid nitrogen and stored at -80°C until further use. Hearts were homogenized using an ultra-turrax tissue separator (IKA, Germany) in T-PER tissue protein extraction reagent (Pierce) with extra added protein inhibitors (protease inhibitor cocktail tablets (10 μg/ml; Roche, Germany), 0.1 mmol/L dithiothreitol (DTT; Invitrogen) and 1 mmol/L phenylmethanesulfonylfluoride (PMSF; Sigma Aldrich), 5 mmol/L NaF and 1 mmol/L $Na_3VO_4$). Samples were incubated on ice for 15 minutes and centrifuged at 10.000 RPM at 4°C for 10 minutes and supernatants were transferred to new tubes. Protein concentration was determined by the Bradford assay (BioRad) using bovine serum albumin as a standard. Proteins (50μg/lane) were separated by SDS-page gel electrophoresis and subsequently blotted using Hybond-P membranes (GE Healthcare) 3 hours at RT. Incubation with the following antibodies was performed overnight at 4°C in 5% milk/TBS-Tween (unless stated else): CHAP (1:200, custom made by Eurogentec MW CHAPa=140 kDa, MW CHAPb=110 kDa), actin (1:1000; Millipore BV, MW=43 kDa), RhoA (1:200, 26C4, Santa Cruz, MW=24 kDa), alpha-actinin (1:800, EA-53, Sigma-Aldrich Chemie, MW=100 kDa), Ezrin/Moesin/Radixin (1:1000 in 5% BSA/TBS-Tween, Cell Signaling Technology MW moesin=75 kDa, MW Ezrin and Radixin=80 kDa), Cofilin (1:1000 in 5% BSA/TBS-Tween, Cell Signaling Technology, MW=19 kDa), SRF (1:200, G20, Santa Cruz, MW=40-67 kDa), Myocyte Enhancer Factor 2 (MEF2, 1:200, C21, Santa Cruz, MW=40-65 kDa) and GAPDH (1:10000, 6C5, Millipore, MW=38 kDa). Peroxidase-conjugated antibodies used were anti-mouse IgG HRP linked antibody (1:1000, Cell Signaling Technology) and anti-rabbit HRP linked antibody (1:2000, Cell Signaling Technology). For the detection of protein bands SuperSignal West Pico Chemiluminescent Substrate (Pierce) was (the substrate) used.

*Southern blot analysis*
Genomic DNA of wild-type and CHAPb Tg mouse tails was extracted by adding 0.5 ml tail lysisbuffer (50 mM Tris pH 8.0, 100 mM EDTA pH 8.0, 100mM NaCl, 1% SDS and 10 mg/ml prot K) at 55 °C overnight. DNA was precipitated by phenol-chloroform extraction and 10 μg DNA was digested by adding BamHI (Promega) or XmnI (New England Biolabs) overnight and run on a 1% v/w agarose gel. Probes were generated using the following primers: 5'-

AGGGGTCCAGCTCTTTGAAC-3' and 5'-AGGCTTAAAGCGTCCTCCTC-3'. The PCR products were then radioactively labelled using α-[p32]dATP (PerkinElmer) by random priming (RadPrime, Invitrogen). DNA blots (Hybond-N+, GE Healthcare) were hybridized with the radioactive probe in ExpressHyb Hybridization buffer (Clontech) and visualized by using a Phosphorimager.

*RNA isolation and quantitative PCR*

Transgenic and wild-type hearts were homogenized in TRIzol (Invitrogen) using an ultra-turrax tissue separator (IKA, Germany) and RNA was isolated according to the supplier's protocol. RNA was treated with DNase (DNA-free, Ambion) and cDNA was made with the iScript kit (BioRad). qPCR was performed using the CFX96 Real-Time PCR detection system (Bio-Rad). Primers used are listed in supplemental table 1. Data were analyzed with Bio-Rad CFX Manager.

**Table 1: list of qPCR primers usesd**

| ***Gene name*** | ***Sequence*** | ***Melting temp. (°C)*** | Remarks |
|---|---|---|---|
| *ChapA* | 5'-GAGGAGGTGCAGGTCACATT-3'<br>5'-CTGAAGAGCCTGGGAAACAG-3' | 58 | |
| *ChapB* | 5'-CCGCCGCTTCTTAAACATAA-3<br>5'-GGCTTTAAAGGGCCTTGG-3' | 58 | endogenous |
| *ChapB* | 5'- CCAAGCCAGCTGTGACAAA -3'<br>5'- CCGCCGCTTCTTAAACATAA -3' | 58 | Endogenous + transgenic |
| *Connexin40* | 5'- CTGGCTCACTGTCCTGTTCA -3'<br>5'- GCAACCAGGCTGAATGGTAT -3' | 60 | |
| *Connexin43* | 5'- TGGACAAGGTCCAAGCCTAC -3'<br>5'- ACAGCGAAAGGCAGACTGTT -3' | 60 | |
| *Connexin45* | 5'- AAGAGCAGAGCCAACCAAAA -3'<br>5'- CCCACCTCAAACACAGTCCT -3' | 60 | |
| *CollagenI* | 5'- GAGCGGAGAGTACTGGATCG -3'<br>5'- GTTCGGGCTGATGTACCAGT -3' | 60 | |
| *CollagenIII* | 5'- ACCAAAAGGTGATGCTGGAC-3'<br>5'- GACCTCGTGCTCCAGTTAGC -3' | 60 | |
| *Nppa* | 5'- GGGGGTAGGATTGACAGGAT -3'<br>5'- CAGAATCGACTGCCTTTTCC -3' | 60 | |
| *Nppb* | 5'- ACAAGATAGACCGGATCGGA -3'<br>5'- ACCCAGGCAGAGTCAGAAAC -3' | 60 | |
| *Myh7* | 5'- GAGCCTTGGATTCTCAAACG -3'<br>5'- CTTGCTACCCTCAGGTGGCT -3' | 60 | |
| *Serca2* | 5'- TACTGACCCTGTCCCTGACC -3'<br>5'- CACCACCACTCCCATAGCTT -3' | 60 | |
| *GAPDH* | 5'-GTTTGTGATGGGTGTGAACCAC-3'<br>5'- CTGGTCCTCAGTGTAGCCCAA -3' | 58 | Reference gene |
| *H2A* | 5'-GTCGTGGCAAGCAAGGAG-3'<br>5'- GATCTCGGCCGTTAGGTACTC -3' | 60 | Reference gene |
| *PGK* | 5'-TGAGAAAGGAAGTGAGCTGTAAA-3'<br>5'-AGATTGCCATGCTGAGTC -3' | 52 | Reference gene |

*Transmission Electron Microscopy (TEM)*
Hearts of CHAPb Tg mice and wild type littermates were collected and left ventricles were used for TEM. Tissues were cut into smaller pieces (1 $mm^3$). For electron microscopy samples were fixed in glutaraldehyde (2.5%) in 0.1 mol/L phosphate buffer for 24 hours, post fixed in 1% $Os0_4$ in 0.1 mol/L cacodylate buffer for 1 hour at 4°C, dehydrated in a graded ethanol series and embedded in an epoxy resin. Ultrathin sections were post stained with uranyl acetate and lead citrate and viewed and imaged with a FEI Tecnai 12 transmission electron microscope, operated at 120 kV and equipped with an Eagle 4kx4k camera (FEI, Eindhoven, The Netherlands)

*Immunohistochemistry*
For histological and immunohistochemical analysis hearts were obtained at different time points (1, 3 and 6 months). Mice were sedated by injection of a mixture of 100 µl ketamine, 50 µl rompun and 10 µl atropine in 1ml 0.9% NaCl.
For paraffin sections mice were perfused with 0.9% NaCl and subsequently with 4% paraformaldehyde (PFA). Hearts and other organs (lungs, kidney and liver) were dissected, fixed over night in 4% PFA, dehydrated by ethanol-xylene series and embedded in paraffin. Serial heart sections (5 µm) were made, mounted on starfrost slides (Knittel) and followed by heamatoxilin-eosin (HE) staining, Sirius red staining, and immunohistochemistry as indicated. For all antibody stainings, except Myosin Light Chain 2a (MLC2a), microwave antigen retrieval in citrate buffer (pH 6) was applied. Endogenous peroxidase was blocked by incubating the slides in 0.3% $H_2O_2$ in PBS. Sections were incubated overnight at room temperature with Connexin40 antibody (1:100; Santa Cruz), Connexin43 (1:500; Zymed), MLC2a (1:4000 gift from S. Kubalak) and Troponin I (TnI, 1:800; Santa Cruz). Secondary antibody used was biotin-labeled goat anti-rabbit (Vector Labs) or biotin-labeled horse anti-goat (Vector Labs). Subsequently, the sections were incubated with Vectastain ABC staining kit (Vector Labs) for 45 min. Slides were rinsed in PBS and Tris/Maleate (pH 7.6). 3-3'-diaminobenzidine tetrahydrochloride (DAB, Sigma-Aldrich Chemie) was used as chromogen and Mayer's heamatoxylin as counterstaining. Finally, slides were dehydrated and mounted with Entellan (Merck).
For cryosections mice were perfused with 0.9% NaCl only, then hearts were isolated. Processing of hearts for cryosections was adapted from Bajanca et al.[12]. In brief hearts were fixed in 0.2% PFA solution containing 4% sucrose, 0.12 mmol/L $CaCl_2.2H_2O$, 0.2 mol/L $Na_2HPO_4.2H_2O$, 0.2 mol/L $NaH_2PO_4.H_2O$ over night at 4°C. Thereafter, hearts were washed in the same solution without PFA during the day at 4°C followed by a solution containing 0.24 mol/L phosphate buffer and 30% sucrose over night at 4°C. The next day hearts were embedded in Tissue-Tek (Sakura) on dry ice and stored at -20°C until sectioning. Serial sections (5 µm) were made and mounted on starfrost slides (Knittel) and antibody staining was performed as previously described[13]. Antibodies used were CHAP (1:50), myomesin (1:50 E. Elher), α-actinin (Sigma Aldrich), RhoA (1:100, 26C4, Santa Cruz) and pERM (1:50, Cell Signaling Technology). Secondary antibodies used are Cy-3 conjugated anti-mouse (1:250, Jackson Immunoresearch Laboratories) and Alexa488 conjugated anti-rabbit (1:200, Invitrogen). Cell nuclei were counterstained with DAPI (Molecular Probes). Stainings were analyzed with SP5 confocal microscope (Leica).

*Volume measurements*
The volume of the atria and ventricle was estimated by the Cavalieri principle. For this serial sections were stained for an atrial marker, MLC2a, or TnI to identify the ventricle. Then a grid was used to estimate the surface of the stained section and the distance between the sections was used to estimate the volume.

*Magnetic Resonance Imaging (MRI)*
For MRI measurements 4 wild type and 5 CHAPb transgenic mice of 6 months of age were used. Animals were sedated by 4% isofluran and MRI images were produced as described below.
Hardware
All experiments were performed on a vertical 9.4T magnet (Bruker, Ettlingen, Germany) supplied with an actively shielded Micro2.5 gradient system of 1T/m and a 30 mm transmit/receive birdcage RF coil, using Para vision 4.0 software.
MRI protocols
*In vivo*:
At the start of each examination, several 2D FLASH scout images were recorded in the transverse and axial plane of the heart to determine the orientation of the heart
A modified FLASH sequence with a navigator echo (IntraAngio) was used for retrospective CINE MRI with the following parameters:
Short-axis (oriented roughly perpendicular to the septum) and long-axis (oriented through the apex and aortic valve) cardiac cine MRI images with the navigator positioned through the aortic arch were acquired with the following parameters: hermite-shaped RF pulse 1 ms; FA 10°; 200 avarages, TR 68.1 ms; TE 1.86 ms; reconstruction of 18 cardiac frames; FOV 2.56*2.56 cm2; matrix 192*192; in-plane resolution 133 μm, slice thickness 1.0 mm; total acquisition time approximately 30 min.

Heart function was assessed using MASS for Mice 5.1 software package (Leiden, The Netherlands) by manual delineation of LV and RV borders.
Based on these segmented areas, LV and RV area, end-diastolic volume (EDV), end-systolic volume (ESV), LV stroke volume (SV), and LV ejection fraction were computed automatically.

*Electrocardiogram (ECG) measurements*
ECG measurements on wild type and CHAPb Tg mice of 6 months of age were performed as described in Henkens et al.[14]. In brief animals were sedated by 4% isofluran and ECG measurements were recorded for at least one minute. The data were analysed with the program LEADS and heart rate, PR duration and P duration were calculated.

*Sarcomere measurements*
Hearts of CHAPb Tg mice and wild type litter mates were isolated at different time points (1 month and 3 months) and snap frozen in liquid nitrogen. Single cardiomyocytes were obtained by grinding hearts in liquid nitrogen. Cardiomyocytes were defrosted in relaxing solution (pH 7.0; 1 mmol/L free $Mg^{2+}$ 1, 145 mmol/L KCl, 2 mmol/L EGTA, 4 mmol/L ATP, 10 mmol/L imidazole). Then cardiomyocytes were treated with relaxing solution containing 1% Triton-x-100 for 5 minutes, to remove the membranes. Cardiomyocytes were washed twice in relaxing solution to remove Triton-X-100. Single cardiomyocytes were placed between a force

tranducer and piezoelectric motor. Isometric force measurements were performed at 15°C and a sarcomere length, measured in relaxing solution, of 2.2 µm. The calcium concentrations of relaxing and activation solution (pH 7.1) were $10^{-3}$ and 30 µmol/L, respectively. Solutions with intermediate free [$Ca^{2+}$] were obtained mixing relaxing and activation solution. The first control activation was performed at maximum [$Ca^{2+}$] and thereafter, the resting sarcomere length was set to 2.2 µm again. The second control measurement was performed to calculate the maximum isometric tension (force divided by cross-sectional area). The next measurements (4-5) were performed in submaximal [$Ca^{2+}$], followed by a control measurement. Force values obtained from submaximal [$Ca^{2+}$] were normalized to control values.

*Protein phosphorylation*

Protein phosphorylation of sarcomeric proteins was measured in hearts of CHAPb Tg and wild type litter mates at 3 months of age. A detailed description of the procedure can be found in R. Zaremba et al.[15]. Briefly, samples were separated by SDS-page gels. Subsequently, gels were stained by SYPRO Ruby stain or Pro-Q Diamond Phosphoprotein Stain.

*Statistical analysis*

Data were analysed with GraphPad Prism. All data are expressed as mean + the standard error of the mean (SEM). Statistical analysis was performed using Student's unpaired t-test. $P < 0.05$ was considered to be statistically different.

# Results

*Ectopic CHAP expression in transgenic mice*

Many genes expressed during heart development, but not in the adult, are re-expressed in cardiac pathology. We previously identified CHAP as such a developmentally regulated and functional cardiac gene and here investigated whether it also has a role in the adult heart. For this purpose we generated transgenic mice that expressed either the CHAPa or CHAPb isoform in the heart using a construct under control of the cardiac-specific α-myosin heavy chain (MHC) promoter and proceeded by an N-terminal FLAG-tag (Figure 1A). DNA vector

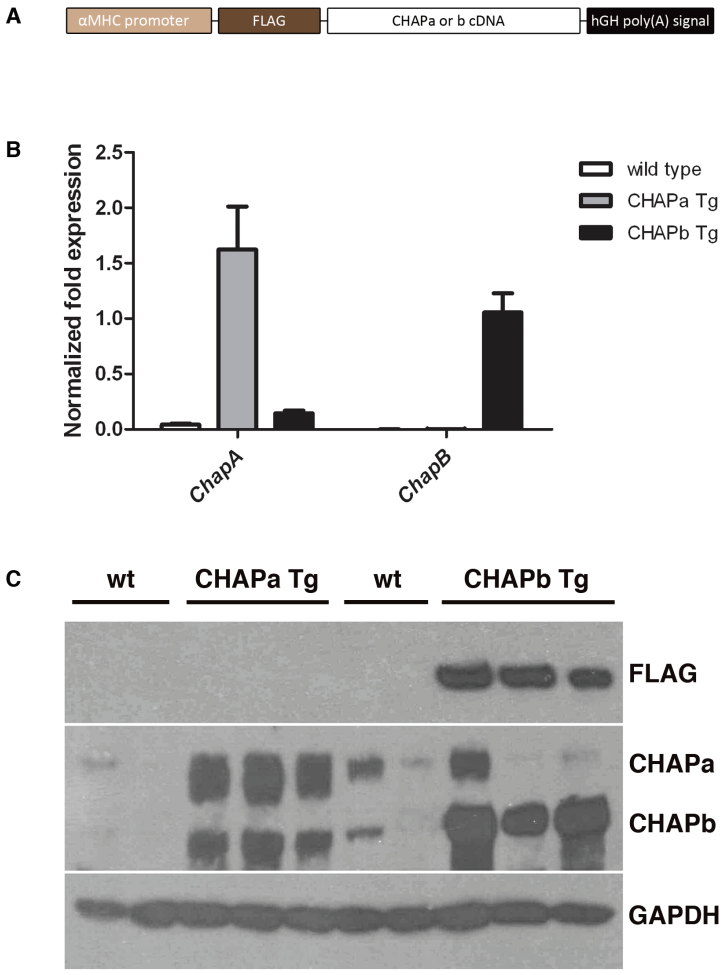


**Figure 1: Expression analysis of CHAPa- and b Tg founders. A) Schematic overview showing the construct used to generate transgenic mice. FLAG-CHAPa- or b cDNA is downstream of the α-MHC promoter and upstream a human Growth Hormone polyA signal. B) qPCR analysis of *ChapA* and *ChapB* in wt (white bars, n=6), CHAPa Tg (gray bars, n=4) and CHAPb Tg hearts (black bars, n=3). GAPDH was used as internal control. C) Western blot showing CHAP and flag expression in two wt and CHAPa Tg and two wt and CHAPb Tg hearts. GAPDH was used as loading control.**

constructs were linearized and injected into C57BL/6-CBA zygotes. This resulted in two CHAPa transgenic (Tg) founders among 29 animals and three CHAPb Tg founders among 30 animals. First, we analysed the mRNA expression of *ChapA* and *ChapB* in the hearts of the offspring of the different transgenic lines. The two CHAPa Tg lines had comparable expression of *ChapA*. Analysis of *ChapA* mRNA in hearts of CHAPa Tg hearts by qPCR showed an expected upregulation (40-fold) compared to wild type (wt) mice (Figure 1B). Next, we analyzed the expression of CHAPa protein using an antibody that recognizes both CHAP isoforms. In wild type hearts, faint expression of CHAPa (140 kDa) was detected, whereas in CHAPa Tg mice strong expression of CHAPa could be detected. However, surprisingly, when using the anti-FLAG antibody no expression was observed. This could indicate that CHAPa was partially degraded or folded incorrectly at the site of the FLAG-epitope (Figure 1C). Histological analysis of CHAPa Tg hearts did not show any abnormalities at one and three months of age. Similarly, at one year of age no differences between wild type hearts and CHAPa Tg hearts was detected.
The three CHAPb Tg lines showed different copy number levels as determined by Southern blot (supplemental figure 1A). Analysis of hearts of the CHAPb Tg mouse line with intermediate copy numbers by qPCR demonstrated upregulation of *ChapB* compared to wt mice (Figure 1B). Western blot analysis of CHAPb Tg hearts showed a clear increase in CHAPb protein levels (110 kDa), when compared to wt hearts. This was confirmed by the presence of anti-FLAG immunoreactivity in the Tg hearts only (Figure 1C).

*Analysis of CHAPb Tg founder phenotype*
Southern blot analysis of founders showed high CHAPb copy number in transgenic line 29 and intermediate CHAPb copy number in line 14 compared to endogenous genomic levels of CHAP (supplemental figure 1A). CHAPb Tg founders died from around 6 months of age and onwards. The highest CHAPb expressing founder (CHAPb Tg line 29) died after 7 months, without progeny. Histological analysis of the heart of this founder is shown in supplemental figure 1B-D, left panels. Progeny of the CHAPb Tg line 14 died spontaneously at the earliest time point of approximately 6 months (supplemental figure 1B-D, right panels). Hearts of both transgenic lines (14 and 29) displayed comparable phenotypes with enlargement of left and right atrium (supplemental figure 1B,C). Histological analysis revealed that the left atrium was filled with a chronic and organized thrombus. Furthermore, thickness of the septum, left and right ventricle wall was increased, suggesting cardiac hypertrophy (supplemental figure 1B). This was confirmed by enlargement and apparent hypertrophy of cardiomyocytes on histological sections at higher magnifications (supplemental figure 1D).

*Overexpression of fetal isoform CHAPb in adult hearts leads to cardiac hypertrophy*
We analyzed CHAPb Tg mice at one, three and six months of age. At one month, heart of wt and CHAPb Tg mice were indistinguishable (supplemental figure 2A-C). At 3 months of age the left atrium of CHAPb Tg hearts was enlarged but without any signs of thrombus formation (figure 2A). Tg hearts showed obvious cardiomyocyte hypertrophy with enlarged nuclei (figure 2B) and interstitial fibrosis, as indicated by Sirius Red staining (figure 2C). To determine the extent of cardiac hypertrophy, we measured atrial and ventricular volume at one and three months of age. Myosin Light Chain 2a (MLC2a) and Troponin I (TnI) staining were used to identify the atria and ventricle, respectively. As expected, the myocardial volume of the left and right atrium at one month of age was similar in wt and CHAPb Tg mice

(supplemental figure 2D and E) but at 3 months, the left atrial volume of CHAPb Tg mice was significantly greater than in wt (wt 2.046 ± 0.1346 n=4 $mm^3$, CHAPb Tg 4.598 $mm^3$ ± 0.3853 n=4, p< 0.01; figure 2E) although the volumes of the right atria were similar (wt 2.041 $mm^3$ ± 0.2431 n=4, CHAPb Tg 2.114 $mm^3$ ± 0.03001 n=4, p=NS). Furthermore, despite the hypertrophy evident in individual cardiomyocytes of the left ventricle, the overall ventricular wall volume was not different in CHAPb Tg mice (wt 57.81 $mm^3$ ± 6.352 n=4, CHAPb Tg 51.31 $mm^3$ ± 2.705 n=4, p=NS).

By 6 months of age, left atrial enlargement was consistently more pronounced in Tg mice and was associated with cardiomyocyte hypertrophy and interstitial fibrosis (Figure 2B, C). Occasionally, intraventricular thrombi were identified (Figure 2D). In general, changes in CHAPb Tg hearts were more pronounced at 6 months of age, displaying features that resemble cardiomyopathy, including sudden death.

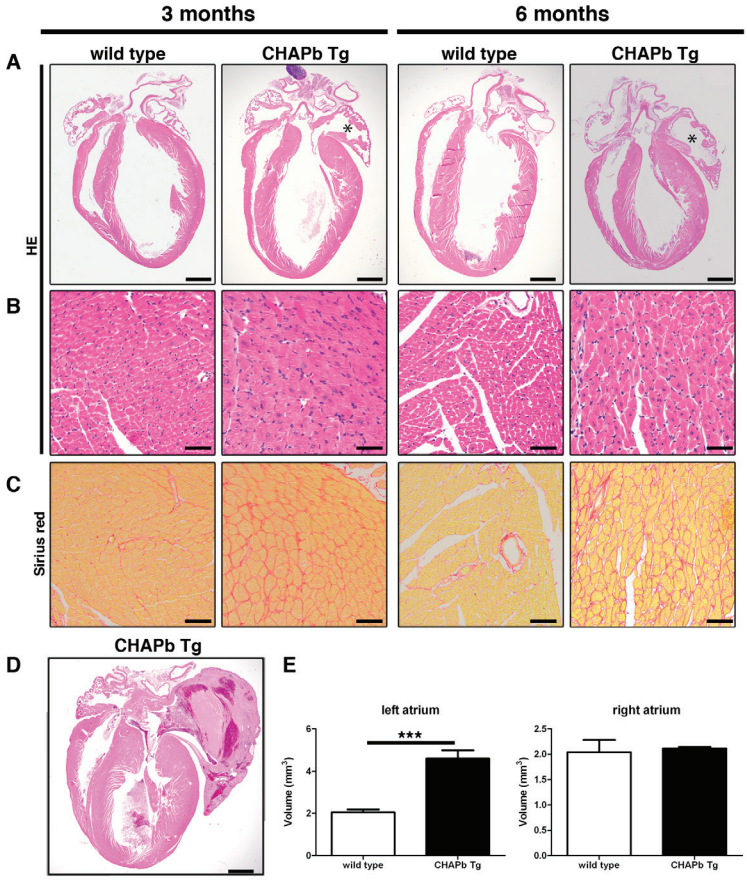


Figure 2: HE and Sirius red staining of CHAP Tg hearts. Wt (left panels) and CHAPb Tg (right panels) at 3 and 6 months of age (A-C). A) HE stained overview section. The left atrium in CHAPb Tg hearts is enlarged (indicated by *) compared to wt litter mates. B) Higher magnification of left ventricle. In the left ventricle of CHAPb Tg hearts the cardiomyocytes are hypertrophic. C) Sirius red staining of the left ventricle showing increase in interstitial fibrosis in CHAPb Tg. D) CHAPb Tg heart with severe phenotype showing pronounced atrial enlargement, filled by a thrombus and thickening of the ventricles. E) Myocardial volume of the left atrium (left panels) and right atrium (right panels) in wt (white bars) and CHAPb Tg (black bars) hearts at 3 months of age. Scale bars 1 mm in A and D, 50 µm in B, C.

*Activation of hypertrophic gene program and collagens in CHAPb Tg hearts*

A hallmark of hypertrophy is re-expression of fetal cardiac genes, such as atrial natriuretic factor (ANF, *Nppa*), brain natriuretic peptide (BNP, *Nppb*) and β-MHC (*Myh7*). To investigate if the hypertrophy induced by CHAPb in Tg mice was also accompanied with upregulation of these genes, we isolated RNA from left ventricles of 6 month old wt (n=3) and CHAPb Tg (n=3) mice. qPCR analysis showed significant upregulation of *Nppa* (17.2x, p<0.01, Figure 3A), *Nppb* (3.6x, p<0.01, Figure 3B) and *Myh7* (28.3x, p= 0.0634, Figure 3C) in Tg hearts. Activation of the same genes was also evident in the right ventricle (data not shown). These findings corroborate the hypertrophic response observed morphologically.

Fibrosis is characterized by increased collagen production. To confirm Sirius red evidence, we analyzed the expression of *Collagen I* and *III,* the major fibrin forming collagen types, in the left ventricles of wt and CHAPb Tg mice. Increased expression of *Collagen I* (3.2x, p=0.0506, Figure 3D) and *III* (3.7x, p=0.0404, Figure 3E) was indeed observed in CHAPb Tg animals, as expected. Moreover, mRNA expression of *Serca2*, which encodes a protein involved in $Ca^{2+}$ cycling[16] and is generally downregulated in cardiac hypertrophy, was also decreased in CHAPb Tg hearts (Figure 3F). Expression of hypertrophic genes and collagens was also increased in the right ventricle (data not shown).

Finally, we examined endogenous *Chap* isoforms in CHAPb Tg mice. *ChapA* mRNA expression was the same in wt and CHAPb Tg hearts (Figure 3G) and although endogenous *ChapB* appeared slightly increased, this was not statistically significant (Figure 3I). Exogenous *ChapB* (Figure 3H) was, as expected, strongly upregulated in CHAPb Tg hearts compared to wt.

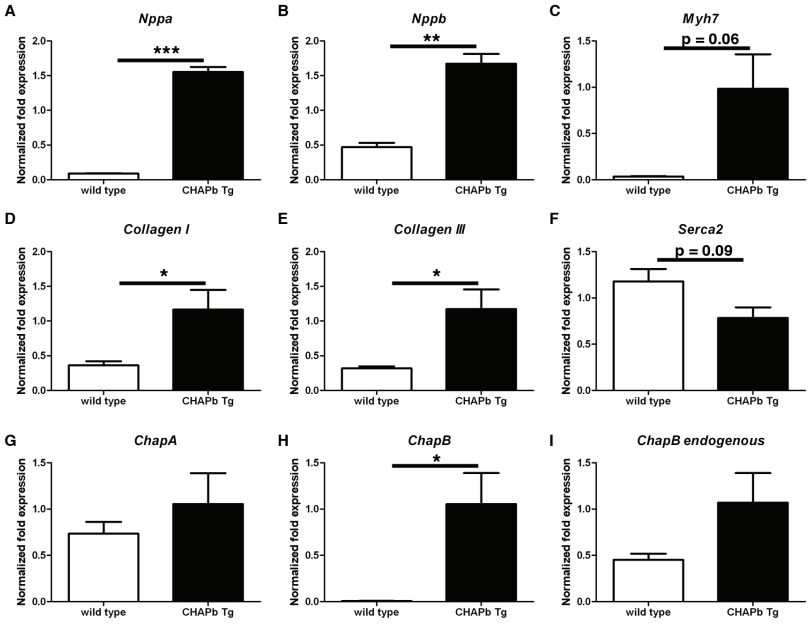


**Figure 3: Expression of hypertrophy markers and collagens in left ventricle. qPCR analysis showing mRNA expression of *Nppa* (A), *Nppb* (B), *Myh7* (C), *CollagenI* (D) *CollagenIII* (E), *Serca2* (F), *ChapA* (G), *ChapB* (H) and endogenous *ChapB* (I) in the left ventricle of wt (white bars) and CHAPb Tg (black bars) mice. *GAPDH, PGK* and *H2A* were used as internal controls.**

*Expression of CHAPb in adult heart leads to loss of Connexin expression in the left atria and conduction disturbances*

Since cardiomyopathies are associated with disturbed electrical conductance and cardiac arrhythmia, we investigated the most predominant Connexin (Cx) isoforms in atria and ventricles. Cx40 is the main isoform expressed in atria. Cx43 is expressed at higher levels in ventricles, although Cx43 it is also expressed at low levels in the atria[17]. At one month of age, there was no difference in Cx40 and Cx43 expression between wt and CHAPb Tg (supplemental figure 3A and B). At three months, however, enlargement of the left atrium was accompanied by loss of expression of Cx's: both Cx40- and Cx43 immunoreactivity was reduced in the left atrium, although in the right atrium (supplemental figure 3C and D) and ventricles they were unchanged. This decrease in Cx40 and Cx43 levels in the left atrium was more pronounced at 6 months (figure 4A). These findings were confirmed by qPCR, which indeed showed that Cx40 (-23x, $p<0.01$, figure 4B) and 43 (-6.9x, $p<0.01$, supplemental figure 3E) were both downregulated in the left atrium. Similar to the protein data, mRNA expression of Cx40 and Cx43 in the right atrium was unchanged (Figure 4C and supplemental figure 3F). Expression of Cx45, which is specifically expressed in the sinoatrial- and atrioventricular nodes and is co-expressed with other isoforms in the rest of the conduction system[17], was unchanged in the left atrium.

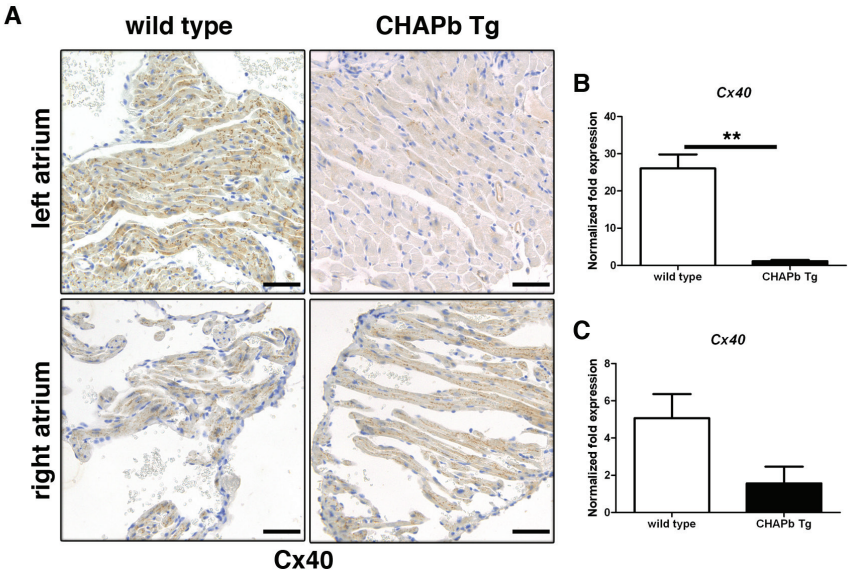


**Figure 4: Decreased Connexin 40 expression in CHAPb Tg left atrium at 6 months of age. Immunohistochemical staining showing Connexin 40 (A) expression in wt (left panels) and CHAPb Tg (right panels) left (upper panels) and right (lower panels) atria. qPCR analysis of *Connexin 40* (B and C) expression in the left (B) and right (C) atrium. Scale bars 50 µm.**

To investigate whether the loss of expression of Cx40 and 43 was correlated with conduction disturbances, we performed ECG measurements of wt and CHAPb Tg mice. These measurements showed that the PR interval was increased in CHAPb Tg mice (wt 40,89 ms ± 1,150 n=3, CHAPb Tg 49,83 ± 1,784 n=8, $p<0.05$; Figure 5A) indicating a conduction delay from atria to ventricles. No signs of atrial fibrillation were observed, as the duration of the P-top was not changed (wt 7,367 ms ± 0,9260 n=3, CHAPb Tg 6,955 ms ± 0,4934 n=8, p=ns; Figure 5B)[18].

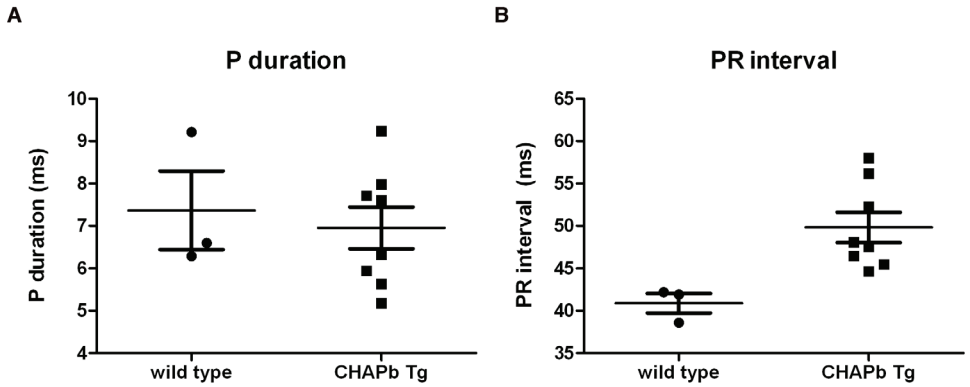


**Figure 5: Conduction disturbances in CHAPb Tg mice at 6 months of age. ECG analysis of wt and CHAPb Tg mice showing PR interval (A) and P duration (B).**

*CHAPb Tg mice show decreased cardiac performance*

To determine whether the phenotypic changes in CHAPb Tg hearts affected cardiac performance, we performed MRI measurements on 5 male wt and 5 male CHAPb Tg mice at 6 months of age. Enlargement of the left atrium was clearly visible in the scans. We then calculated the functional parameters of the left and right ventricle. The results of the left ventricle are shown in figure 6. Representative scans for wt and CHAPb Tg are shown in figure 6A. Both the end diastolic volume (wt 45.81 µl ± 2.297 n=4, CHAPb Tg 29.08 µl ± 1.176 n=5, $p<0.01$; Figure 6B) and end systolic volume (wt 15.72 µl ± 2.570 n=4, CHAPb Tg 7.474 µl ± 1.702 n=5, $p<0.05$; Figure 6C) were significantly decreased in the left ventricle, which resulted in the ejection fraction being similar in wt and CHAPb Tg mice (wt 66.26 % ± 3.972 n=4, CHAPb Tg 74.35 % ± 5.376 n=5, p=ns; Figure 6D). However, the cardiac output was significantly decreased in CHAPb Tg mice compared to wt (wt 1559 µl/min ± 32.20 n=4, CHAPb Tg 1083 µl/min ± 117.6 n=5, $p<0.01$; Figure 6E). Both the left ventricular mass of end diastole (wt 77.79 mg ± 2.572 n=4, CHAPb Tg 58.11 mg ± 5.399 n=5, $p<0.05$; Figure 6F) and end systole (wt 93.97 ± 1.784 n=4, CHAPb Tg 71.39 ± 5.127 n=5, $p<0.01$; Figure 6G) were decreased in CHAPb Tg mice. Similar data were obtained for the right ventricle (supplemental figure 4). Overall, these data show that CHAPb expression impairs diastolic and systolic function in both the left and right ventricle compared to wt mice.

*CHAPb Tg mice display decreased force generating capacity of cardiac sarcomeres*

To investigate the functional properties of cardiac sarcomeres, we measured force development at different calcium concentration in membrane-permeabilzed single cardiomyocytes (Figure 6H) from wt and CHAPb Tg sarcomeres at 1 month of age. At the highest calcium concentration (30 µmol/L) force development was decreased in CHAPb Tg cardiomyocytes (wt 50.40 $kN/m^2$ ± 4.911 n=12, CHAPb Tg 30.23 $kN/m^2$ ± 4.346 n=11, p= 0,006; figure 6I). Furthermore, sarcomere $Ca^{2+}$-sensitivity ($pCa_{50}$, the calcium concentration at which half of the maximum force was generated) was also decreased in CHAPb Tg sarcomeres compared to wt (wt 5.53 ± 0.02 n=12, CHAPb Tg 5.45 ± 0.02 n=11, p= 0,0046; figure 6J). The reduction in both maximal force and $pCa_{50}$ shows that the CHAPb sarcomeres have less force generating capacity compared to wt sarcomeres. The phosphorylation status of the sarcomeric proteins troponin I and T, myosin binding protein C and myosin light chain 2, remained unchanged

(data not shown). These results correlated with the lower cardiac output observed in CHAPb Tg mice compared to wt mice, where we found decreased diastolic function, indicating a stiffer heart.

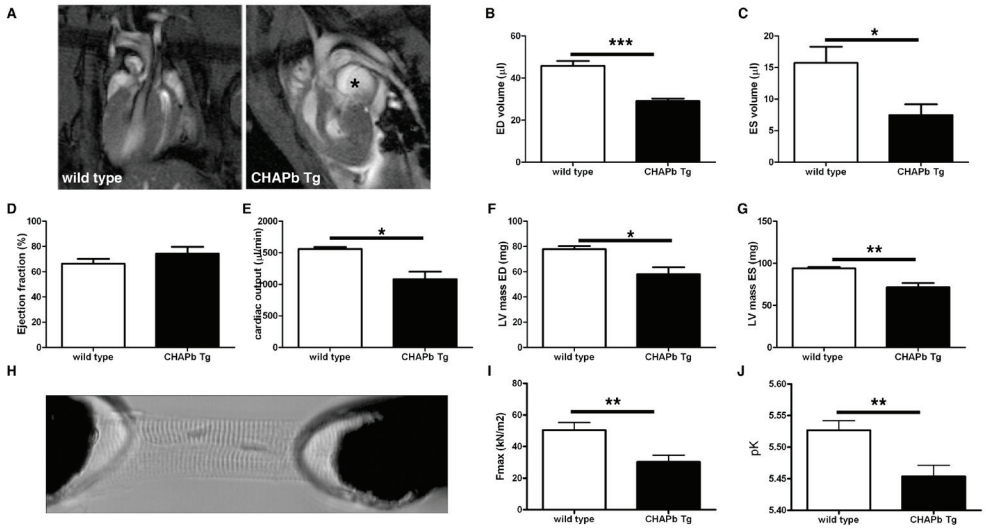


**Figure 6: Functional analysis of CHAPb Tg hearts. A) Example images of wt and CHAPb Tg longitudinal sections. Enlarged LA in CHAPb Tg is indicated with *. B-G) MRI measurements of the left ventricle of wt (white bars) and CHAPb Tg (black bars) animals at 6 months of age. ED volume (B), ES volume (C), ejection fraction (D), cardiac output (E), LV mass ED (F) and LV mass ES (G). H) Experimental setup for single membrane-permeabilized cardiomyocyte measurements to determine sarcomere function. Sarcomere force measurements at one month of age showed reductions in maximum force (I; Fmax) and $Ca^{2+}$-sensitivity (J; $pCa_{50}$) in CHAPb Tg (black bars) compared to wt (white bars) . ED (end diastolic), ES (end systolic) and LV (left ventricular).**

*Sarcomeric organization is disturbed in CHAPb Tg hearts*

Next we investigated the sarcomeric organization in cryosections of wt and CHAPb Tg hearts. Immunohistochemical staining for CHAP, α-actinin (Z-disc protein) and myomesin (M-band protein) showed that both CHAP and α-actinin were co-localized at the Z-disc of cardiomyocytes in wt hearts (Figure 7A), whereas CHAP did not overlap with myomesin (supplemental figure 5). In CHAPb Tg hearts, CHAP was also localized at the Z-disc with α-actinin (Figure 7A) and did not overlap with myomesin (supplemental figure 5). However, in the CHAPb Tg hearts, CHAP was also localized in fibers, which appeared to be perpendicular to the sarcomeres and resembled the formation of stress fibers. These fibers stained with α-actinin (Figure 7A), but not myomesin (supplemental figure 5). The formation of these stress fibers was already visible at 1 month. To study this in more detail we performed Transmission Electron Microscopy on 6 months old wt and Tg hearts. In wt hearts the organization of the sarcomeres was regular with well-formed Z-discs and intercalated discs. In CHAPb Tg hearts the sarcomeres were clearly irregular and both Z-disc and intercalated discs were disorganized (Figure 7B). These data indicate that in CHAPb Tg hearts the organization of the Z-discs and intercalated discs are disturbed.

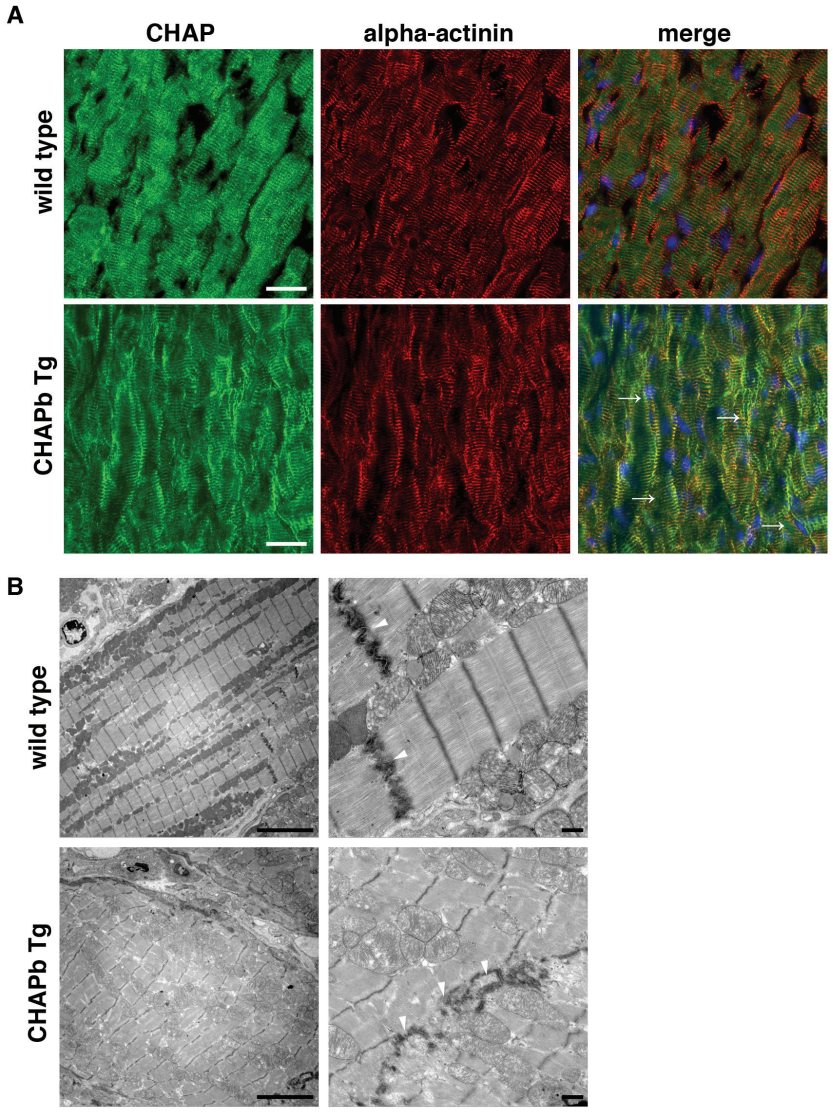


**Figure 7: Sarcomeric organization is disturbed in CHAPb Tg hearts. Hearts stained for CHAP (green) / α-actinin (red; A), merge images are shown. CHAP is localized in the Z-disc of cardiomyocytes of wt (upper panels) hearts. In cardiomyocytes of CHAPb Tg (lower panels) CHAP also stains stress fibers (arrows), which co-stain for α-actinin. B) Electron microscopy analysis of wt and CHAPb Tg hearts at 6 months of age. In CHAPb Tg the sarcomeres were irregular and Z-discs and intercalated discs (arrow heads) are disorganized. Scale bars 20 µm in A, 5 µm in left panels and right panels 1 µm of B.**

*Activation of the actin signalling pathway in CHAPb Tg hearts*

Since synaptopodin, a CHAP family member, has been associated with actin signalling in other tissues such as brain and kidney and since the actin signalling pathway is also involved in cardiac hypertrophy, we investigated whether components of the actin signalling pathway were activated in CHAPb Tg hearts. Staining of GTPase RhoA, a key component of the actin signalling pathway, in hearts at 6 months of age showed sarcomeric expression pattern in wt

hearts, while in CHAPb Tg hearts RhoA expression was increased and, interestingly, was displaced from its sarcomeric localization in cardiomyocytes (Figure 8A). To further confirm the CHAPb dependent activation of actin signalling, we examined downstream effectors. Indeed, phosphorylation of Ezrin/radixin/moesin (ERM), a family of proteins involved in Rho-dependent signalling and linking the actin cytoskeleton to the plasma membrane[19, 20], was increased in CHAPb Tg hearts and co-localized with CHAP (supplemental figure 6) and RhoA. Increased protein expression levels of RhoA, actin, α-actinin, ERM, cofilin, and downstream actin-dependent transcription factors serum response factor (SRF) and myocyte enhancer factor-2 (MEF2) in hearts of CHAPb Tg compared to wt (figure 8B) confirmed these findings. These results suggested CHAPb dependent activation of the actin-signalling pathway, from membrane to the nucleus, which may contribute to the molecular, phenotypic and functional alterations observed in the transgenic mice.

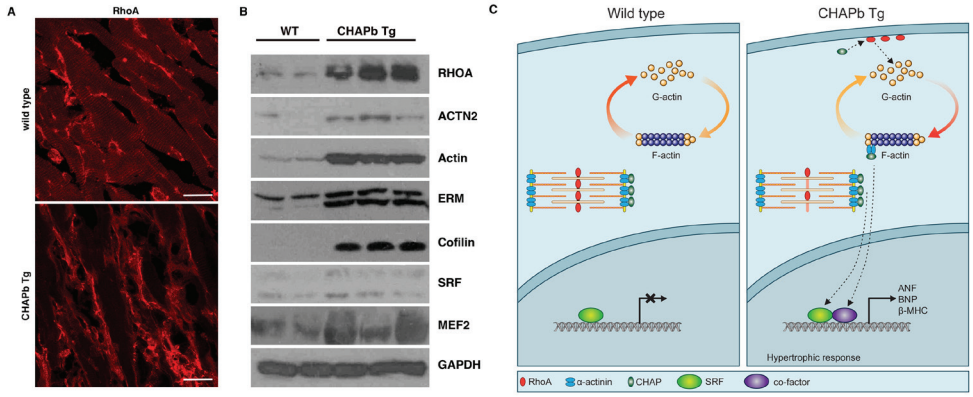


**Figure 8: Increased actin signaling in CHAPb Tg hearts. A) Wt (upper panels) and CHAPb Tg (lower panels) hearts at 6 months of age stained for RhoA (red). In wt mice RhoA is localized at the membrane of cardiomyocytes and shows a sarcomeric expression pattern. In CHAPb Tg hearts sarcomeric expression of RhoA is decreased and membrane expression is increased. B) Western blot analysis of 2 wt and 3 CHAPb Tg hearts at 6 months of age for RhoA, α-actinin, actin, Ezrin(80 kDa)/moesin(80 kDa)/radixin (75 kDa; ERM), cofilin, SRF (40 – 67kDa) and MEF2. GAPDH is used as loading control. C) Summarizing model: in wt mice CHAPa is localized at the Z-disc with α-actinin and there is no expression of CHAPb, leading to high G-actin expression resulting in low expression of SRF target genes. In CHAPb Tg mice CHAPb expression results in activation of RhoA, leading to a shift from G-actin to F-actin, binding of co-factors to SRF and activation of SRF target genes, such as ANF, BNP and β-MHC. In addition signaling of CHAPb to SRF might also be directly through binding of CHAPb and α-actinin to F-actin fibers or through the Z-disc. Scale bars: 20 μm.**

# Discussion

Here we show for the first time that the Z-disc protein CHAP can initiate cardiac disease. CHAP was initially identified as a gene upregulated during the differentiation of human embryonic stem cell-derived to cardiomyocytes [5]. In mice and human two CHAP splice variants were identified which differ in their temporal expression patterns: the shorter isoform CHAPb is expressed during embryonic development in the heart, somites and muscle precursors, whilst CHAPa is expressed in the adult heart and skeletal muscle. Morpholino knockdown of *Chap* in zebrafish showed that it is essential for heart development. Furthermore, overexpression of "embryonic" CHAPb, but not "adult" CHAPa, in rat cardiomyocytes led to dissociation of α-actinin-2 from the Z-disc[6]. In agreement with these findings, we found that overexpression of CHAPa in the adult mouse heart had no effect on cardiac morphology or function, whilst CHAPb Tg mice displayed features which are comparable to cardiomyopathy, such as cardiac hypertrophy, interstitial fibrosis, diastolic dysfunction, and disturbed electrical conductance, which led to higher mortality.

*CHAPb induces cardiac hypertrophy, left atrial enlargement and fibrosis*

CHAPb overexpression in transgenic hearts was apparent both in qPCR and Western blot analysis. This had no effect at one month of age but by 3 months, molecular and cellular hypertrophy without ventricular wall thickening, left atrial enlargement and interstitial fibrosis were clearly evident. This was more pronounced at 6 months of age and by then was occasionally accompanied by wall thickening of the left and right ventricles and septum. In agreement with increasing severity of the phenotype, CHAPb Tg mice died spontaneously from 6 months of age and onwards. Occasionally thrombi were found in the left atria, which may have disturbed blood flow in the left atrium and impaired ventricular filling. Reduced ventricular filling may eventually contribute to pulmonary venous congestion and development of pulmonary oedema. Although we did not observe pulmonary oedema overall (indicated by preserved lung weights) in CHAPb Tg mice, we cannot exclude that this occurred in individual mice. Indeed, occasionally MRI, revealed white/grey areas in lungs of CHAPb Tg mice, suggesting fluid retention.

*Impaired structural and electrical organization at intercalated discs in CHAPb Tg hearts*

In addition to the morphological and histological changes in CHAPb Tg heart, we also observed changes at the intercalated discs of cardiomyocytes. In particular, gap junction proteins Cx40 and Cx43 were clearly downregulated in the left atrium of CHAPb Tg hearts, which was already visible at 3 months of age but more pronounced at 6 months. Since gap junctions are crucial for fast spreading of action potentials between cardiomyocytes, impaired expression of gap junctions would be expected to affect electrical guidance. Indeed, decreased connexins expression in the left atrium correlated with conduction disturbances, evidenced by increased PR interval, the time required for conduction between atria and ventricles. Loss of expression of Cx40 and 43 has been associated previously with conduction disturbances in mice. In $Cx40^{-/-}$ mutant mice, various conduction disturbances have been reported, including increased PR interval[21, 22]. In $Cx43^{+/-}$ mice ventricular conduction was delayed[23], although no change in atrial conduction was observed[24]. In other hypertrophy mouse models, down-regulation of Cx's in the atria also correlated with conduction disturbances[25-27].

Although decreased expression of connexins and impaired electrical guidance in CHAP

Tg mice was limited to the atria, detailed analysis of individual cardiomyocytes by electronmicroscopy showed that there was disorganization of Z-discs and intercalated discs throughout the whole heart. Sarcomeric disorganization would suggest impaired contractility and/or relaxation of cardiac muscle, affecting cardiac function.

*CHAPb Tg mice display cardiac diastolic dysfunction*

MRI measurements indicated that CHAPb Tg mice had normal left ventricular ejection fraction. Similarly, in patients with heart failure, almost half (47%) still have a normal ejection fraction[28]. Ejection fraction is determined by differences in both end diastolic and end systolic volumes and if both parameters are changed, as occurs in CHAPb Tg mice, ejection fraction may be unaffected. The decreased diastolic volumes observed in CHAPb Tg mice may suggest impaired relaxation during diastole (diastolic dysfunction), which relates to impaired $Ca^{2+}$ cycling in cardiomyocytes. Contraction of cardiomyocytes is achieved by entry of $Ca^{2+}$ through L-type channels, which causes $Ca^{2+}$ release into the cytosol, immediately followed by $Ca^{2+}$ release from the sarcoplasmic reticulum (SR). Subsequently, $Ca^{2+}$ binds to sarcomeric protein troponin C to initiate contraction. On the other hand, relaxation occurs through uptake of the $Ca^{2+}$ into the SR via SERCA2. In CHAPb Tg cardiomyocytes, re-uptake of $Ca^{2+}$ might be affected, due to reduced levels of SERCA2[16, 29]. Indeed, we found that SERCA2 mRNA expression is reduced in the hearts of CHAPb Tg. In addition, measurements in membrane-permeabilized cardiomyocytes revealed reduced force generating capacity of CHAPb Tg sarcomeres, which may in part underlie the significant reduction in cardiac output observed in CHAPb Tg compared to wt mice. In primary cardiomyopathy, alterations in $Ca^{2+}$-sensitivity have been reported, which may depend on the location of the mutation in affected genes. Perturbations in $Ca^{2+}$-sensitivity of the sarcomeres may result in development of HCM or DCM[30]. As overexpression of CHAPb reduced $Ca^{2+}$-sensitivity, it would be interesting to investigate the role of CHAP in primary cardiomyopathy cases.

*Activated actin signalling in CHAPb Tg hearts*

We found that expression of RhoA is increased in CHAPb Tg hearts. RhoA belongs to the family of the small GTPases. Its effects on the actin cytoskeleton are mediated through stimulation of Rho Kinase (ROCK)[31]. RhoA is expressed in the heart during embryonic development, is downregulated after birth and re-expressed in cardiac hypertrophy[32]. Furthermore, RhoA transgenic mice develop a phenotype that resembles dilated cardiomyopathy (DCM), which is accompanied with conduction disturbances[33]. Alternatively, inhibition of ROCK reduces pressure overload-induced hypertrophy in rats[34]. It has been previously shown that synaptopodin, which has significant homology to CHAP, is involved in actin stress fiber formation by preventing proteasomal degradation of RhoA[10]. Like synaptopodin, CHAPb might be involved in the stabilization of RhoA, which may lead to actin stress fiber formation and induction of hypertrophy via the Rho-ROCK pathway.

*CHAP is involved in the SRF/MEF-2 actin signalling pathway*

We observed increased expression of transcription factors SRF and MEF-2 in CHAPb Tg hearts. Previously, it has been demonstrated that Striated muscle activator of Rho signaling (STARS), an actin-bundling protein that is localized at the Z-disc, is associated with both SRF and MEF-2 signalling. STARS is induced by MEF-2, which in turn regulates the formation of F-actin fibers via RhoA, leading to depletion of the monomeric globular

actin (G-actin) pool. Consequently, a reduction of G-actin may lead to activation of SRF mediated transcription[35-37]. Previous studies in mice have indicated the relevance of SRF in the development of cardiomyopathy[38, 39]. In addition, the importance of SRF in cardiomyocyte function, maintenance and regulation was shown in experiments in which it was knocked-down: expression of cytoskeletal genes, such as α- and β-MHC, cardiac α-actin and smooth muscle actin were decreased and also, interestingly, CHAP [40, 41]. With respect to the MEF2 transcription factor family (MEF-2a,c and d), Tg mice overexpressing these genes in the heart also showed cardiac hypertrophy and stress-dependent cardiac remodelling[42-44]. The phenotypes of the different Tg models do not overlap completely with the phenotype observed here, suggesting that additional pathways may be involved in the CHAPb induced hypertrophy. In summary, our study suggests a model in which increased levels of CHAPb may activate actin signalling leading to subsequent activation of cardiac transcription factors MEF2 and SRF, initiating a hypertrophic response and structural and functional changes in cardiomyocytes (figure 8C).

*Conclusion*

We show that overexpression of the "embryonic" isoform of CHAP, CHAPb, in mice causes cardiomyopathy with diastolic cardiac dysfunction and conduction disturbances, which is associated with sarcomere dysfunction and activation of actin signalling and of the downstream transcription factors MEF-2 and SRF. In contrast, overexpression of "adult" isoform CHAPb did not lead to cardiac phenotypical and fucntional changes. Recently, Kong[45] *et al* demonstrated that apart from alterations in gene expression, changes in mRNA splicing of sarcomeric genes particularly are associated with heart failure. These findings and our study demonstrate the importance of correctly spliced sarcomeric genes and substantiates further investigation in developmentally (dys-) regulated alternative splicing of other cardiac genes.

Taken together our results identify CHAPb as a novel component in the pathology of cardiomyopathy and a potential new candidate gene for screening mutations in familial cardiomyopathies.

# Acknowledgements

We thank L. Wisse, J. Korving, A.M. Mommaas-Kienhuis for technical assistance. We would like to thank Bas Blankevoort for graphics.

# References


(1) Barry SP, Davidson SM, Townsend PA. Molecular regulation of cardiac hypertrophy. *Int J Biochem Cell Biol* 2008;40(10):2023-39.

(2) Wilkins BJ, Molkentin JD. Calcium-calcineurin signaling in the regulation of cardiac hypertrophy. *Biochem Biophys Res Commun* 2004 October 1;322(4):1178-91.

(3) Rohini A, Agrawal N, Koyani CN, Singh R. Molecular targets and regulators of cardiac hypertrophy. *Pharmacol Res* 2010 April;61(4):269-80.

(4) Sanoudou D, Vafiadaki E, Arvanitis DA, Kranias E, Kontrogianni-Konstantopoulos A. Array lessons from the heart: focus on the genome and transcriptome of cardiomyopathies. *Physiol Genomics* 2005 April 14;21(2):131-43.

(5) Beqqali A, Kloots J, Ward-van Oostwaard D, Mummery C, Passier R. Genome-wide transcriptional profiling of human embryonic stem cells differentiating to cardiomyocytes. *Stem Cells* 2006 August;24(8):1956-67.

(6) Beqqali A, Monshouwer-Kloots J, Monteiro R, Welling M, Bakkers J, Ehler E, Verkleij A, Mummery C, Passier R. CHAP is a newly identified Z-disc protein essential for heart and skeletal muscle function. *J Cell Sci* 2010 April 1;123(Pt 7):1141-50.

(7) van Eldik W, Beqqali A, Monshouwer-Kloots J, Mummery C, Passier R. Cytoskeletal heart-enriched actin-associated protein (CHAP) is expressed in striated and smooth muscle cells in chick and mouse during embryonic and adult stages. *Int J Dev Biol* 2011;55(6):649-55.

(8) Weins A, Schwarz K, Faul C, Barisoni L, Linke WA, Mundel P. Differentiation- and stress-dependent nuclear cytoplasmic redistribution of myopodin, a novel actin-bundling protein. *J Cell Biol* 2001 October 29;155(3):393-404.

(9) Asanuma K, Kim K, Oh J, Giardino L, Chabanis S, Faul C, Reiser J, Mundel P. Synaptopodin regulates the actin-bundling activity of alpha-actinin in an isoform-specific manner. *J Clin Invest* 2005 May;115(5):1188-98.

(10) Asanuma K, Yanagida-Asanuma E, Faul C, Tomino Y, Kim K, Mundel P. Synaptopodin orchestrates actin organization and cell motility via regulation of RhoA signalling. *Nat Cell Biol* 2006 May;8(5):485-91.

(11) Faul C, Dhume A, Schecter AD, Mundel P. Protein kinase A, Ca2+/calmodulin-dependent kinase II, and calcineurin regulate the intracellular trafficking of myopodin between the Z-disc and the nucleus of cardiac myocytes. *Mol Cell Biol* 2007 December;27(23):8215-27.

(12) Bajanca F, Luz M, Duxson MJ, Thorsteinsdottir S. Integrins in the mouse myotome: developmental changes and differences between the epaxial and hypaxial lineage. *Dev Dyn* 2004 October;231(2):402-15.

(13) van Laake LW, Passier R, Monshouwer-Kloots J, Nederhoff MG, Ward-van Oostwaard D, Field LJ, van Echteld CJ, Doevendans PA, Mummery CL. Monitoring of cell therapy and assess ment of cardiac function using magnetic resonance imaging in a mouse model of myocardial infarction. *Nat Protoc* 2007;2(10):2551-67.

(14) Henkens IR, Mouchaers KT, Vliegen HW, van der Laarse WJ, Swenne CA, Maan AC, Draisma HH, Schalij I, van der Wall EE, Schalij MJ, Vonk-Noordegraaf A. Early changes in rat hearts with developing pulmonary arterial hypertension can be detected with three-dimensional electrocardiography. *Am J Physiol Heart Circ Physiol* 2007 August;293(2):H1300-H1307.

(15) Zaremba R, Merkus D, Hamdani N, Lamers JM, Paulus WJ, Dos RC, Duncker DJ, Stienen GJ, van der Velden J. Quantitative analysis of myofilament protein phosphorylation in small cardiac biopsies. *Proteomics Clin Appl* 2007 October;1(10):1285-90.

(16) van der Velden J. Diastolic myofilament dysfunction in the failing human heart. *Pflugers Arch* 2011 April 13.

(17) Severs NJ, Bruce AF, Dupont E, Rothery S. Remodelling of gap junctions and connexin expression in diseased myocardium. *Cardiovasc Res* 2008 October 1;80(1):9-19.

(18) Perez MV, Dewey FE, Marcus R, Ashley EA, Al-Ahmad AA, Wang PJ, Froelicher VF. Electrocardio graphic predictors of atrial fibrillation. *Am Heart J* 2009 October;158(4):622-8.

(19) Louvet-Vallee S. ERM proteins: from cellular architecture to cell signaling. *Biol Cell* 2000 August;92(5):305-16.

(20) Lee JH, Katakai T, Hara T, Gonda H, Sugai M, Shimizu A. Roles of p-ERM and Rho-ROCK signal ing in lymphocyte polarity and uropod formation. *J Cell Biol* 2004 October 25;167(2):327-37.

(21) Bevilacqua LM, Simon AM, Maguire CT, Gehrmann J, Wakimoto H, Paul DL, Berul CI. A targeted

disruption in connexin40 leads to distinct atrioventricular conduction defects. *J Interv Card Electrophysiol* 2000 October;4(3):459-67.

(22) Kirchhoff S, Nelles E, Hagendorff A, Kruger O, Traub O, Willecke K. Reduced cardiac conduction velocity and predisposition to arrhythmias in connexin40-deficient mice. *Curr Biol* 1998 February 26;8(5):299-302.

(23) Guerrero PA, Schuessler RB, Davis LM, Beyer EC, Johnson CM, Yamada KA, Saffitz JE. Slow ventricular conduction in mice heterozygous for a connexin43 null mutation. *J Clin Invest* 1997 April 15;99(8):1991-8.

(24) Thomas SA, Schuessler RB, Berul CI, Beardslee MA, Beyer EC, Mendelsohn ME, Saffitz JE. Disparate effects of deficient expression of connexin43 on atrial and ventricular conduction: evidence for chamber-specific molecular determinants of conduction. *Circulation* 1998 February 24;97(7):686-91.

(25) Wei L, Taffet GE, Khoury DS, Bo J, Li Y, Yatani A, Delaughter MC, Klevitsky R, Hewett TE, Robbins J, Michael LH, Schneider MD, Entman ML, Schwartz RJ. Disruption of Rho signaling results in progressive atrioventricular conduction defects while ventricular function remains preserved. *FASEB J* 2004 May;18(7):857-9.

(26) Ikeda Y, Sato K, Pimentel DR, Sam F, Shaw RJ, Dyck JR, Walsh K. Cardiac-specific deletion of LKB1 leads to hypertrophy and dysfunction. *J Biol Chem* 2009 December 18;284(51):35839-49.

(27) Bierhuizen MF, Boulaksil M, van SL, van der Nagel R, Jansen AT, Mutsaers NA, Yildirim C, van Veen TA, De Windt LJ, Vos MA, van Rijen HV. In calcineurin-induced cardiac hypertrophy expression of Nav1.5, Cx40 and Cx43 is reduced by different mechanisms. *J Mol Cell Cardiol* 2008 September;45(3):373-84.

(28) Owan TE, Hodge DO, Herges RM, Jacobsen SJ, Roger VL, Redfield MM. Trends in prevalence and outcome of heart failure with preserved ejection fraction. *N Engl J Med* 2006 July 20;355(3):251-9.

(29) Kindermann M, Reil JC, Pieske B, van Veldhuisen DJ, Bohm M. Heart failure with normal left ventricular ejection fraction: what is the evidence? *Trends Cardiovasc Med* 2008 November;18(8):280-92.

(30) Robinson P, Griffiths PJ, Watkins H, Redwood CS. Dilated and hypertrophic cardiomyopathy mutations in troponin and alpha-tropomyosin have opposing effects on the calcium affinity of cardiac thin filaments. *Circ Res* 2007 December 7;101(12):1266-73.

(31) Brown JH, Del Re DP, Sussman MA. The Rac and Rho hall of fame: a decade of hypertrophic signaling hits. *Circ Res* 2006 March 31;98(6):730-42.

(32) Ahuja P, Perriard E, Pedrazzini T, Satoh S, Perriard JC, Ehler E. Re-expression of proteins involved in cytokinesis during cardiac hypertrophy. *Exp Cell Res* 2007 April 1;313(6):1270-83.

(33) Sah VP, Minamisawa S, Tam SP, Wu TH, Dorn GW, Ross J, Jr., Chien KR, Brown JH. Cardiac-specific overexpression of RhoA results in sinus and atrioventricular nodal dysfunction and contractile failure. *J Clin Invest* 1999 June;103(12):1627-34.

(34) Phrommintikul A, Tran L, Kompa A, Wang B, Adrahtas A, Cantwell D, Kelly DJ, Krum H. Effects of a Rho kinase inhibitor on pressure overload induced cardiac hypertrophy and associated diastolic dysfunction. *Am J Physiol Heart Circ Physiol* 2008 April;294(4):H1804-H1814.

(35) Kuwahara K, Teg Pipes GC, McAnally J, Richardson JA, Hill JA, Bassel-Duby R, Olson EN. Modula tion of adverse cardiac remodeling by STARS, a mediator of MEF2 signaling and SRF activity. *J Clin Invest* 2007 May;117(5):1324-34.

(36) Arai A, Spencer JA, Olson EN. STARS, a striated muscle activator of Rho signaling and serum re sponse factor-dependent transcription. *J Biol Chem* 2002 July 5;277(27):24453-9.

(37) Kuwahara K, Barrientos T, Pipes GC, Li S, Olson EN. Muscle-specific signaling mechanism that links actin dynamics to serum response factor. *Mol Cell Biol* 2005 April;25(8):3173-81.

(38) Parlakian A, Charvet C, Escoubet B, Mericskay M, Molkentin JD, Gary-Bobo G, De Windt LJ, Ludosky MA, Paulin D, Daegelen D, Tuil D, Li Z. Temporally controlled onset of dilated cardiomyopathy through disruption of the SRF gene in adult heart. *Circulation* 2005 November 8;112(19):2930-9.

(39) Zhang X, Chai J, Azhar G, Sheridan P, Borras AM, Furr MC, Khrapko K, Lawitts J, Misra RP, Wei JY. Early postnatal cardiac changes and premature death in transgenic mice overexpressing a mutant form of serum response factor. *J Biol Chem* 2001 October 26;276(43):40033-40.

(40) Balza RO, Jr., Misra RP. Role of the serum response factor in regulating contractile apparatus gene expression and sarcomeric integrity in cardiomyocytes. *J Biol Chem* 2006 March 10;281(10):6498-510.

(41) Miano JM, Ramanan N, Georger MA, de Mesy Bentley KL, Emerson RL, Balza RO, Jr., Xiao Q, Weiler H, Ginty DD, Misra RP. Restricted inactivation of serum response factor to the cardiovascular system. *Proc Natl Acad Sci U S A* 2004 December 7;101(49):17132-7.

(42) van Oort RJ, van RE, Bourajjaj M, Schimmel J, Jansen MA, van der NR, Doevendans PA, Schneider MD, van Echteld CJ, De Windt LJ. MEF2 activates a genetic program promoting chamber dilation and contractile dysfunction in calcineurin-induced heart failure. *Circulation* 2006 July 25;114(4):298-308.

(43) Kim Y, Phan D, van RE, Wang DZ, McAnally J, Qi X, Richardson JA, Hill JA, Bassel-Duby R, Olson EN. The MEF2D transcription factor mediates stress-dependent cardiac remodeling in mice. *J Clin Invest* 2008 January;118(1):124-32.

(44) Xu J, Gong NL, Bodi I, Aronow BJ, Backx PH, Molkentin JD. Myocyte enhancer factors 2A and 2C induce dilated cardiomyopathy in transgenic mice. *J Biol Chem* 2006 April 7;281(14):9152-62.

(45) Kong SW, Hu YW, Ho JW, Ikeda S, Polster S, John R, Hall JL, Bisping E, Pieske B, dos Remedios CG, Pu WT. Heart failure-associated changes in RNA splicing of sarcomere genes. *Circ Cardiovasc Genet.* 2010 Apr;3(2):138-46.

# Supplemental figures

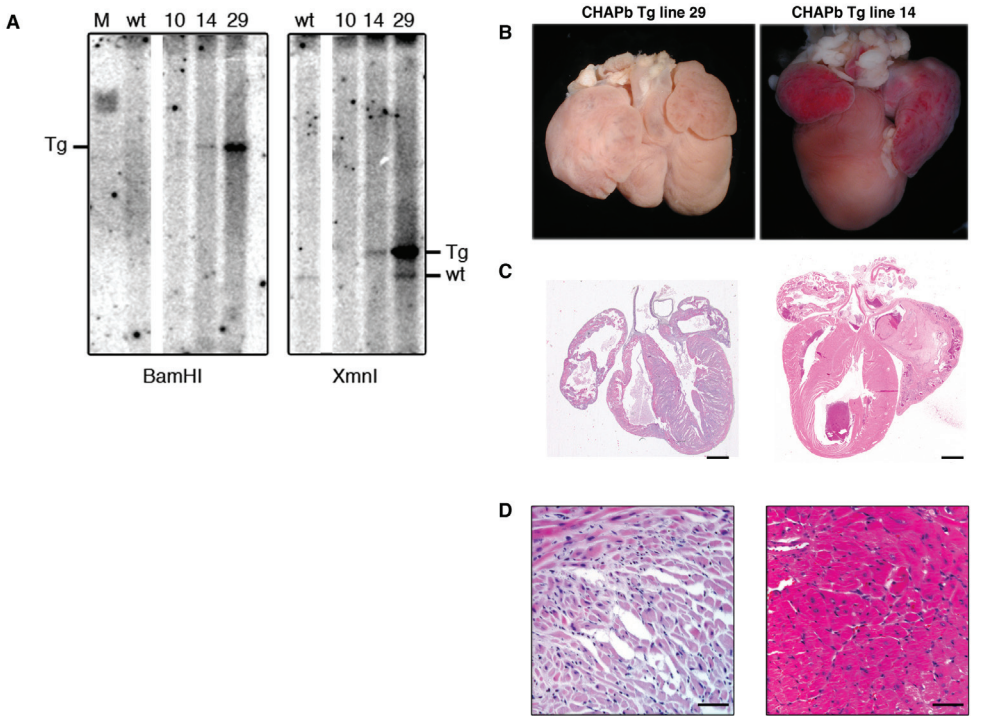


**Supplemental figure 1: Hearts of CHAPb Tg founders that died spontaneously. A) Southern blot analysis of genomic wild type and CHAPb Tg DNA showing intermediate copy number in line 14 and high copy number in line 29, compared to wild type copy numbers. Hearts of CHAPb founder line 29 (left panels) and line 14 (right panels). B) Hearts showing enlarged atria and malformed ventricles. C) HE stained overview section showing enlarged atria and thickened ventricles. D). Higher magnification of the left ventricle. Scale bars in B 1 mm, in C 50 µm.**

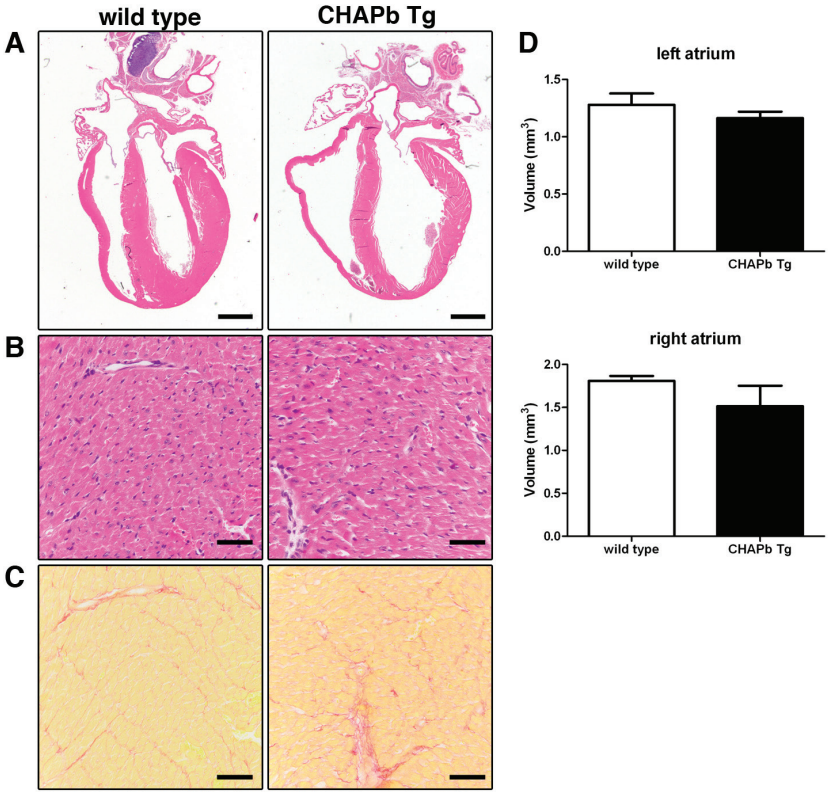


**Supplemental figure 2: HE and Sirius red staining of CHAPb Tg hearts at one month of age. Wt (left panels) and CHAPb Tg (right panels) at 1 month of age (A-C). A) HE stained overview section. B) Higher magnification of left ventricle. C) Sirius red staining of the left ventricle. D and E) Volume of the left atrium (D) and right atrium (E) in wt (white bars) and CHAPb Tg (black bars) hearts. Scale bars 1 mm in A, 50 µm in B, C.**

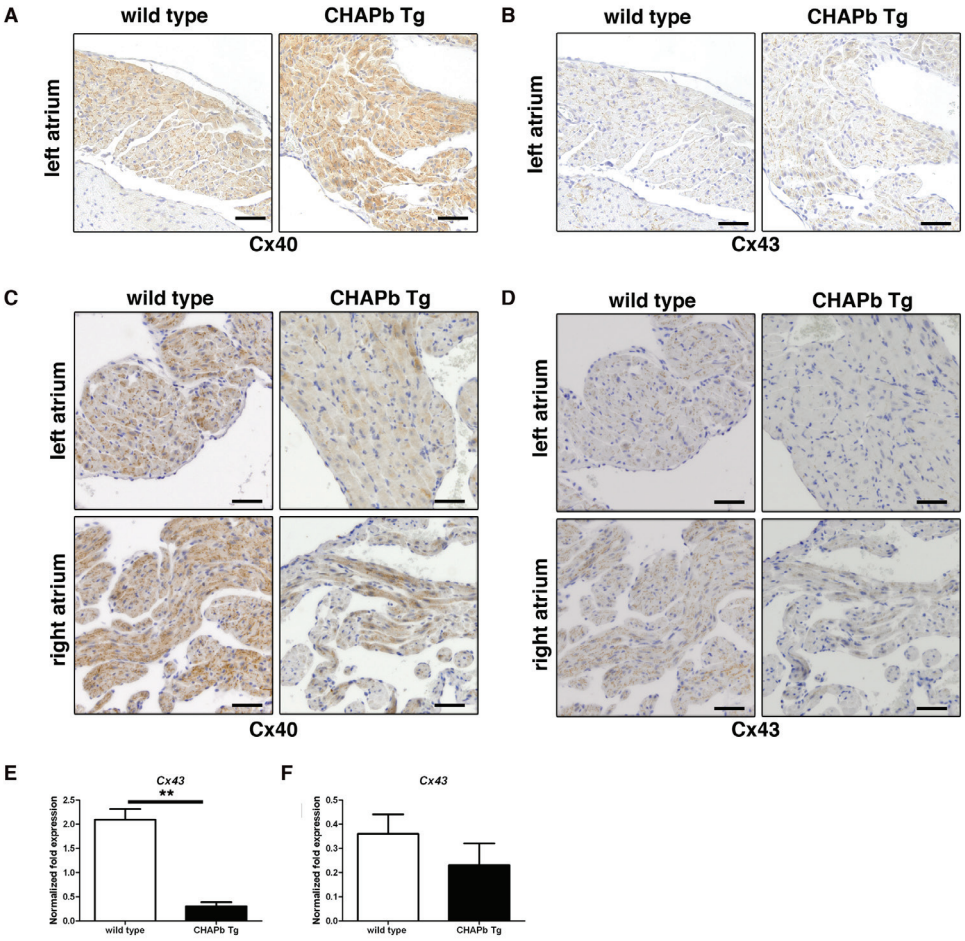


**Supplemental figure 3: Expression of Connexin 40 and 43 at 1, 3 and 6 months. Immunohistochemical staining showing Connexin 40 (A and C) and 43 (B and D) expression in wt (left panels) and CHAPb Tg (right panels) left atria (A, B and upper panels of C and D) and right atria (lower panels of C and D) at one month (A and B) and 3 months of age (C and D) of age. qPCR analysis of *Connexin 43* (E and F) expression in the left (E) and right (F) atrium at 6 months of age. Scale bars 50 μm.**

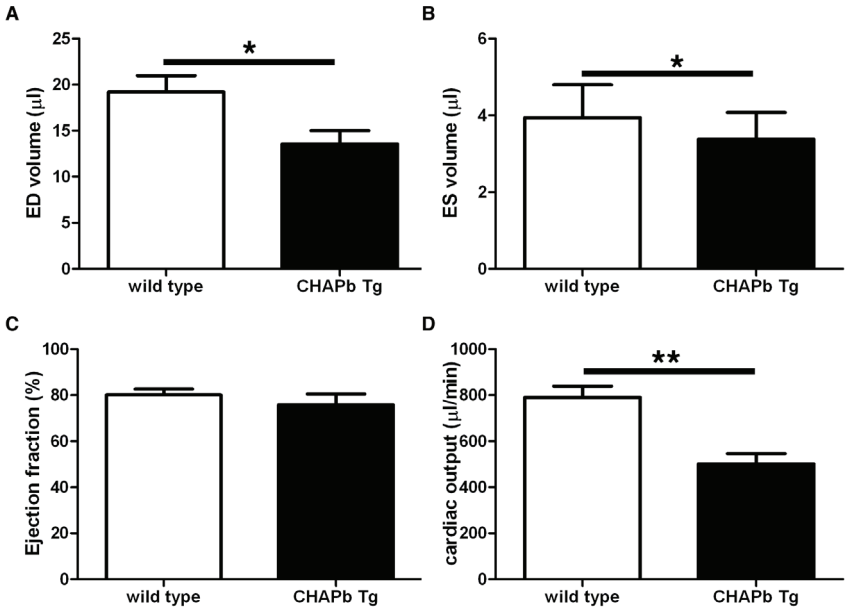


Supplemental figure 4: Functional analysis of CHAPb Tg hearts. MRI measurements of the right ventricle of wt (white bars) and CHAPb Tg (black bars) animals at 6 months of age (A-F). ED volume (A), ES volume (B), ejection fraction (C) and cardiac output (D). ED (end diastolic), ES (end systolic) and LV (left ventricular).

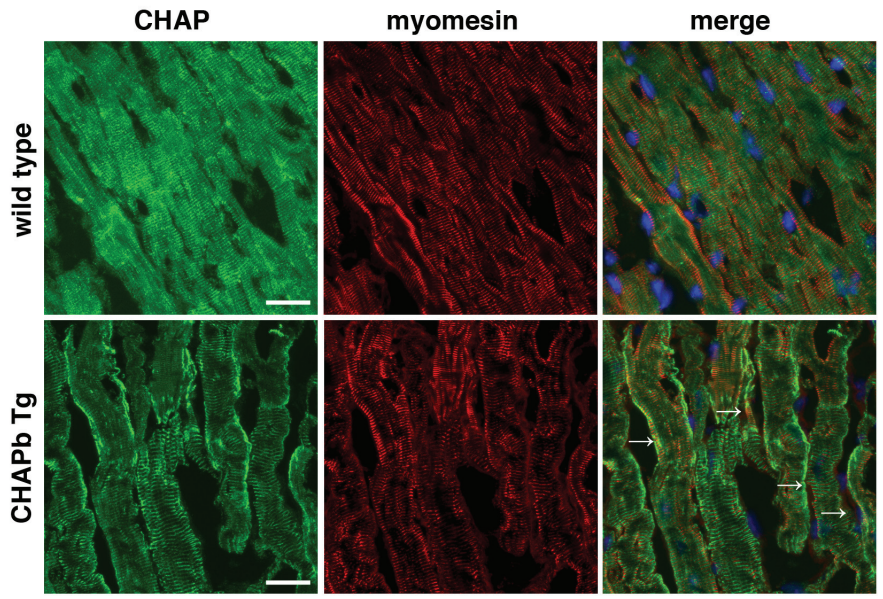


Supplemental Figure 5: Expression of m-band marker myomesin is not affected in CHAPb Tg hearts. Hearts stained for CHAP (green) / myomesin (red), merge images are shown. CHAP is localized in the z-disc of cardiomyocytes of wt (upper panels) hearts. In cardiomyocytes of CHAPb Tg (lower panels) CHAP also stained stress fibers (arrows), which did not stain for myomesin. Scale bars: 20 µm.

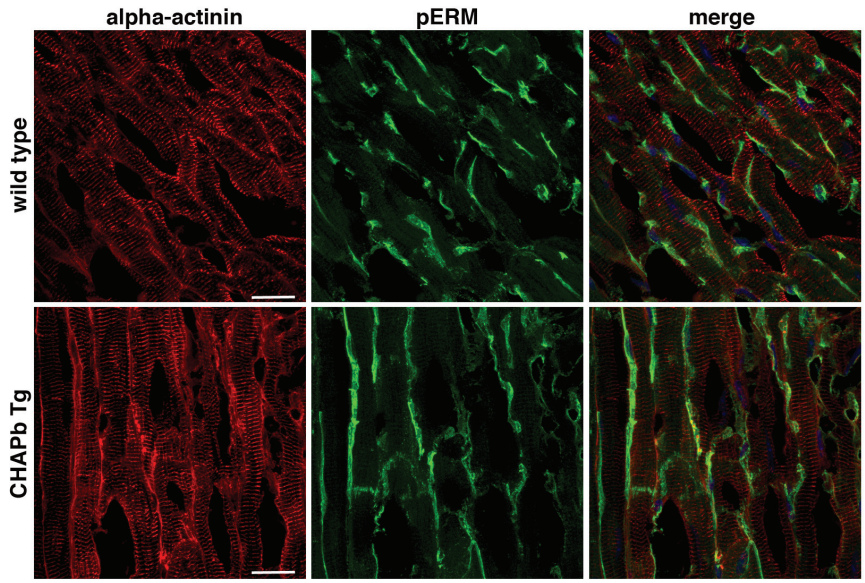


**Supplemental figure 6: Ectopic pERM expression in CHAPb Tg hearts. Wt (upper panels) and CHAPb Tg (lower panels) hearts at 6 months of age stained for pERM (green) and alpha-actinin (red). Nuclei are stained blue, merge images are shown. Scale bars: 20 µm.**

# Chapter 5

## *In vitro* overexpression of CHAPa and CHAPb in mouse cardiomyocytes and skeletal muscle cells interferes with Z-disc integrity and decreases fetal gene expression

Willemijn van Eldik, Abdelaziz Beqqali, Jantine Monshouwer-Kloots,
Twan de Vries, Christine Mummery, Robert Passier

# Abstract

In the previous chapter we have described that CHAPb transgenic mice displayed features of cardiomyopathy and cardiac dysfunction, whereas CHAPa transgenic mice did not display any abnormalities. In order to determine direct effects of both CHAP isoforms, we infected mouse cardiomyocytes (E17.5) and skeletal muscle cells myoblast cells (C2C12) with adenoviral constructs for CHAPa and CHAPb.
*In vitro* overexpression of CHAPa resulted in Z-disc disruption, as shown by α-actinin-2 staining in both C2C12 cells and cardiomyocytes. CHAPb overexpression in C2C12 and cardiomyocytes resulted in stress fiber formation, which stained for F-actin. Although RhoA and phosphorylated Ezrin/Moesin/Radixin, proteins involved in linking the actin cytoskeleton to the plasma membrane, were ectopically expressed in cardiomyocytes, no activation of the actin signaling pathway was observed. Surprisingly, in both CHAPa and CHAPb infected cells downregulation of hypertrophy markers *Nppa*, *Nppb* and *Myh7* was observed, whereas *Myh6* was upregulated. In agreement with these findings we observed that a key player in muscle hypertrophy and development, the transcription factor Nuclear Factor of Activated T-cells-c2 (NFATc2), was translocated from the nucleus to the cytoplasm. These results show that CHAPa and CHAPb have an important role in maintaining the integrity of muscle cells. Furthermore, interestingly our findings suggest that CHAPa and b isoforms may directly affect transcriptional regulation regarding maturation and/or blocking hypertrophy of cardiomyocytes.

# Introduction

Cardiac hypertrophy is a compensatory mechanism of the heart to increased workload as a result of loss of cardiomyocytes that occurs in pathophysiological events (for example myocardial infarction). During a hypertrophic response cardiomyocytes increase their cell volume to compensate for the loss of cardiomyocytes. Cardiomyocytes respond to stress by expressing a specific subset of fetal genes, such as Atrial Natriuretic Factor (ANF), Brain Natriuretic Peptide (BNP) and β-Myosin Heavy Chain (β-MHC), leading to the described hypertrophic response[1-3]. The basic contractile unit of cardiomyocytes is the sarcomere, which is delineated by the Z-disc[4], which consists of a protein complex, including α-actinin-2 and CHAP. Z-disc proteins may sense stress signals, and activate signaling pathways leading to activation of the fetal gene program[5, 6].In the previous chapters we have seen that CHAP is expressed in skeletal and heart muscle cells during embryonic development and in adulthood. Two isoforms of CHAP exists: CHAPa is the longest isoform and contains a PDZ domain and nuclear localization signal (NLS), whereas the shorter isoform CHAPb lacks the PDZ domain. Whereas CHAPa is predominantly expressed in adult tissues, CHAPb is expressed at higher levels in the developing heart and muscles[7]. CHAP is homologous to synaptopodin and myopodin, which have both been implicated in actin signaling. Myopodin is expressed in the Z-disc of cardiac and skeletal muscle and interacts with α-actinin-2[8]. Synaptopodin interacts with α-actinin-2 and -4[11], and is involved in actin signaling in kidney podocytes by the formation of actin stress fibers via RhoA[12].

Besides localization at the Z-disc, Myopodin is also able to translocate to the nucleus, which is mediated by 14-3-3[9].It has been shown that interaction between 14-3-3 and Myopodin can be regulated by various kinases and phosphatases, such as Protein Kinase A (PKA), $Ca2^{+}$/calmodulin-dependent kinase II (CaMKII) and the phosphotase calcineurin, a key player in cardiac hypertrophy[10].

In the previous chapter, we described the phenotypes of heart-specific CHAPa- and b transgenic (Tg) mice. CHAPa Tg mice did not show a phenotype after one year of age or after myocardial infarction (Chapter 4 and data not shown), although misfolding or partially degradation could not be excluded. CHAPb Tg mice, on the other hand developed features of cardiomyopathy, including cardiac hypertrophy and diastolic dysfunction. Furthermore, stress fibers were apparent in CHAPb Tg hearts which was associated with activation of the actin signaling pathway.

To study the direct effects of CHAP we induced expression for both isoforms by adenoviral transduction in skeletal muscle cells (C2C12) and embryonic 17.5 (E17.5) mouse cardiomyocytes. We found that CHAPa- and b both disrupted the Z-disc structure of cardiomyocytes and differentiated C2C12 cells. However, only CHAPb induced stress fibers, similar to the stress fibers found in CHAPb Tg hearts. In contrast to the CHAPb Tg hearts we did not observe a significant upregulation of the actin signaling and reactivation of fetal cardiac genes, a hallmark of pathological cardiac hypertrophy. In fact, we observed an opposite effect on re-expression of fetal cardiac genes, which included a switch in expression of MHC isoforms and downregulation of ANF and BNP. These changes were further accompanied by translocation of Nuclear Factor of Activated T-cells (NFAT), suggesting that direct effects of CHAP may be involved in further maturation of muscle cells or even have anti-hypertrophic effect on striated muscle cells.

# Materials and methods

*Animals and cardiomyocyte isolation*
Swiss mice were intercrossed for collection of embryos at embryonic day 17.5 (E17.5). Embryos were collected and rinsed in PBS. Hearts were removed and rinsed in PBS. Subsequently, hearts were rotated over night in 1x trypsin/EDTA (Sigma-Aldrich Chemie). The next day trypsin/EDTA was removed by transferring hearts over a 70 µm strainer (BD Biosciences). In a next step, cardiomyocytes were isolated by shaking the hearts in fractions of collagenase mix (0.5 ml 22% BSA (Sigma-Aldrich Chemie) and 15 µl Collagenase type 1A (36.9 u/µl; Sigma-Aldrich Chemie) in 30 ml 0.9% NaCl for 3 minutes at 37 °C. After each fraction, hearts were put over a new 70 µm strainer (BD Biosciences) and filtered. Each fraction was collected in 2 ml fetal calf serum (FCS, Sigma-Aldrich Chemie), followed by rinsing the strainer with 5 ml cardiomyocyte medium (Dulbecco's Modified Eagle Medium F12 [DMEM F12, Invitrogen], 15% FCS and pen/strep [Invitrogen]). The remainder of the hearts was put in a new fraction with collagenase mix and the procedure was applied until all hearts were dissolved. All fractions were collected, cells were spun down, resuspended in new cardiomyocyte medium and finally cells were counted and plated on gelatin-coated dishes. The amount of cells plated was 75,000 per 24-well and 380,000 per 6-well. The next day medium was refreshed with cardiomyocyte medium without FCS.

*Cell culture*
First-generation human adenovirus type 5 (HAdV5) vectors were produced in PER.tTA. Cre76 cells[13]. These HAdV5 early region 1 (E1)-transformed human embryonic retinoblasts were maintained in DMEM (Invitrogen) containing 10% fetal bovine serum (FBS; Invitrogen) and 10 mM $MgCl_2$ and cultured at 37°C in a humidified atmosphere of 90% air and 10% $CO_2$. Endpoint titrations of HAdV5 vector preparations were carried out in HeLa cells, which were fed DMEM containing 5% FCS (Sigma Aldrich). C2C12 cells were cultured in DMEM with 10% FCS and pen/strep added. For differentiation of C2C12 cells, cells were incubated with DMEM with 2% horse serum (Invitrogen) and pen/strep added. Medium was refreshed every other day.
The latter cell types were cultured at 37°C in a humidified atmosphere of 95% air and 5% $CO_2$.

*Generation of first-generation HAdV5 vectors encoding murine CHAP isoforms a and b.*
The codinq sequences of murine CHAPa and CHAPb were amplified by Platinum Taq DNA Polymerase High fidelity (Invitrogen) polymerase chain reaction from cDNA templates that were generated earlier[7] using the forward primers 5'-GCGGCCGCCCACC**ATG**GGTGCTGAGGAGGAGGT-3' and 5'-GCGGCCGCCCACC**ATG**GAGACCACCATCCAAGA-3', respectively, together with a single reverse primer (5'-GTCGACACTGGTGCCCTGCCCC-3'), the stopcodon was included in a c-terminal flag-tag. The amplification products were subcloned into pCRII (Invitrogen) and subjected to nucleotide sequence analysis. The pShuttle-IRES-hrGFP-1 vector was used for generating adenoviruses of CHAPa (AdCHAPa) and CHAPb (AdCHAPb). This vector contains a CMV promoter, a multiple cloning site which is followed by internal ribosome entry site (IRES), which directs the translation of human recombinant Green Fluorescent Protein (hrGFP) as a second open reading frame. Errorless coding sequences of murine CHAPa and CHAPb were transferred to pShuttle-IRES-hrGFP-1 (Agilent

Technologies) using NotI and SalI to produce pShuttle-mCHAPa-IRES-hrGFP-1 and pShuttle-mCHAPb-IRES-hrGFP-1, respectively. These two HAdV5 shuttle constructs were linearized with PmeI and used in combination with pAdEasy-1 DNA for the generation by *in vivo* recombineering[14] of plasmids pAdEasy-1-mCHAPa-IRES-hrGFP-1 and pAdEasy-1-mCHAPb-IRES-hrGFP-1 carrying full-length HAdV5 vector genomes. Following treatment with PacI to release the HAdV5 vector termini, pAdEasy-1-mCHAPa-IRES-hrGFP-1 and pAdEasy-1-mCHAPb-IRES-hrGFP-1 DNA was individually transfected with the aid of linear 25-kDa polyethyleneimine (Polysciences) into PER.tTA.Cre76 cells[13] to produce seed stocks of AdEasy-1-mCHAPa-IRES-hrGFP-1 and AdEasy-1-mCHAPb-IRES-hrGFP-1, respectively. These seed stocks were used for large-scale production of both HAdV5 vectors in PER.tTA.Cre76 cells essentially as described by Gonçalves *et al.*[13]. The functional titers of the resulting AdEasy-1-mCHAPa-IRES-hrGFP-1 and AdEasy-1-mCHAPb-IRES-hrGFP-1 vector preparations were determined by limiting dilution assays in HeLa cells using flow cytometric analysis of *hrGFP-1* expression as readout and were expressed in terms of HeLa cell-transducing units (HTU)/ml. An adenovirus expressing GFP only was used as control and is described in Knaän-Shanzer et al[15].

*Infection of cells*

Cells were infected with multiplicity of infection (MOI) of 10. After 6-12 hours medium was refreshed. Then cells were left for 24 hours, 48 hours or 7 days.

*Immunofluorescence*

Cells were grown on gelatin coated coverslips. Cells were washed with PBS and fixed for 30 minutes in 2% PFA at room temperature, followed by 3 washes in PBS. Cells were permeabilized with 0.1% Triton-x-100 in PBS for 8 minutes. Cells were washed 3 times with PBS and blocked for 1 hour in 4% normal goat serum (Vector labs) in PBS. First antibody was applied over night at 4 °C in PBS/normal goat serum. Antibodies used were anti-CHAP (1:50), anti-α-actinin (1:800, Sigma-Aldrich Chemie), myomesin (1:50, kind gift from E. Ehler), anti-RhoA (1:100, Santa Cruz), anti-phosphorylated Ezrin/Moesin/Radixin (1:50, Cell Signaling Technology) or anti-NFATc2 (1:50, G1 D10, Santa Cruz). The next day cells were washed 3 times with PBS/0.05% Tween-20 (PBS-T) for 10 minutes. Secondary antibodies were dissolved in 4% normal goat serum/PBS. Antibodies used were Alexa Fluor® 647 donkey anti-rabbit IgG (1:100, Invitrogen), goat anti-mouse/IgG(H+L)/Cy3 (1:250, Jackson Immuno research). Cells were 3 times washed in PBS-T for 20 minutes, and then 1 time in PBS. F-actin fibers were stained using Alexa555 conjugated phalloidin (1:100, Invitrogen). Cells were counter stained with DAPI for 8 minutes. Coverslips were enclosed with Molviol. Immunofluorescent stainings were analyzed with SP5 confocal microscope (Leica).

*Protein isolation and western blot*

For protein isolation cells were grown on 6 well plates. Cells were infected and 24 hours, 48 hours or 7 days later protein was isolated (see previous section). For this cells were washed twice with PBS. Then 250 µl ice-cold RIPA buffer (50 mM Tris-HCl pH8, 150 mM NaCl, 1% NP-40 (Sigma-Aldrich Chemie), 0.2% sodium deoxycholate and 0.1% SDS) with extra added protein inhibitors (protease inhibitor cocktail tablets (10 µg/ml; Roche, Germany), 0.1 mmol/L dithiothreitol (DTT; Invitrogen) and 1 mmol/L phenylmethanesulfonylfluoride (PMSF; Sigma Aldrich), 5 mmol/L NaF and 1 mmol/L $Na_3VO_4$) was added to the cells, which

were then left on ice for 15 minutes. Then cells were scraped on ice and transferred to an eppendorf tube. Lysed cells were spun down (10000 g, 4 °C, 15 minutes) and supernatant was transferred to a new tube. Protein concentration was measured with the Bradford assay (Bio-rad) using bovine serum albumin (BSA) for a standard curve. Then 5x sample buffer (100 mM Tris-HCl pH 6.8, 10% SDS, 50% glycerol, 25% β-mercaptoethanol and bromphenol blue) was added and samples were boiled for 5 minutes at 95 °C. Protein gels were loaded with 30 µg protein. Gels were blotted (Hybond-P, GE healthcare) for 3 hours at room temperature and blocked for one hour with 5% milk/Tris Buffered Saline-tween (TBS-T: 50mM Tris-HCl pH 7.5, 125 mM NaCl, 0.02% Tween-20). First antibody diluted in 5% milk/TBS-T (unless stated else) was applied over night at 4 °C. Antibodies used were anti-RhoA (1:200, Santa Cruz), anti-actin (1:1000, Millipor), anti-α-actinin (1:1000, Sigma-Aldrich Chemie), anti-Ezrin/moesin/radixin (1:1000 in 5% BSA/TBS-T, Cell Signaling Technology), anti-Flag (1:5000, Sigma-Aldrich Chemie) and anti-GAPDH (1:10000, Millipor). Secondary antibody was applied for 1 hour at room temperature. Secondary antibodies used were anti-mouse IgG HRP (1:1000, Cell Signaling Technology) or anti-rabbit IgG HRP (1:2000, Cell Signaling Technology) dissolved in 5% milk/TBS-T. Blots were visualized by using SuperSignal West Pico Chemiluminescent Substrate (Pierce).

*RNA isolation and cDNA synthesis*

Infected cells were grown in 6 well plates, washed twice with PBS and dissolved in Trizol (Invitrogen). Then RNA was isolated according to the manufactures protocol. RNA was treated with DNase (DNA-free, Ambion) and subsequently translated in cDNA (iScript, BioRad). qPCR analysis was done using the CFX96 Real-Time PCR detection system (Bio-Rad). Primers used are listed in table in the Material and Method section of chapter 4, except for *Myh6*: 5'- CTTCATCCATGGCCAATTCT-3' and 5'- GCGCATTGAGTTCAAGAAGA-3'. Data were analyzed with Bio-Rad CFX Manager.

# Results

*Generation of adenoviral CHAP constructs*

To study the effects of overexpression of CHAPa- and b *in vitro*, we generated adenoviruses encoding flag-tagged CHAPa or –b cDNA (AdCHAPa and AdCHAPb, with additional IRES-GFP expression). An adenovirus expressing GFP (AdGFP) only was used as control. We first investigated the expression of the CHAP adenoviruses in mouse E17.5 cardiomyocytes. For this, cells were infected with AdGFP, AdCHAPa, AdCHAPb and non-infected cells were used as control. After 2 days RNA and protein samples were obtained and expression levels were analyzed with qPCR and western blot. We found a robust overexpression by qPCR for both *ChapA* (Figure 1A) and *ChapB* (Figure 1B) when compared to control virus and the non-infected endogenous CHAP isoforms. Also at the protein level the products of CHAPa and CHAPb could be detected with a flag antibody (Figure 1C), whereas no bands could be detected in the control samples. These results show a specific, robust and stable overexpression of both CHAPa and CHAPb isoforms.

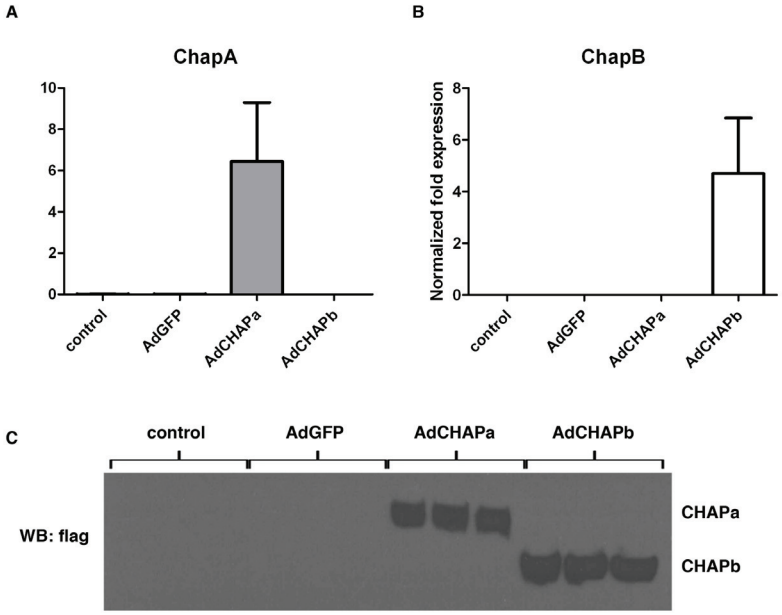


**Figure 1: Generation of AdCHAPa and AdCHAPb viruses. Mouse cardiomyocytes were infected with AdCHAPa or Ad-CHAPb. A+B) Expression of *ChapA* (A) or *ChapB* (B) was analyzed by qPCR, *Gapdh*, *H2A* and *Pgk* were used as internal controls. C) Western blot stained with flag antibody shows overexpression of CHAPa and CHAPb at the protein level.**

*Overexpression of CHAP affects Z-disc organization in both skeletal muscle cells and cardiomyocytes*

Next, we studied the role of CHAP in skeletal and heart muscle cells *in vitro*. In chapter 3 we have seen that CHAP is expressed in developing and adult skeletal muscle cells of mouse and chick embryos (see chapter 3). To investigate the role of CHAPa and CHAPb in skeletal muscle differentiation we used a mouse myoblast cell line, C2C12, which can be differentiated to skeletal muscle cells by culturing cells in media containing 2% horse serum. This results in

the formation of multinucleated twitching myotubes in which striations can be detected by α-actinin-2 staining. C2C12 cells were infected with AdGFP, AdCHAPa or AdCHAPb, after the infection medium was replaced for differentiation medium and cells were differentiated for 6 days. Then cells were stained for CHAP and α-actinin-2. The control AdGFP-infected cells formed multinucleated myotubes and striations could be detected in these myotubes with α-actinin-2 staining (Figure 2, upper panels, arrows). However, formation of multinucleated myotubes was disrupted in both AdCHAPa and AdCHAPb infected cells (Figure 2, middle and lower panels). Whereas in AdCHAPa infected cells only the sarcomere structure was disrupted (arrows in middle panel, Figure 2), in AdCHAPb cells additional stress fibers were formed (arrows in lower panel, Figure 2). In undifferentiated C2C12 cells overexpression of CHAPb also induced stress fibers (data not shown).

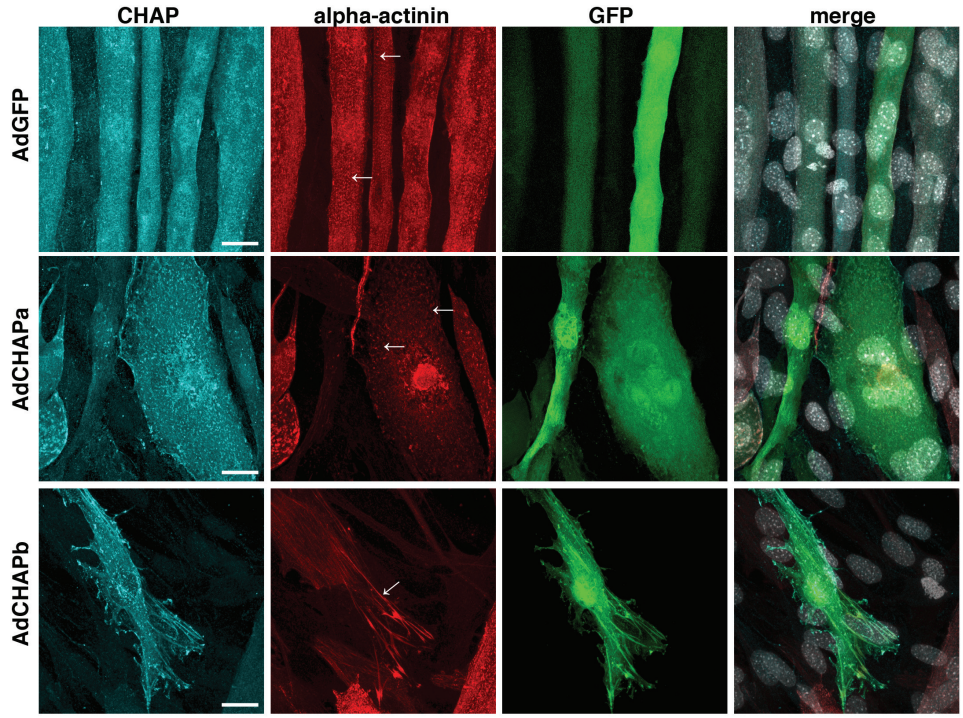


**Figure 2: Overexpression of CHAPa and CHAPb affects skeletal muscle differentiation. C2C12 cells were infected with AdGFP, AdCHAPa or AdCHAPb, differentiated and stained for α-actinin-2 (red) and CHAP (cyan). Infected cells can be identified by GFP signal (green), nuclei are stained gray, merge images are shown. In AdGFP infected cells (upper panels) multinucleated myotubes were formed, in which striations could be detected by α-actinin-2 staining (arrows). In AdCHAPa infected cells no multinucleated myotubes were formed and Z-disc was disrupted, which was shown by α-actinin-2 staining (middle panels, arrows). In AdCHAPb infected cells no myotubes were formed, instead, stress fibers were formed, that stained for α-actinin-2 and CHAP (lower panel, arrow).**

Next, we investigated overexpression of AdCHAPa and AdCHAPb in E17.5 cardiomyocytes. In CHAPb Tg mice overexpression of CHAPb induces stress fibers, which co-stained for α-actinin-2 and not for myomesin. In AdGFP infected cells CHAP co-localized in the Z-disc with α-actinin-2 (Figure 3A, upper panels) and not with myomesin (Figure 3B, upper panels), which is in agreement with our previous findings[7]. Infection of E17.5 cardiomyocytes with AdCHAPa resulted in disruption of Z-disc structure, which was apparent by both CHAP

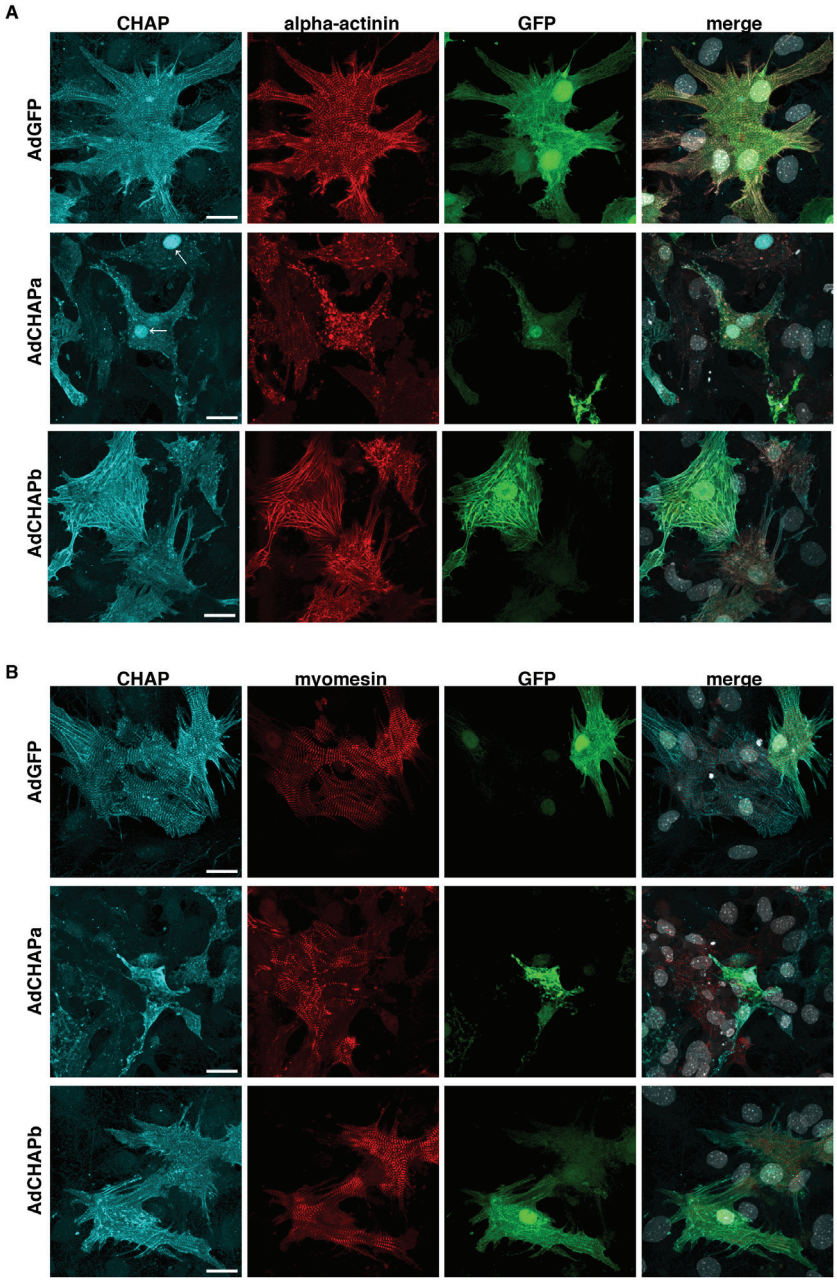


**Figure 3: Overexpression of CHAPa and CHAPb results in distinct phenotypes in E17.5 mouse cardiomyocytes. Mouse cardiomyocytes were infected with AdGFP, AdCHAPa or AdCHAPb and stained for α-actinin-2 (red)/CHAP (cyan, A) or Myomesin (red)/CHAP (cyan, B). Infected cells can be identified by GFP signal (green), nuclei are stained gray, merge images are shown. In AdGFP infected cardiomyocytes CHAP localizes at the Z-disc with α-actinin (A, upper panels) and not with myomesin (B, upper panels). In AdCHAPa infected cardiomyocytes the Z-disc is disrupted (A, middle panels, α-actinin), while the m-band is not affected (B, middle panels, myomesin). In AdCHAPb infected cells stress fibers are formed that stain for α-actinin-2 (A, lower panels), while myomesin is not affected (B, lower panels).**

and α-actinin-2 staining (Figure 3A, middle panels). Occasionally, infection of AdCHAPa in E17.5 mouse cardiomyocytes resulted in nuclear localization of CHAP (Figure 3A, middle panel, arrows). Infection of E17.5 cardiomyocytes with AdCHAPb resulted in the formation of stress, which stained for CHAP and α-actinin-2 (Figure 3A, lower panels). Staining for myomesin showed that in both AdCHAPa and AdCHAPb infected cells the M-band structure was not affected (Figure 3B, middle and lower panels). Thus formation of stress fibers in AdCHAPb infected cells led to a subsequent loss of Z-disc integrity, whereas the M-band was unaffected. In summary, both CHAP isoforms led to sarcomeric disruption, whereas formation of stress fibers was only evident in AdCHAPb infected cardiomyocytes.

*CHAP does not directly affect actin signaling in is not affected in muscle cells*

To investigate if the fibers in cells with CHAPb were F-actin fibers, we stained the cells for F-actin (phalloidin) and co-stained for α-actinin-2. In AdGFP infected E17.5 cardiomyocytes phalloidin had a sarcomeric staining pattern (Figure 4, upper panel, arrows). In AdCHAPa infected cells a disrupted pattern for F-actin was observed (Figure 4, middle panel, arrows) and in AdCHAPb infected cells phalloidin indeed stained the fibers, which co-stained for α-actinin-2. These results show that CHAPb induces actin stress fibers.

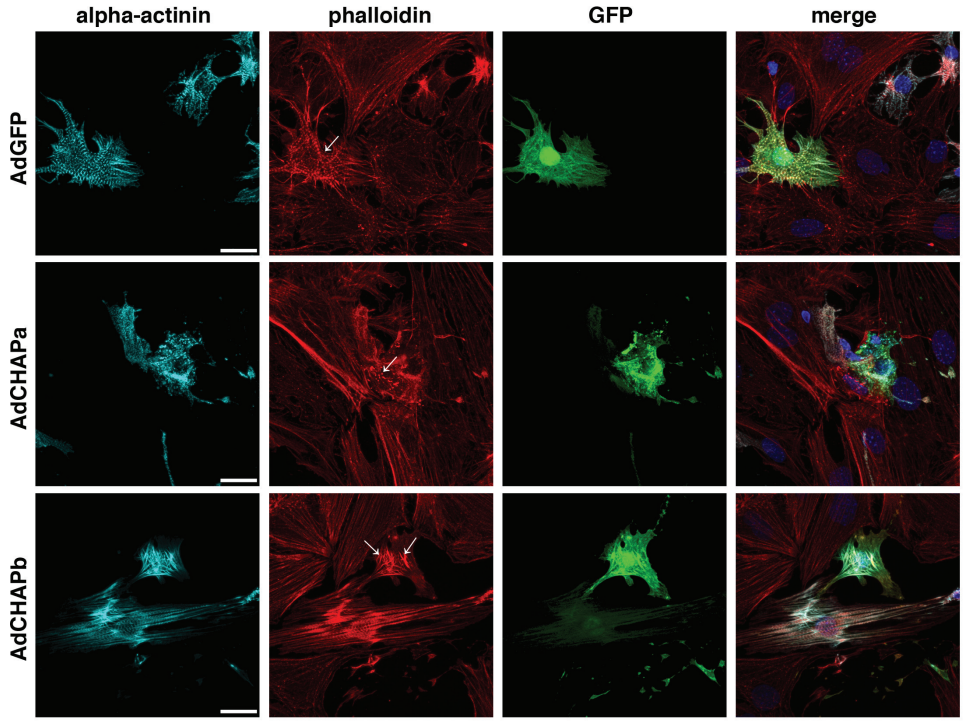


**Figure 4: CHAPb, but not CHAPa, overexpression induces F-actin fibers. Mouse cardiomyocytes were infected with AdGFP, AdCHAPa or AdCHAPb and stained for phalloidin (F-actin, red)/CHAP (cyan). Infected cells can be identified by GFP signal (green), nuclei are stained blue, merge images are shown. In AdGFP infected cardiomyocytes (upper panels) phalloidin has a sarcomeric staining pattern. In AdCHAPa infected cardiomyocytes (middle panels) the sarcomeric phalloidin staining is disrupted, while in AdCHAPb infected cardiomyocytes (lower panels) phalloidin stains the fibers.**

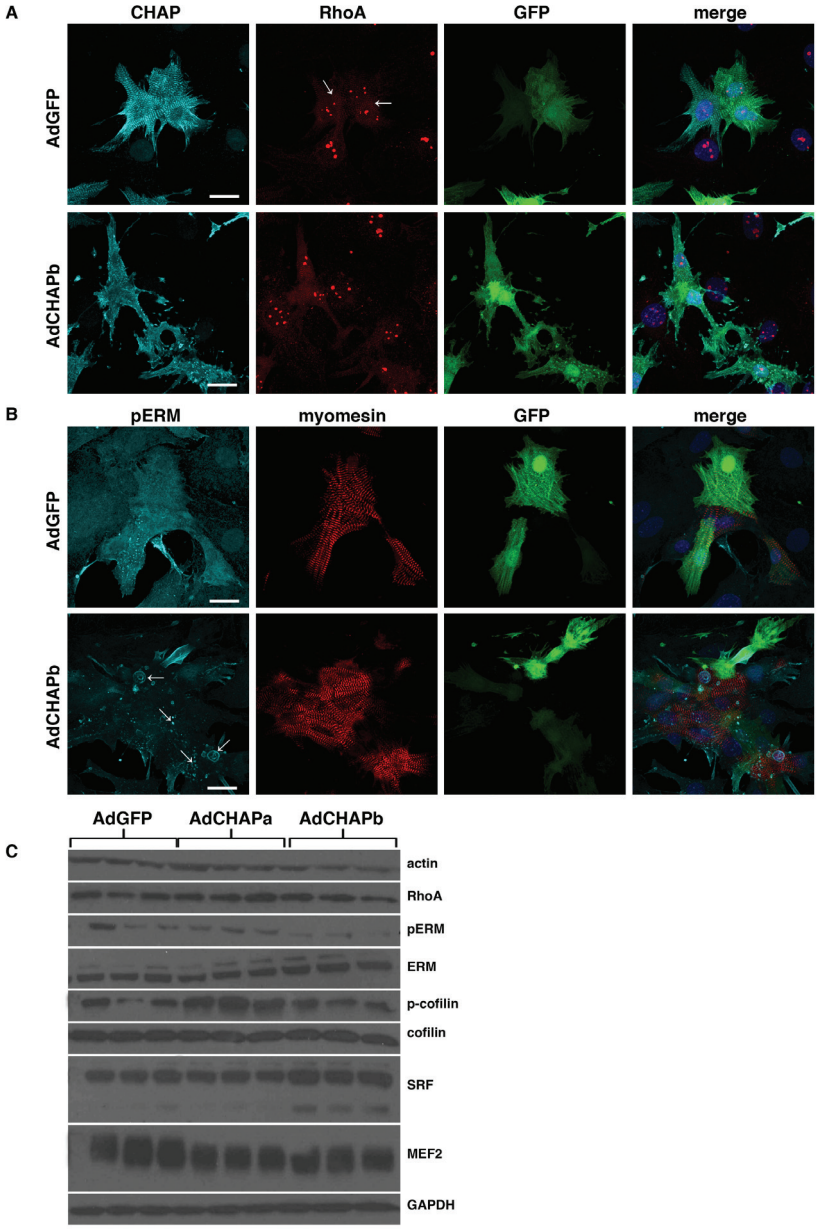


**Figure 5: Actin signaling in AdCHAPb infected cells. Mouse cardiomyocytes were infected with AdGFP or AdCHAPb and stained for CHAP (cyan)/ RhoA (red, A) or pERM (cyan)/myomesin (red, B). A) Infected cells can be identified by GFP signal (green), nuclei are stained blue, merge images are shown. In AdGFP infected cardiomyocytes RhoA has a sarcomeric staining pattern (upper panels, arrows), while in AdCHAPb infected cardiomyocytes RhoA sarcomeric expression pattern is lost (lower panels). B) In AdGFP infected cardiomyocytes pERM expression is diffuse (upper panels), whereas in AdCHAPb infected cells pERM localizes at the cell membrane (lower panel, arrows). C) Western blot showing expression of actin, RhoA, pERM, ERM, p-cofilin, cofilin, SRF and MEF2 in mouse cardiomyocytes after infection with AdGFP (n=3), AdCHAPa (n=3) or AdCHAPb (n=3). GAPDH was used as loading control.**

Since we previously observed activation of actin-dependent signaling in CHAPb Tg mice (Chapter 4), indicated by upregulated levels of RhoA, actin, α-actinin-2, Ezrin/Moesin/Radixin (ERM), and SRF) at 6 months of age, we investigated whether cellular changes seen in AdCHAPa- or b infected cells were also mediated trough the actin signaling pathway.
In AdGFP infected E17.5 cardiomyocytes RhoA was expressed at high levels in the nucleus in a dotted pattern combined with a sarcomeric expression (Figure 5A, upper panels, arrows). In AdCHAPb infected cells the sarcomeric expression of RhoA was lost, whereas the nuclear expression was not affected (Figure 5A, lower panels). Expression of pERM in AdGFP infected cells was diffuse (Figure 5B, upper panels), whereas expression in AdCHAPb infected cells pERM was expressed at the membrane of the cells (Figure 5B, lower panels, arrows). Next, we investigated the protein expression levels of other components of the actin signaling pathway, actin, RhoA, pERM, ERM, p-cofilin, cofilin, Serum Response Factor (SRF) and Myocyte Enhancer Factor 2 (MEF2) in AdGFP, AdCHAPa and AdCHAPb infected cells. No difference in expression levels were found between the different conditions (Figure 5C). Although, in one experiment, we observed a slight upregulation in p-cofilin in AdCHAPa infected cells and pERM and SRF in AdCHAPb infected cells, these results could not be repeated in other experiments using a different batch of cardiomyocytes. Furthermore, shorter exposure (24 hours) and analysis at a later time point after infection (7 days) did not display any differences between the various conditions (data not shown). These results show that the actin signaling pathway is not directly activated. Although, expression patterns for both RhoA and pERM were affected in AdCHAPb infected cells, compared to the AdGFP control cells, the expression levels of the actin signaling pathway are not affected.

*CHAP causes downregulation of hypertrophic markers and translocation of NFAT*
In the previous chapter we have seen that CHAPb Tg mice displayed cardiac hypertrophy which was combined with activation of genetic markers of cardiac hypertrophy. In order to study whether CHAP isoforms have a direct effect on the activation of hypertrophic markers we studied hypertrophic markers following adenoviral overexpression. Surprisingly, we observed a clear downregulation of hypertrophy markers. Both ANF (Figure 6A, *Nppa*) and BNP (Figure 6B, *Nppb*) were downregulated to the same extent in AdCHAPa and AdCHAPb cells when compared to AdGFP cells. β-MHC (Figure 6D, *Myh7*) displayed a stronger downregulation in AdCHAPa than in AdCHAPb infected cardiomyocytes. Moreover, α-MHC gene expression (Figure 6C, *Myh6*), which is usually downregulated in cardiac hypertrophy, was increased in AdCHAPa and AdCHAPb infected cells. In addition we also investigated the expression levels of SERCA2A, endogenous *ChapB*, Connexin40, 43 and CollagenI and III, but no differences were detected (data not shown).
The calcineurin-Nuclear Factor of Activated T-cells (NFAT) pathway has been described in many studies as a crucial pathway in the onset and progression of cardiac hypertrophy. Therefore, we investigated the expression of NFAT2c isoform in infected E17.5 cardiomyocytes. Whereas in AdGFP infected cells NFAT2c was localized in the nucleus (Figure 7, upper panels, arrows), in AdCHAPa and AdCHAPb infected cells NFAT2c was translocated to the cytoplasm, suggesting that overexpression of CHAP is able to inhibited calcineurin-NFAT dependent pathway (Figure 7, middle and lower panels, arrow heads).

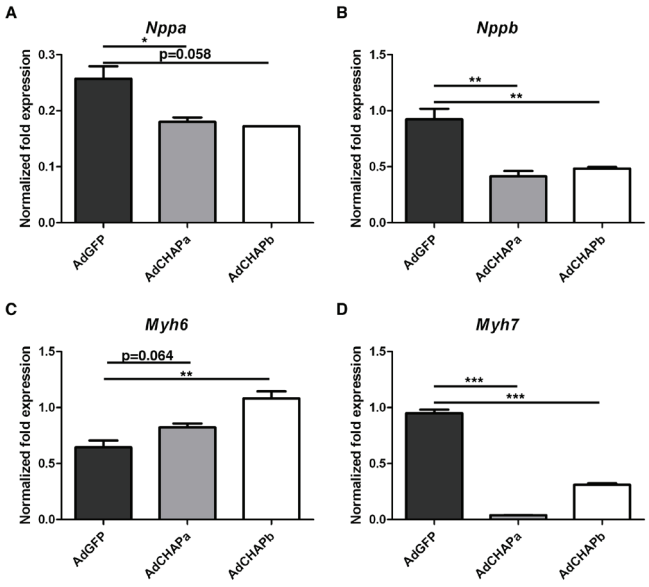


**Figure 6: qPCR analysis of hypertrophy markers. Mouse cardiomyocytes were infected with AdGFP (dark grey bars), AdCHAPa (light grey bars) or AdCHAPb (white bars) and expression of *Nppa* (A), *Nppb* (B), *Myh6* (C) or *Myh7* (D) was analyzed. *Gapdh*, *Pgk* and *H2A* were used as internal controls.**

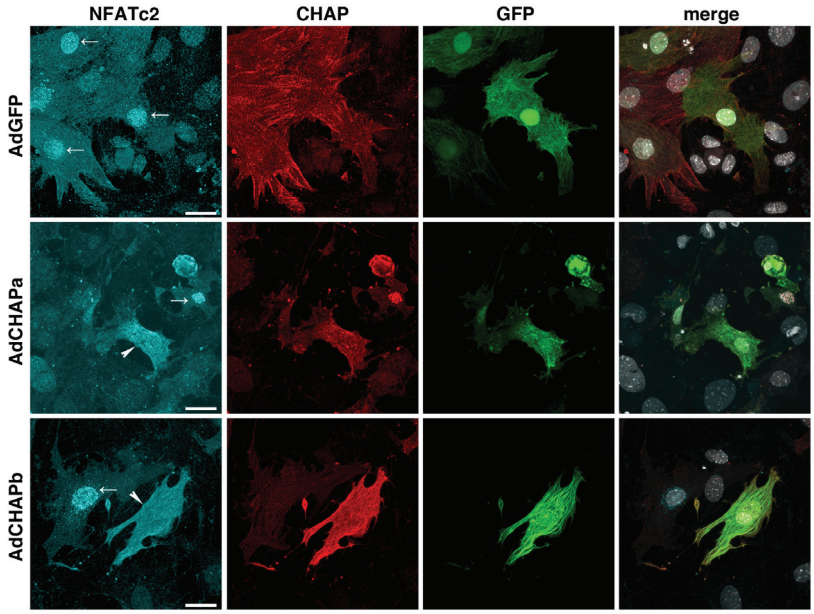


**Figure 7: NFATc2 localization is affected by CHAPa and CHAPb. Mouse cardiomyocytes were infected with AdGFP, AdCHAPa or AdCHAPb and stained for NFATc2 (cyan)/CHAP (red). Infected cells can be identified by GFP signal (green), nuclei are stained gray, merge images are shown. In AdGFP infected cells NFATc2 is localized in the nucleus (arrows). In AdCHAPa and AdCHAPb infected cells a cytoplasmic localization for NFATc2 is observed (arrow heads). In some AdCHAPa infected cells both CHAP and NFATc2 were localized in the nucleus and co-staining of these proteins was observed (middle panels).**

# Discussion

Previously we generated transgenic (Tg) mice that overexpress one of both isoforms of CHAP specifically in the heart. Whereas the CHAPa Tg mice did not develop a phenotype, CHAPb Tg mice developed features of cardiomyopathy, which includes cardiac hypertrophy with diastolic dysfunction. Furthermore, regionalized suppression of connexin 40, formation of stress fibers, increased collagen production and activation of the actin signaling pathway were observed. In order to understand the direct effects of CHAP we have analyzed the *in vitro* function of CHAPa and CHAPb by overexpressing these proteins in mouse cardiomyocytes and skeletal muscle cells (C2C12). To study the effects of CHAP overexpression we developed CHAPa and CHAPb adenoviruses.

*CHAPa regulates Z-disc integrity*

We have shown in a previous study that CHAPa is co-localized with actin and localizes to the Z-disc as shown by overexpression in rat neonatal cardiomyocytes, suggesting a putative interaction of CHAPa with α-actinin-2, a Z-disc marker[7]. Besides that CHAPa is expressed in adult heart and skeletal muscle (see chapter 2). Therefore, we expect CHAPa to be essential for adult cardiac and skeletal muscle function. Here we generated CHAPa adenovirus to investigate the function of CHAPa *in vitro*. Infection of mouse cardiomyocytes with AdCHAPa resulted in a robust overexpression. Overexpression of CHAPa in E17.5 cardiomyocytes, as wells as skeletal muscle cells (C2C12) resulted in Z-disc disruption. Both, CHAPa and α-actinin-2 were ectopically expressed, while myomesin, a m-band marker, is not affected. Several mouse models have shown that disruption of the Z-disc results in development of dilated cardiomyopathy (DCM). Cypher (Oracle/ZASP) is a PDZ-LIM protein that is expressed in the heart[16, 17] and interacts with α-actinin-2 at the Z-disc[17]. Disruption of Cypher expression leads to the development to DCM in humans, mice and zebrafish[18-22]. Enigma homologue protein (ENH) is another PDZ-LIM protein which interacts with α-actinin-2, Cypher and calsarcin-1[23], and disruption of its expression results in loss of Cypher and calsarcin-1 expression, which leads to development of a DCM phenotype[24]. Cypher and ENH interact with Z-disc protein α-actinin-2 through their PDZ-domains[17, 23]. Given the fact that CHAPa localizes at the Z-disc and bares a PDZ-domain as well, makes it tempting to speculate that the PDZ-domain in CHAPa is responsible for interaction with α-actinin-2. However, CHAPb, the isoform lacking the PDZ-domain, can interact with α-actinin-2 as well[7], therefore it would also possible that the PDZ-domain in CHAPa is not responsible for interaction with α-actinin-2, but interacts with a different subset of cytoskeletal proteins. Therefore, it would be of interest to investigate interaction partners of the CHAPa PDZ-domain by immunoprecipitation experiments. In addition, investigating the function of CHAPa in the cypher/ENH complex would be possible by deleting it conditionally from the heart.

*CHAPb induces actin stress fibers*

Activation of RhoA promotes both the inhibition of actin depolymerization via the Rho-associated kinase (ROCK)-LIM-kinase-cofilin pathway and the polymerization of actin via profilin, leading to a shift from G-actin to F-actin[25, 26]. Synaptopodin and myopodin are involved in actin bundling via α-actinin [8, 11]and RhoA[12]. Myocardin-related transcription factors (MRTFs) are inhibited by G-actin and depletion of the G-actin pool leads to nuclear localization of the MRTFs. In the nucleus they can act as transcriptional cofactors for SRF[26].

Striated muscle activator of Rho Signaling (STARS) is a novel muscle specific activator of RhoA and regulates thereby the activity of SRF in muscle cells[27, 28]. The transcription of STARS in turn is regulated by MEF2[29]. Cardiac-specific overexpression of MEF2A and MEF2C results in development of DCM[30], whereas knockout models of MEF2A and MEF2D have shown that these factors are involved in the expression of genes regulating contractility and energy metabolism and genes involved in stress-dependent remodeling of the heart, respectively[31, 32]. We have shown the formation of stress fibers by staining for α-actinin-2 by CHAPb *in vivo* (chapter 4). In CHAPb Tg mice the formation of stress fibers was correlated with the induction of actin signaling, demonstrated by the increased expression of RhoA, actin, ERM, cofilin, SRF and MEF2. Furthermore, in hearts of CHAPb Tg mice we showed etopic expression of pERM and RhoA. Here we show, that overexpression of CHAPb *in vitro*, in E17.5 cardiomyocytes as well as skeletal muscle cells, results in similar F-actin. Although we obtained similar results for RhoA and pERM localization, there is no increased expression of the actin signaling pathway. This could imply that the induction of actin signaling is a secondary effect in CHAPb Tg mice. Another explanation could be that members of the actin signaling pathway are already high expressed in embryonic cardiomyocytes. RhoA, for example, is high expressed during development and down regulated in adult heart[33]. Furthermore, the F-actin to G-actin balance might differ between embryonic and adult cardiomyocytes. In addition it maybe possible that stress fiber formation in this model is regulated via a different mechanism, for example via calcineurin-NFAT signaling (see next section).

*Role of CHAPa and CHAPb in cardiomyocyte hypertrophy and the calcineurin-NFAT signaling pathway*

The calcineurin-NFAT signaling pathway is an essential pathway in the development of hypertrophy. In this pathway the phosphatase calcineurin dephosphorylates NFAT, which leads to its nuclear localization and induction of hypertrophy marker genes like ANF, BNP and β-MHC[3]. Transgenic mice expressing a constitutively active form of the calcineurin catalytic subunit in the heart developed hypertrophy[34], which was mediated by NFATc2 and NFATc3[35, 36]. The nuclear localization of myopodin is regulated by calcineurin as well; phosphorylation dependent binding of 14-3-3 protein to myopodin and subsequent nuclear localization is regulated by PKA and CaMKII, which phosphorylate myopodin and calcineurin, involved in dephosphorylating myopodin[10]. Furthermore, the stability of synaptopodin and its actin-bundling activity is regulated through a similar mechanism in kidney podocytes, in this way linking actin dynamics and calcineurin signaling[37]. It would be of interest to investigate if CHAP stability can be regulated via similar phosphorylation processes. Overexpression of CHAPa or CHAPb in E17.5 cardiomyocytes resulted in translocation of NFATc2 from the nucleus to the cytoplasm. In line with this, the expression levels of the hypertrophy markers were decreased after overexpression of CHAPa or CHAPb. Interestingly, whereas β-MHC was decreased, α-MHC expression on the other hand was increased. Changes in the ratio of both MHC proteins is not only indicative for cardiac hypertrophy, but as well for the maturation phase of cardiac cells, with high levels of α-MHC and low levels of β-MHC. Therefore, decrease in the above mentioned markers may indicate that CHAP either has an anti-hypertrophic activity or a maturation-promoting effect in striated muscle cells. However, these results are in contrast to the observed increase of hypertrophy markers in CHAPb Tg mice (chapter 4), which might indicate an indirect upregulation of these markers in the CHAPb Tg mice. Furthermore, we have to take into account that the cardiomyocytes used for these experiments

are fetal and will have a fetal expression pattern of genes. Therefore, expression of ANF, BNP and β-MHC is expected to be high, whereas α-MHC expression is low. In the adult CHAPb Tg mice however, expression of these markers are low and increase with age. Therefore, the decrease of these factors in AdCHAPa and AdCHAPb infected cardiomyocytes might reflect a morphological change, partially to a more mature or adult phenotype. To investigate the effect of CHAPa and CHAPb on gene expression the use of reporter genes would be an alternative.

*Conclusion*
Here we show that by *in vitro* overexpressing of CHAPa and CHAPb these two proteins have distinct functions. Whereas CHAPa is involved in Z-disc integrity, CHAPb induces F-actin fibers. It would be interesting to investigate the roles of CHAPa and CHAPb in vivo by conditionally deleting one of both isoforms. For example, we generated floxed CHAP$^{f/+}$ mouse embryonic stem cells (chapter 3) and mouse lines generated from this line can be intercrossed with specific Cre transgenic mice. A CHAPb knock out can be obtained by making use of a α-MHC-Cre or Nkx2.5-Cre, whereas CHAPa can be conditionally deleted by crossing with a tamoxifen inducible mouse line. Furthermore, using a CHAP knock out approach, the role of CHAP in calcineurin-induced hypertrophy can also be investigated *in vivo*, by crossing CHAP knock out mice to calcineurin Tg mice.
In addition, investigating the role of PKA, CaMKII and calcineurin in the stability of CHAP by *in vitro* phosphorylation and inhibition experiments, could clarify the role of calcineurin signaling in CHAP mediated stress fiber formation.

Thus in contrast to what was found in CHAPb Tg mice, overexpression of both CHAPa and CHAPb in vitro leads to downregulation of the hypertrophy markers ANF, BNP and β-MHC, which might be caused by a translocation of NFATc2 from the nucleus to the cytosol upon CHAPa and CHAPb overexpression.

# References


(1) Beqqali A, van Eldik W, Mummery C, Passier R. Human stem cells as a model for cardiac differentiation and disease. *Cell Mol Life Sci* 2009 March;66(5):800-13.

(2) Barry SP, Davidson SM, Townsend PA. Molecular regulation of cardiac hypertrophy. *Int J Biochem Cell Biol* 2008;40(10):2023-39.

(3) Wilkins BJ, Molkentin JD. Calcium-calcineurin signaling in the regulation of cardiac hypertrophy. *Biochem Biophys Res Commun* 2004 October 1;322(4):1178-91.

(4) Lange S, Ehler E, Gautel M. From A to Z and back? Multicompartment proteins in the sarcomere. *Trends Cell Biol* 2006 January;16(1):11-8.

(5) Frank D, Kuhn C, Katus HA, Frey N. The sarcomeric Z-disc: a nodal point in signalling and disease. *J Mol Med* 2006 June;84(6):446-68.

(6) Cox L, Umans L, Cornelis F, Huylebroeck D, Zwijsen A. A broken heart: a stretch too far: an overview of mouse models with mutations in stretch-sensor components. *Int J Cardiol* 2008 December 17;131(1):33-44.

(7) Beqqali A, Monshouwer-Kloots J, Monteiro R, Welling M, Bakkers J, Ehler E, Verkleij A, Mummery C, Passier R. CHAP is a newly identified Z-disc protein essential for heart and skeletal muscle function. *J Cell Sci* 2010 April 1;123(Pt 7):1141-50.

(8) Weins A, Schwarz K, Faul C, Barisoni L, Linke WA, Mundel P. Differentiation- and stress-dependent nuclear cytoplasmic redistribution of myopodin, a novel actin-bundling protein. *J Cell Biol* 2001 October 29;155(3):393-404.

(9) Faul C, Huttelmaier S, Oh J, Hachet V, Singer RH, Mundel P. Promotion of importin alpha-mediated nuclear import by the phosphorylation-dependent binding of cargo protein to 14-3-3. *J Cell Biol* 2005 May 9;169(3):415-24.

(10) Faul C, Dhume A, Schecter AD, Mundel P. Protein kinase A, Ca2+/calmodulin-dependent kinase II, and calcineurin regulate the intracellular trafficking of myopodin between the Z-disc and the nucleus of cardiac myocytes. *Mol Cell Biol* 2007 December;27(23):8215-27.

(11) Asanuma K, Kim K, Oh J, Giardino L, Chabanis S, Faul C, Reiser J, Mundel P. Synaptopodin regulates the actin-bundling activity of alpha-actinin in an isoform-specific manner. *J Clin Invest* 2005 May;115(5):1188-98.

(12) Asanuma K, Yanagida-Asanuma E, Faul C, Tomino Y, Kim K, Mundel P. Synaptopodin orchestrates actin organization and cell motility via regulation of RhoA signalling. *Nat Cell Biol* 2006 May;8(5):485-91.

(13) Goncalves MA, van dV, I, Janssen JM, Maassen BT, Heemskerk EH, Opstelten DJ, Knaan-Shanzer S, Valerio D, de Vries AA. Efficient generation and amplification of high-capacity adeno-associated virus/adenovirus hybrid vectors. *J Virol* 2002 November;76(21):10734-44.

(14) Luo J, Deng ZL, Luo X, Tang N, Song WX, Chen J, Sharff KA, Luu HH, Haydon RC, Kinzler KW, Vogelstein B, He TC. A protocol for rapid generation of recombinant adenoviruses using the AdEasy system. *Nat Protoc* 2007;2(5):1236-47.

(15) Knaan-Shanzer S, van dV, I, Havenga MJ, Lemckert AA, de Vries AA, Valerio D. Highly efficient targeted transduction of undifferentiated human hematopoietic cells by adenoviral vectors displaying fiber knobs of subgroup B. *Hum Gene Ther* 2001 November 1;12(16):1989-2005.

(16) Passier R, Richardson JA, Olson EN. Oracle, a novel PDZ-LIM domain protein expressed in heart and skeletal muscle. *Mech Dev* 2000 April;92(2):277-84.

(17) Zhou Q, Ruiz-Lozano P, Martone ME, Chen J. Cypher, a striated muscle-restricted PDZ and LIM domain-containing protein, binds to alpha-actinin-2 and protein kinase C. *J Biol Chem* 1999 July 9;274(28):19807-13.

(18) Zhou Q, Chu PH, Huang C, Cheng CF, Martone ME, Knoll G, Shelton GD, Evans S, Chen J. Ablation of Cypher, a PDZ-LIM domain Z-line protein, causes a severe form of congenital myopathy. *J Cell Biol* 2001 November 12;155(4):605-12.

(19) Zheng M, Cheng H, Li X, Zhang J, Cui L, Ouyang K, Han L, Zhao T, Gu Y, Dalton ND, Bang ML, Peterson KL, Chen J. Cardiac-specific ablation of Cypher leads to a severe form of dilated cardiomyopathy with premature death. *Hum Mol Genet* 2009 February 15;18(4):701-13.

(20) Cheng H, Zheng M, Peter AK, Kimura K, Li X, Ouyang K, Shen T, Cui L, Frank D, Dalton ND, Gu Y, Frey N, Peterson KL, Evans SM, Knowlton KU, Sheikh F, Chen J. Selective deletion of long but not short Cypher isoforms leads to late-onset dilated cardiomyopathy. *Hum Mol Genet* 2011 May 1;20(9):1751-62.

(21) Vatta M, Mohapatra B, Jimenez S, Sanchez X, Faulkner G, Perles Z, Sinagra G, Lin JH, Vu TM, Zhou Q, Bowles KR, Di LA, Schimmenti L, Fox M, Chrisco MA, Murphy RT, McKenna W, Elliott P, Bowles NE, Chen J, Valle G, Towbin JA. Mutations in Cypher/ZASP in patients with dilated cardiomyopathy and left ventricular non-compaction. *J Am Coll Cardiol* 2003 December 3;42(11):2014-27.

(22) van der Meer DL, Marques IJ, Leito JT, Besser J, Bakkers J, Schoonheere E, Bagowski CP. Zebrafish cypher is important for somite formation and heart development. *Dev Biol* 2006 November 15;299(2):356-72.

(23) Nakagawa N, Hoshijima M, Oyasu M, Saito N, Tanizawa K, Kuroda S. ENH, containing PDZ and LIM domains, heart/skeletal muscle-specific protein, associates with cytoskeletal proteins through the PDZ domain. *Biochem Biophys Res Commun* 2000 June 7;272(2):505-12.

(24) Cheng H, Kimura K, Peter AK, Cui L, Ouyang K, Shen T, Liu Y, Gu Y, Dalton ND, Evans SM, Knowlton KU, Peterson KL, Chen J. Loss of enigma homolog protein results in dilated cardiomyopathy. *Circ Res* 2010 August 6;107(3):348-56.

(25) Maekawa M, Ishizaki T, Boku S, Watanabe N, Fujita A, Iwamatsu A, Obinata T, Ohashi K, Mizuno K, Narumiya S. Signaling from Rho to the actin cytoskeleton through protein kinases ROCK and LIM-kinase. *Science* 1999 August 6;285(5429):895-8.

(26) Olson EN, Nordheim A. Linking actin dynamics and gene transcription to drive cellular motile functions. *Nat Rev Mol Cell Biol* 2010 May;11(5):353-65.

(27) Arai A, Spencer JA, Olson EN. STARS, a striated muscle activator of Rho signaling and serum re sponse factor-dependent transcription. *J Biol Chem* 2002 July 5;277(27):24453-9.

(28) Kuwahara K, Barrientos T, Pipes GC, Li S, Olson EN. Muscle-specific signaling mechanism that links actin dynamics to serum response factor. *Mol Cell Biol* 2005 April;25(8):3173-81.

(29) Kuwahara K, Teg Pipes GC, McAnally J, Richardson JA, Hill JA, Bassel-Duby R, Olson EN. Modula tion of adverse cardiac remodeling by STARS, a mediator of MEF2 signaling and SRF activity. *J Clin Invest* 2007 May;117(5):1324-34.

(30) Xu J, Gong NL, Bodi I, Aronow BJ, Backx PH, Molkentin JD. Myocyte enhancer factors 2A and 2C induce dilated cardiomyopathy in transgenic mice. *J Biol Chem* 2006 April 7;281(14):9152-62.

(31) Kim Y, Phan D, van RE, Wang DZ, McAnally J, Qi X, Richardson JA, Hill JA, Bassel-Duby R, Olson EN. The MEF2D transcription factor mediates stress-dependent cardiac remodeling in mice. *J Clin Invest* 2008 January;118(1):124-32.

(32) Naya FJ, Black BL, Wu H, Bassel-Duby R, Richardson JA, Hill JA, Olson EN. Mitochondrial deficiency and cardiac sudden death in mice lacking the MEF2A transcription factor. *Nat Med* 2002 November;8(11):1303-9.

(33) Ahuja P, Perriard E, Pedrazzini T, Satoh S, Perriard JC, Ehler E. Re-expression of proteins involved in cytokinesis during cardiac hypertrophy. *Exp Cell Res* 2007 April 1;313(6):1270-83.

(34) Molkentin JD, Lu JR, Antos CL, Markham B, Richardson J, Robbins J, Grant SR, Olson EN. A calcineurin-dependent transcriptional pathway for cardiac hypertrophy. *Cell* 1998 April 17;93(2):215-28.

(35) Wilkins BJ, De Windt LJ, Bueno OF, Braz JC, Glascock BJ, Kimball TF, Molkentin JD. Targeted disruption of NFATc3, but not NFATc4, reveals an intrinsic defect in calcineurin-mediated cardiac hypertrophic growth. *Mol Cell Biol* 2002 November;22(21):7603-13.

(36) Bourajjaj M, Armand AS, da Costa Martins PA, Weijts B, van der NR, Heeneman S, Wehrens XH, De Windt LJ. NFATc2 is a necessary mediator of calcineurin-dependent cardiac hypertrophy and heart failure. *J Biol Chem* 2008 August 8;283(32):22295-303.

(37) Faul C, Donnelly M, Merscher-Gomez S, Chang YH, Franz S, Delfgaauw J, Chang JM, Choi HY, Campbell KN, Kim K, Reiser J, Mundel P. The actin cytoskeleton of kidney podocytes is a direct target of the antiproteinuric effect of cyclosporine A. *Nat Med* 2008 September;14(9):931-8.

# Chapter 6

## Expression of CHAP in adult mouse tissues is correlated with filamentous actin expression

Willemijn van Eldik, Jantine Monshouwer-Kloots, Christine Mummery, Robert Passier

# Abstract

Previously, we have shown that CHAP is expressed in striated muscles during developmental stages and in adult tissues. Here, we analyzed CHAP expression in multiple mouse adult tissues and show that besides expression in striated and smooth muscle, CHAP is expressed in small intestine, kidney and brain in an isoform specific manner. Expression of CHAP in small intestine and kidney was co-localized with expression of filamentous actin. These results suggest that CHAP may be involved in actin signaling with a broader function as previously expected.

# Introduction

Actin is the major component of the cytoskeleton of eukaryotic cells. Many cellular processes, such as division, cell migration, vesicle transport, contractile force generation, cell polarity and cell shape changes are regulated by changes in actin dynamics[1-3]. In mammals and birds there are six different actin isoforms, which are encoded by six different genes. Four of these actin isoforms are muscle specific: α-skeletal actin, α-cardiac actin, α-smooth actin and γ2-smooth actin. The γ1-actin and β-actin are non-muscle isoforms and function in the assembly of the cytoskeleton of non-muscle cells[1, 3]. Monomeric actin (globular or G-actin) can assemble in filamentous actin (F-actin), and this balance is regulated by several actin binding proteins. Cofilin enhances actin filament turnover by severing actin filaments and promoting dissociation of actin monomers from the pointed ends of actin filaments. Profilin on the other hand, promotes assembly of F-actin fibers. Myosin binding to F-actin is essential for contraction in muscle cells. The myosin-actin interaction is also in important for other cellular processes, such as cytokinesis and cell migration[1, 3].

In the previous chapters we have described a novel Z-disc protein, which we named Cytoskeletal Heart-enriched Actin-associated Protein (CHAP)[7]. Two isoforms of CHAP exist: a longer isoform CHAPa and a shorter isoform CHAPb. Whereas CHAPb is expressed in the heart and somites during embryonic development CHAPa is expressed in adult heart and skeletal muscle[8]. We have previously shown that overexpression of CHAP resulted in actin stress fiber formation *in vivo* and *in vitro* (see chapter 4 and 5), suggesting a possible role in actin signaling. This is further corroborated by the fact that CHAP belongs to synaptopodin protein family, of which its other members have also been shown to be involved in actin bundling[4, 5]. Synaptopodin, the first described protein of this family, regulates formation of actin stress fibers, via RhoA signaling[6] and is expressed in brain and kidney[4]. Furthermore, myopodin, a second member of this family, is expressed in muscle cells and is also involved in actin signaling as well. It contains an actin binding site, binds directly to actin and has actin bundling activity[5].

In this chapter we analyzed the expression of CHAP in multiple adult tissues. We confirmed predominant expression of CHAPa and CHAPb isoforms in skeletal muscle by western blot analysis. However, low levels of CHAPb could also be detected in adult kidney, brain, small intestine and large intestine. This was confirmed by specific CHAP immunofluorescent staining on adult mouse tissue sections of kidney and intestine, which strongly co-localized with filamentous actin.

# Material and methods

*Animals*
Adult Swiss mice were sacrificed for the collection of organs. For RNA and protein isolation organs were rinsed in PBS, snap frozen in liquid nitrogen and stored at -80 °C until further use.
Organs for cryosections were perfused, collected and rinsed in PBS. Subsequently, organs were processed as described in Bajanca et al[9]. Briefly, organs were fixed in 0.2% PFA solution containing 4% sucrose, 0.12mM $CaCl_2.2H_2O$, 0.2M $Na_2HPO_4.2H_2O$, 0.2M $NaH_2PO_4.H_2O$ over night at 4 °C. Then, organs were washed in the same solution without PFA during the day at 4 °C, followed by 0.24M phosphate buffer and 30% sucrose over night at 4 °C. The next day embryos were embedded in Tissue-Tek (Sakura Finetek) on dry ice and stored at -20 °C until sectioning.

*RNA isolation and cDNA synthesis*
Organs were homogenized in Trizol (Invitrogen) using the Ultra Turrax tissue separator (IKA, Germany). Then RNA was isolated according to the manufacturers protocol. RNA was treated with DNase (DNA-free, Ambion) and cDNA was synthesized (iScript BioRad). qPCR was performed using the CFX96 Real-Time PCR detection system (Bio-Rad). The following primers were used: *ChapA* (sense: 5'-GAGGAGGTGCAGGTCACATT-3'; antisense: 5'-CTGAAGAGCCTGGGAAACAG-3'), *ChapB* (sense: 5'-CCGCCGCTTCTTAAACATAA-3 antisense: 5'-GGCTTTAAAGGGCCTTGG-3') and as reference gene *Gapdh* (sense: 5'-GTTTGTGATGGGTGTGAACCAC-3', antisense: 5'-CTGGTCCTCAGTGTAGCCCAA-3'). Data were analyzed with Bio-Rad CFX Manager and presented as mean +/- standard error.

*Protein isolation and western blot*
For protein isolation organs were crushed on liquid nitrogen and dissolved in T-PER tissue protein extraction reagent (Pierce) with extra added protein inhibitors (protease inhibitor cocktail tablets (10 µg/ml; Roche, Germany), 0.1 mmol/L dithiothreitol (DTT; Invitrogen) and 1 mmol/L phenylmethanesulfonylfluoride (PMSF; Sigma Aldrich), 5 mmol/L NaF and 1 mmol/L $Na_3VO_4$). Samples were incubated on ice for 15 minutes and centrifuged at 10.000 RPM at 4 °C for 10 minutes and supernatants were transferred to new tubes. Protein concentration was measured with the Bradford assay (Bio-rad) using bovine serum albumin (BSA) for a standard curve. Then 5x sample buffer (100 mM Tris-HCl pH 6.8, 10% SDS, 50% glycerol, 25% β-mercaptoethanol and bromphenol blue) was added and samples were boiled for 5 minutes at 95 °C. Protein gels were loaded with 50 µg protein. Gels were blotted (Hybond-P, GE healthcare) for 3 hours at room temperature and blocked for one hour with 5% milk/Tris Buffered Saline-tween (TBS-T: 50mM Tris-HCl pH 7.5, 125 mM NaCl, 0.02% Tween-20). First antibody diluted in 5% milk/TBS-T was applied over night at 4 °C. Antibodies used were CHAP (1:200, custom made by Eurogentec) and GAPDH (1:10000, Millipore). Secondary antibody was applied for 1 hour at room temperature. Secondary antibodies used were anti-mouse IgG HRP (1:1000, Cell Signaling Technology) or anti-rabbit IgG HRP (1:2000, Cell Signaling Technology) dissolved in 5% milk/TBS-T. Blots were visualized by using SuperSignal West Pico Chemiluminescent Substrate (Pierce).

*Immunofluorescence*

Organs were sectioned (5 μM) and mounted on starfrost slides (Knittel). Antibody stainings were performed as described by van Laake et al[10]. Antibodies used were CHAP (1:50, custom made by Eurogentec), α-smooth muscle actin (1:500, 1A4, Sigma-Aldrich Chemie), RhoA (1:100, Santa Cruz). Secondary antibodies were as follows: Cy-3 conjugated anti-rabbit (1:250, Jackson Immunoresearch Laboratories) and Alexa488 conjugated anti-mouse (1:200, Invitrogen). F-actin fibers were stained with phalloidin conjugated Alexa488 (1:100, Invitogen) in PBS for 20 minutes. Cell nuclei were stained with TO-PRO (Invitrogen) and slides were enclosed with Prolong Gold (Invitrogen). Stainings were analyzed with SL confocal microscope.

# Results

We have previously demonstrated that CHAP is expressed embryonic and adult heart and skeletal muscle and also in smooth muscle cells. To analyze CHAP expression in other adult organs we first isolated RNA from different mouse organs, followed by quantitative analysis of *ChapA* and *ChapB* expression levels (Figure 1A). Expression levels for *ChapA* and *ChapB* were, as expected, highest in skeletal muscle. Nevertheless, expression levels for particularly *ChapB* could also be observed in the other tissues: kidney, brain, stomach, intestine, spleen and lung. *ChapA* was expressed at lower levels but still detectable in kidney small intestine and lung. In order to determine whether CHAPa and b proteins were expressed in these tissues we performed western blot analysis (Figure 1B). Whilst in skeletal muscle both CHAPa (140 kDa) and CHAPb (110 kDa) could be clearly detected, in the other tissues examined we only could detect expression at the height, which corresponds to the size of CHAPb, in kidney, brain, small intestine and large intestine, confirming qPCR results the mRNA expression levels. Although there was a slight difference in the height of the bands between the organs, this may be explained by posttranslational modifications.

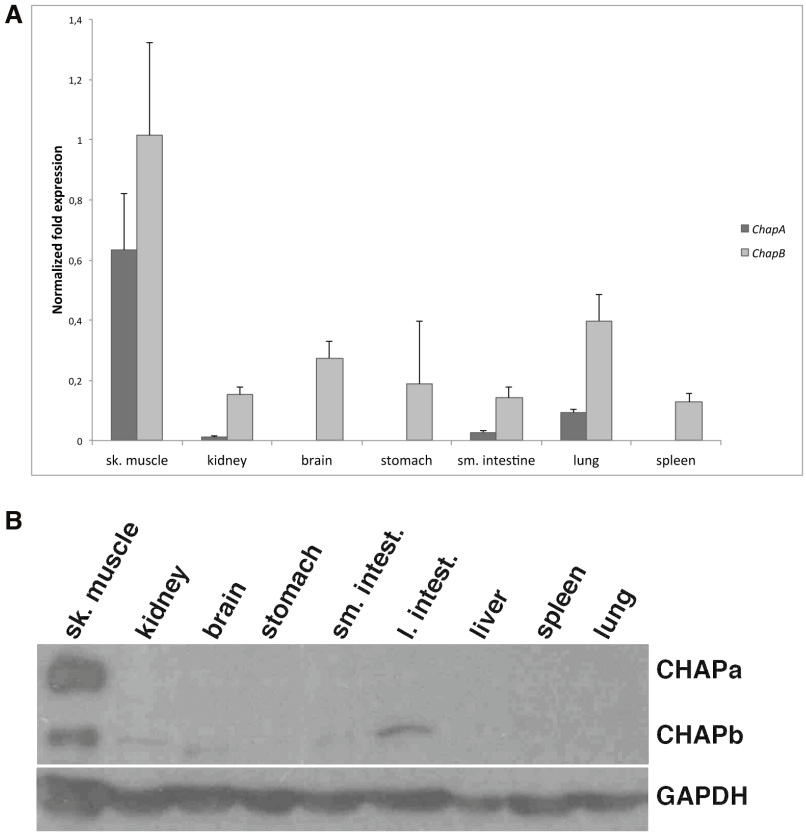


**Figure 1: Expression analysis of CHAP in adult tissues . A) qPCR expression analysis of *ChapA* (dark gray bars) and *ChapB* (light gray bars) in skeletal muscle, kidney, brain, stomach, small intestine, lung and spleen. *Gapdh* was used as internal control. B) Western blot showing expression of CHAP in kidney, brain, small intestine and large intestine. GAPDH was used as loading control.**

Next we analyzed expression of CHAP by immunohistochemistry on cryosections of these organs. Since we have recently described that CHAP is expressed in smooth muscle cells we co-stained sections of the intestine with α-smooth muscle actin (ASMA). However, no significant CHAP staining was observed in the smooth muscle layer of the small intestine (Figure 2A). Instead, we found CHAP to be expressed in the villus of the small intestine. CHAP expression was not detected in the bottom of the crypt, but was found in differentiated endothelial cells in a dotted pattern and expression was lost at the tip of the villus. Thus expression of CHAP was restricted to the central part of the villus, which contains differentiated endothelial cells. Besides this expression of CHAP, expression was also found in the center of the villus (Figure 2B). The homolog of CHAP, Synaptopodin, is involved in actin polymerization via RhoA and found that RhoA was upregulated and ectopically expressed in CHAPb Tg mice (see chapter 4). Therefore, we co-stained the small intestine for RhoA. Similar to the localization of CHAP, RhoA was expressed in the center of the villus. However, no co-immunostaining of CHAP and RhoA was found (Figure 2C), indicating that CHAP and RhoA were not expressed in the similar cells.

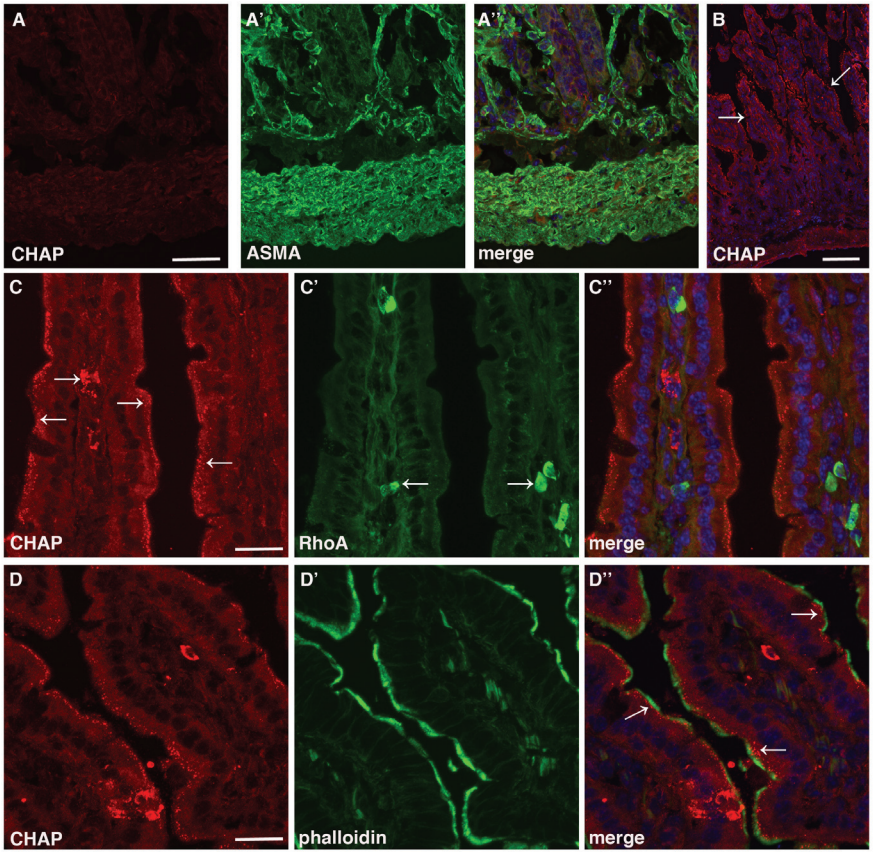


**Figure 2: CHAP expression in the small intestine. A) Staining of the smooth muscle layer for CHAP (red; A) and α-smooth muscle actin (green, A'), merge images are shown (A"). B) CHAP is expressed in the villi of the small intestine in a dotted pattern (arrows). C) Staining of the villus for CHAP (red; C) and RhoA (green; C'), merge images are shown (C"). D) Staining of the villus for CHAP (red; D) and phalloidin (green, D'), merge images are shown (D"). Scale bars 20 µm in A, C and D and 100 µm in B.**

In the hearts of CHAPb Tg mice we observed actin stress fibers and upregulation of the actin pathway (see chapter 4). To investigate if CHAP localization correlated with filamentous actin (F-actin) localization, we co-stained with phalloidin. F-actin stained the microvilli of a villus. No co-localization of CHAP with F-actin was observed. Instead, CHAP was expressed adjacent to the F-actin stained microvilli (Figure 2D), showing that expression of CHAP was restricted to the roots of the microvilli.
Next we analyzed expression of CHAP in the kidney. Synaptopodin is expressed in kidney podocytes of the glomerulus. Staining of the kidney for CHAP showed that CHAP was expressed in the kidney tubules but not in the glomerulus (Figure 3A and B). Similar as in the small intestine, no co-staining was found of CHAP with RhoA, which was expressed in the glomerulus (Figure 3A). However, co-staining of CHAP with F-actin, which stains the tubule microvilli, showed that as in the small intestine, CHAP localization was adjacent to that of F-actin in the kidney tubules (Figure 3B and C). Thus, CHAP expression was restricted to the roots of the kidney tubule microvilli, suggesting a similar staining pattern as observed in the small intestine.
We also analyzed the expression of CHAP in the brain, however no specific CHAP immunostaining could be detected, although we cannot exclude CHAP expression in specific locations in the brain, that we may have missed in the current analysis.

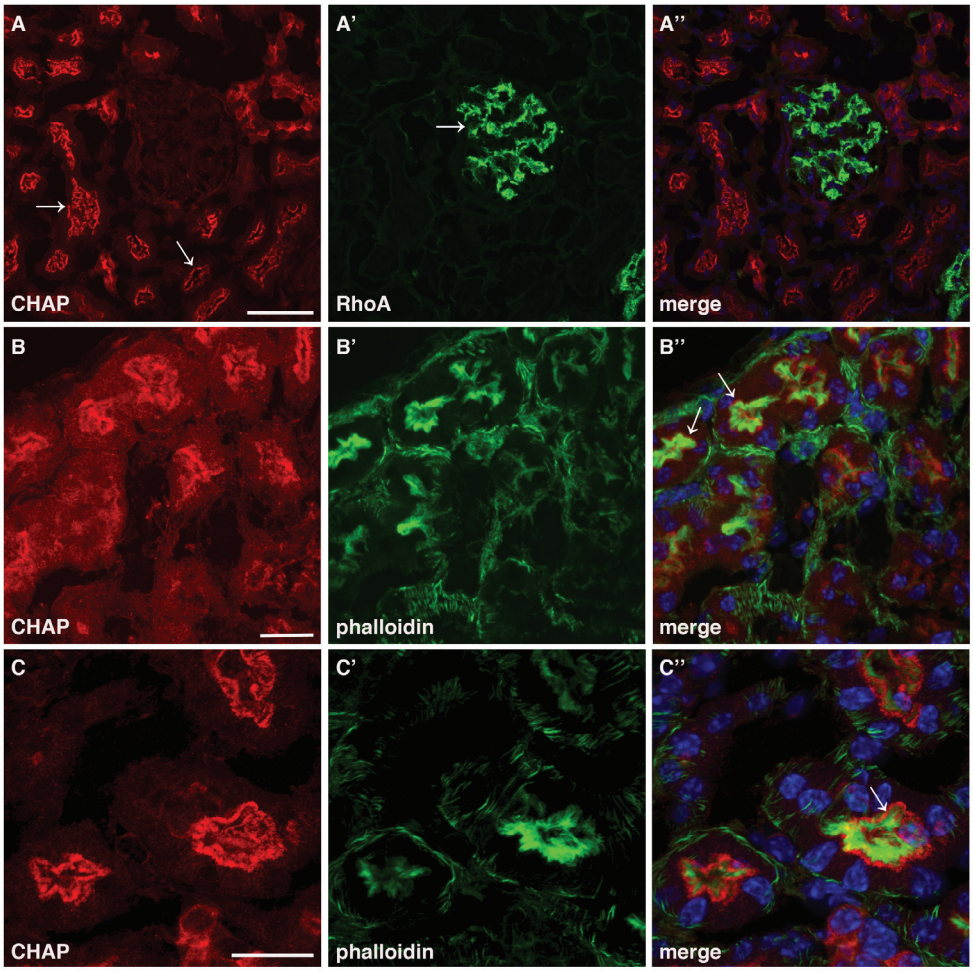


Figure 3: CHAP expression in the kidney. A) CHAP (red) is expressed in the kidney tubules and not in the glomeruli, where RhoA (green) is expressed. Merge images are shown (A"). B and C) Staining of kidney tubules for CHAP (red; B and C) and phalloidin (green; B' and C'). Merge images are shown (B" and C"). Scale bars 50 µm in A, 20 µm in B and C.

# Discussion

In this chapter we analyzed the expression of CHAP in a variety of adult organs Previously we have shown that CHAP is expressed in striated muscles (heart and skeletal muscle) and also in smooth muscle cells. Here, we show that CHAP is also expressed in brain, small intestine and kidney. Based on western blot analysis, we conclude that in these organs only CHAPb is expressed. From previous chapters (chapter 4 and 5), we have observed that CHAPb is involved in actin bundling activity (chapter 4 and 5). Immunofluorescence stainings show that CHAP is expressed in the roots of the microvilli of the small intestine and kidney tubules. Microvilli are cylindrical membrane protrusions and have been identified in the small intestine, kidney proximal tubules, and brain. Functions of the villi are increasing the surface area, vesicle releasement, fluid flow sensing and mechano-transduction. Microvilli are composed of actin bundels, which are oriented with the barbed end at the villus tip and the pointed end at the bottom of the bundle. The actin bundles are cross-linked by several cross-linking and membrane-linking proteins, such as myosins. At the bottom of the villus proteins are found that prevent the depolymerization of the actin filaments[11]. For example, tropomyosin is a rootlet protein in microvilli of the small intestine[12] and kidney[13], and has been shown to prevent actin depolymerization by competing with binding to actin with cofilin[13, 14]. Like tropomyosin, CHAP could be involved in preventing actin depolymerization as well.

It would be interesting to investigate expression of CHAP in relation to actin. For example, stereocillia are specialized microvilli on the sensory hair cells of the cochlea and vestibular apparatus[11], where CHAP could be expressed as well. In addition, filopodia are single actin membrane protrusion, involved in cell movement[11], where CHAP expression can be investigated as well. Finally, in cancer cells, actin is necessary for cell movement and in these cells CHAP could function as a tumor suppressor by preventing actin polymerization. Indeed, myopodin has been identified as a tumor suppressor in prostate cancer, as it is (partially) deleted in invasive prostate cancers[15, 16] and inhibits tumor growth *in vitro* and *in vivo*[16].

The results of this chapter show that CHAPb is expressed in a pattern, which is closely related to the presence of filamentous actin and is expressed in different tissue besides heart and skeletal muscle. On the other hand, CHAPa seems to be more restricted to the striated muscles, although we cannot exclude that western blot analysis was not sensitive enough to detect CHAPa protein levels. Furthermore, these results show that CHAPa is muscle-specific expressed, whereas CHAPb is expressed during muscle development and in non-muscle adult tissues.

# References


(1) Perrin BJ, Ervasti JM. The actin gene family: function follows isoform. *Cytoskeleton (Hoboken )* 2010 October;67(10):630-4.

(2) Ono S. Dynamic regulation of sarcomeric actin filaments in striated muscle. *Cytoskeleton (Hoboken )* 2010 November;67(11):677-92.

(3) Hild G, Bugyi B, Nyitrai M. Conformational dynamics of actin: effectors and implications for biological function. *Cytoskeleton (Hoboken )* 2010 October;67(10):609-29.

(4) Asanuma K, Kim K, Oh J, Giardino L, Chabanis S, Faul C, Reiser J, Mundel P. Synaptopodin regulates the actin-bundling activity of alpha-actinin in an isoform-specific manner. *J Clin Invest* 2005 May;115(5):1188-98.

(5) Weins A, Schwarz K, Faul C, Barisoni L, Linke WA, Mundel P. Differentiation- and stress-dependent nuclear cytoplasmic redistribution of myopodin, a novel actin-bundling protein. *J Cell Biol* 2001 October 29;155(3):393-404.

(6) Asanuma K, Yanagida-Asanuma E, Faul C, Tomino Y, Kim K, Mundel P. Synaptopodin orchestrates actin organization and cell motility via regulation of RhoA signalling. *Nat Cell Biol* 2006 May;8(5):485-91.

(7) Beqqali A, van Eldik W, Mummery C, Passier R. Human stem cells as a model for cardiac differentiation and disease. *Cell Mol Life Sci* 2009 March;66(5):800-13.

(8) Beqqali A, Monshouwer-Kloots J, Monteiro R, Welling M, Bakkers J, Ehler E, Verkleij A, Mummery C, Passier R. CHAP is a newly identified Z-disc protein essential for heart and skeletal muscle function. *J Cell Sci* 2010 April 1;123(Pt 7):1141-50.

(9) Bajanca F, Luz M, Duxson MJ, Thorsteinsdottir S. Integrins in the mouse myotome: developmental changes and differences between the epaxial and hypaxial lineage. *Dev Dyn* 2004 October;231(2):402-15.

(10) van Laake LW, Passier R, Monshouwer-Kloots J, Nederhoff MG, Ward-van OD, Field LJ, van Echteld CJ, Doevendans PA, Mummery CL. Monitoring of cell therapy and assessment of cardiac function using magnetic resonance imaging in a mouse model of myocardial infarction. *Nat Protoc* 2007;2(10):2551-67.

(11) Nambiar R, McConnell RE, Tyska MJ. Myosin motor function: the ins and outs of actin-based membrane protrusions. *Cell Mol Life Sci* 2010 April;67(8):1239-54.

(12) Burgess DR, Broschat KO, Hayden JM. Tropomyosin distinguishes between the two actin-binding sites of villin and affects actin-binding properties of other brush border proteins. *J Cell Biol* 1987 January;104(1):29-40.

(13) Ashworth SL, Wean SE, Campos SB, Temm-Grove CJ, Southgate EL, Vrhovski B, Gunning P, Weinberger RP, Molitoris BA. Renal ischemia induces tropomyosin dissociation-destabilizing microvilli microfilaments. *Am J Physiol Renal Physiol* 2004 May;286(5):F988-F996.

(14) Ono S, Ono K. Tropomyosin inhibits ADF/cofilin-dependent actin filament dynamics. *J Cell Biol* 2002 March 18;156(6):1065-76.

(15) Lin F, Yu YP, Woods J, Cieply K, Gooding B, Finkelstein P, Dhir R, Krill D, Becich MJ, Michalopoulos G, Finkelstein S, Luo JH. Myopodin, a synaptopodin homologue, is frequently deleted in invasive prostate cancers. *Am J Pathol* 2001 November;159(5):1603-12.

(16) Jing L, Liu L, Yu YP, Dhir R, Acquafondada M, Landsittel D, Cieply K, Wells A, Luo JH. Expression of myopodin induces suppression of tumor growth and metastasis. *Am J Pathol* 2004 May;164(5):1799-806.

# Chapter 7

*General discussion*

In this thesis the function of a novel Z-disc protein Cytoskeletal Heart-enriched Actin-associated Protein (CHAP) is described, CHAP was identified previously from a genome-wide transcriptome study in human embryonic stem cells differentiating to cardiomyocytes[1]. In mouse and human genomes two isoforms of CHAP were identified; a longer isoform CHAPa containing a N-terminal PDZ-domain and nuclear localization signal (NLS) and a shorter isoform CHAPb, which lacks the PDZ-domain. Interestingly, mouse CHAP isoforms have a distinct expression pattern; whereas CHAPb is predominantly expressed in heart and skeletal muscle during embryonic development, CHAPa is clearly higher expressed in adult heart and skeletal muscle. We have recently demonstrated that zebrafish *chap* is essential for skeletal muscle and heart development[2]. In this thesis I further explored the function of CHAP by several *in vivo* and *in vitro* approaches. And discuss here the potential role(s) of CHAP during development, adult stages and disease.

*Function of CHAP during heart and skeletal muscle development*

The first clues on CHAP function came from its expression pattern during embryonic development. CHAP is expressed in the developing heart and somites (that give rise to skeletal muscle), and this is conserved between species (zebrafish, mouse and chick; previously studied[2] and chapter 2). We showed in chapter 2 that in chick embryos CHAP is expressed in the linear heart tube from Hamburger and Hamilton (HH) stage 8 onwards and at older stages, found expression in somites as well as the heart. As mentioned before, CHAPb is the predominant isoform during mouse embryonic development. However, both in chick and zebrafish only one isoform of CHAP exists, containing the CHAPa characteristic PDZ domain, suggesting that during embryonic development in chick and zebrafish, CHAP may have a similar role as CHAPb. Alternatively, other proteins that resemble CHAP may substitute for the lack of embryonic CHAPb. In this regard, CHAP belongs to a family of actin-bundling proteins, with synaptopodin being the first described member and myopodin the second member of this family. Whereas synaptopodin is expressed in brain and kidney[3], myopodin is expressed in heart, skeletal muscle and smooth muscle[4] and is thus the most likely candidate protein to partially substitute CHAP functionality during muscle development in chick and zebrafish.
We have demonstrated previously that morpholino-mediated knockdown of *chap* in zebrafish led to impaired heart looping and disturbed muscle development[5], indicating the importance of *chap* during muscle development. However, the role of CHAP in heart and skeletal muscle in higher vertebrates still needed to be investigated, especially with respect to the functions of the different CHAP isoforms. To investigate the role of CHAP in higher vertebrates, we used CHAP specific morpholino's to knockdown CHAP in developing chick embryos and followed different to strategies generate CHAP knockout mice (conditional and LacZ knock-in; chapter 3). Although knockdown of CHAP in chick embryos led to abnormalities during cardiac development, such as cardiac looping, these results were variable and not statistically significant. Therefore, to study the role of CHAP during heart development it is essential to generate CHAP (conditional) knockout mice. However, in first attempts we were unable to achieve germline transmission for CHAP mutant embryonic stem cells, which resulted in the study of CHAP in alternative animal models as a first priority: overexpression of CHAP in mice or in cells/cardiomyocytes *in vitro.*

*The role of CHAP in actin signaling*

What could be the mechanism by which CHAP affects cardiac development, or more

specifically, cardiomyocyte function? One possible role of CHAP involves interference with the actin cytoskeleton. This has been evidenced by previous studies on other family members of CHAP. Synaptopodin has been shown to regulate the actin-bundling activity of α-actinin[3] and also regulates actin-bundling via RhoA[6]. In line with these findings, myopodin also has been shown to have actin-bundling activity and binds directly to actin[5]. Furthermore, we observed co-localization of CHAP and actin, suggesting a role for CHAP in actin signaling[5].
The actin cytoskeleton plays an important role in formation of sarcomeres in muscle cells. It has been postulated that formation of actin bundles may serve as a scaffold for the formation of I-Z-I complexes (referring to the I-bands and Z-discs in sarcomeres). These complexes are composed of Z-bodies containing α-actinin and titin which are linked to the actin bundles and are associated with the membrane. In the next stage, myosin thick filaments are organized with the I-Z-I complexes and dissociate from the membrane, forming immature sarcomeres that already show contraction. In the last stage thin filaments form and sarcomeres mature[7]. RhoA and its down-stream effector Rho-associated kinase (ROCK) have been shown to be involved in the formation of actin fibers and in this way play an important role sarcomere formation[8, 9]. We have shown in chapter 3 that CHAP knockdown and deletion of one allele did not affect sarcomere formation *in vitro*. However, this did not result in a complete loss of CHAP and therefore remaining levels of CHAP may be sufficient for sarcomere formation. Knockdown of *chap* in zebrafish resulted in sarcomeric disorganization[5], suggesting that *chap* knockdown was more efficient in zebrafish or that the timing of interference is crucial. In the future, complete removal of CHAP *in vivo* and *in vitro* will tell us more about the possible function of CHAP in sarcomere formation.
In chapter 4 we showed that cardiac-specific overexpression of CHAPb in mice (CHAPb transgenic [Tg]) induced cardiomyopathy which was accompanied by activation of actin signaling, indicated by the formation of stress fibers. These stained for α-actinin and CHAP, and increased expression of actin, the small GTPase molecule RhoA, Ezrin/Radixin/Moesin (ERM) and actin binding protein cofilin was observed. Furthermore, we showed that sarcomeric expression of RhoA was reduced, whereas expression of RhoA at the membrane was increased. To investigate if these observed effects in the Tg mice were a direct effect of CHAPb we generated CHAPa- and b adenoviruses to express CHAP in embryonic day 17.5 (E17.5) cardiomyocytes in culture and in C2C12 cells, a mouse skeletal myoblast cell line. Overexpression of CHAP in these cells did not result in increased expression of actin, RhoA, cofilin or ERM (chapter 5), suggesting that CHAP does not directly regulate expression of members of the actin-signaling pathway and that secondary effects, timing, or additional factors, that are not present *in vitro* cultures, must be involved *in vivo*.

*CHAP and transcriptional regulation*
Another possible role for CHAP could be on transcriptional regulation. The first indication is provided by the localization of CHAP in the nucleus of undifferentiated myoblast cells, where it co-localizes with RhoA. Both proteins are translocated to the cytoplasm upon muscle differentiation (figure 1). It has been suggested that RhoA is directly involved in maintaining skeletal myoblast cells in an undifferentiated state by activating SRF and suppressing transcription factor MyoD, a key factor for skeletal muscle differentiation[10, 11]. Furthermore, RhoA inhibits M-cadherin mediated muscle cell fusion, suggesting that RhoA activity needs to be suppressed for muscle differentiation[12]. On the other hand, RhoA may regulate Serum Response Factor (SRF), a transcription factor, which plays an important role in skeletal

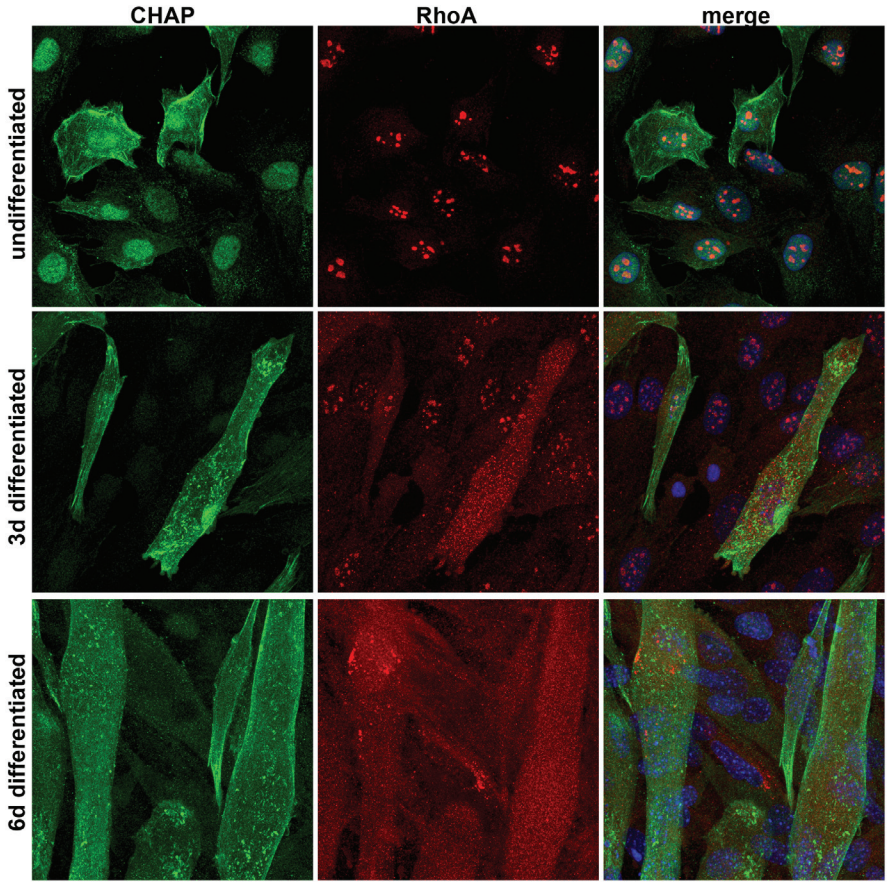


**Figure 1: Localization of CHAP (green) and RhoA (red) in undifferentiated, 3 days differentiated and 6 days differentiated C2C12 cells. Merge images are shown.**

muscle growth and maturation[13]. Thus, the role of RhoA/SRF in skeletal muscle development is rather complex. CHAP expression levels increase during muscle differentiation. However, exogenous expression of CHAPa or CHAPb in C2C12 myoblasts cells prevent muscle fusion (chapter 5), similar to overexpression of a dominant positive isoform of RhoA[12]. Whether CHAP plays a role in muscle differentiation by affecting subcellular localization and/or expression levels of RhoA and SRF or any other mechanism needs to be determined. In CHAPb Tg mice we showed an increase in the expression of transcription factors SRF and Myocyte Enhancer Factor 2 (MEF2). However, adenoviral overexpression of CHAPa and CHAPb in fetal cardiomyocytes did not lead to an upregulation of these transcription factors, suggesting that CHAP may not directly influence transcriptional regulation.

In addition to the RhoA-SRF pathway, CHAP might also influence transcription via the calcineurin-NFAT (nuclear factor of activated T-cells) pathway, a key pathway in cardiac hypertrophy and disease (see below). In CHAP transfected cells the cardiac fetal genes and hypertrophic markers ANF, BNP and beta-MHC were downregulated, which was correlated with translocation of NFATc2 from the nucleus to the cytosol. Furthermore, we recently found that CHAP interacts with the phosphatase calcineurin and with calcineurin-interacting

proteins, such as calsarcins (Beqqali personal communication), suggesting a function for CHAP in calcineurin-mediated hypertrophy. Therefore, it would be interesting to investigate the function of CHAP in this pathway by generating CHAPa- and b knockout models and by analyzing CHAP in different hypertrophy models, such as calcineurin Tg and calsarcin and cypher knockout mice. Furthermore, CHAP might have a direct effect on transcription, because we have observed nuclear localization of CHAP in cardiomyocytes (chapter 5 and unpublished data of A. Beqqali). However, *in vivo* we never observed nuclear localization of CHAP.

*Role of CHAP in sarcomere integrity, cardiac hypertrophy and disease*
We have shown previously that CHAP is expressed at the Z-disc of adult hearts and that it interacts with α-actinin-2[2]. Several Z-disc components have been identified that interact with α-actinin-2 and act as a stretch-sensor. The phosphatase calcineurin is a well-described key regulator of hypertrophy. During cardiac hypertrophy, which occurs in response to various pathophysiological conditions or events, such as myocardial infarction, increased levels of $Ca^{2+}$ lead to activation of calcineurin. Subsequently, activated calcineurin dephosphorylates nuclear factor of activated T-cells (NFAT), leading to nuclear translocation of NFAT and activation of a fetal gene expression program[14, 15]. Calsarcins represent a new family of calcineurin-interacting proteins, bind to other sarcomeric proteins such as α-actinin-2, are expressed in heart and skeletal muscle[16] and protect the heart against calcineurin-induced hypertrophy[17, 18]. Cypher (Oracle) is another α-actinin-2-interacting protein and is expressed in the heart and skeletal muscle[19, 20] and cypher knockout mice displayed decreased calsarcin expression[21] and development of a dilated cardiomyopathy phenotype in mice[21] and zebrafish[22]. Both deletion of calsarcin and cypher leads to disruption of the Z-disc[17, 21]. In addition to calsarcin and cypher, CHAP might regulate sarcomeric integrity and cardiac hypertrophy via calcineurin-NFAT and/or SRF. SRF, which was upregulated in CHAPb Tg hearts (chapter 4), is also involved in maintaining Z-disc integrity in adult skeletal muscle by regulation of transcription of sarcomeric proteins[23].

In order to investigate the role of CHAP *in* vivo, we generated transgenic mice by heart-specific overexpression of both isoforms of CHAP. We did not observe any abnormalities in hearts of CHAPa Tg mice. Although, we found upregulation of *ChapA* mRNA expression by qPCR experiments and CHAP protein by western analysis in CHAPa Tg mice, we could not detect the transgenic protein with a specific FLAG antibody (chapter 4) and therefore cannot exclude the possibility that CHAPa protein was partially degraded and functionally inactive.
In CHAPb Tg mice both mRNA and protein levels of CHAPb were stably expressed. We observed mild hypertrophy and interstitial fibrosis in hearts of CHAPb Tg mice at three months of age. This was more severe at six months of age and was associated with activation of the hypertrophic gene program and expression of collagens. Furthermore, we observed conduction disturbances in CHAPb Tg mice, which coincided with a remarkable suppression of atrial connexins (Cx40 and Cx43), crucial for electrical coupling of cardiomyocytes. Besides electrical dysfunction, CHAPb Tg mice showed diastolic dysfunction *in vivo* and in isolated cardiomyocytes *in vitro*. These features are comparable to the cardiac abnormalities seen in patients with hypertrophic cardiomyopathy (HCM), i.e. cardiac hypertrophy, diastolic dysfunction and increased occurrence of arrhythmia (in particular atrial fibrillation). In order to identify a possible working mechanism for the observed phenotype, we further studied

CHAPb Tg hearts at the cellular level. We observed stress fiber-like structures in the hearts of CHAPb Tg mice, that stained for both CHAP and α-actinin. In addition, we showed that the actin signaling pathway was upregulated in CHAPb Tg hearts, as discussed previously. These observations led us to conclude that the fetal isoform CHAPb can be involved in the onset and progression of cardiac disease, strongly resembling characteristics of cardiac hypertrophy and HCM. This is further corroborated by recent findings, in which we found that expression of CHAPb is upregulated in several models of hypertrophy (personal communication A. Beqqali). These data suggest a role for CHAPb during hypertrophic events and it would be interesting to investigate the possible working mechanisms further. It would also be interesting to analyze the function of CHAP in human disease by sequence analysis of CHAP in HCM and in dilated cardiomyopathy (DCM). In HCM and DCM sarcomeric proteins are mutated and most mutated proteins are beta-MHC, myosin-binding protein C and troponin T[24, 25]. However, several mutations in other Z-disc components were also identified and these mutations interfered with interaction between Z-disc components. For example, a mutation found in cypher (D626N) in DCM patients increased the interaction with protein kinase C, a key regulator of contractility and growth of cardiomyocytes[26]. Mutations in Tcap result in HCM (T137I and R153H) or DCM (E132Q) and resulted in increased interaction with titin and calsarcin-1 or decreased interaction with muscle LIM protein, calsarcin-1 and titin, respectively[27]. Mutations in Z-disc protein nexilin (G650del, Y652C and P611T) leads to disruption of the Z-disc, although the exact mechanism was not identified[28].
Thus, *in vivo* experiments in mice and sequence analysis in HCM and DCM patients may reveal more information about the putative function of CHAP in Z-disc integrity and cardiac disease.

*CHAP in skeletal muscle*
In skeletal muscle we found expression of both CHAPa and CHAPb (chapter 2 and chapter 6), with expression of CHAPa approximately 10 fold higher than CHAPb. CHAPa overexpression in skeletal muscle cells (C2C12) resulted in disruption of the Z-disc, whereas CHAPb overexpression induces stress fibers (chapter 5). As in cardiomyocytes, CHAPa could function in maintaining Z-disc intergrity in skeletal muscle cells. Mutations in cypher have been described in muscular dystrophy and these resulted in disintegration of the Z-disc[29]. Therefore, it would be interesting to search for CHAPa mutations in muscular dystrophy patients. We also found low expression of CHAPb in skeletal muscle cells. In contrast to cardiomyocytes, skeletal muscle cells have the ability to regenerate in adult mice[30]. The function of CHAPb here could be, as suggested by its role in cardiac development, to induce actin polymerization and serve as a scaffold for new Z-disc formation.
In addition to Z-disc integrity CHAP could also be involved in determining the slow muscle fiber phenotype in adult animals. We find highest CHAPa expression in soleus muscle, which is predominantly composed of slow muscle fibers. Calcineurin, NFAT and MEF2 are important regulators of the slow muscle fibers. In slow muscle fibers there is a tonic motor nerve activity that leads keeps $Ca^{2+}$ levels constant and calcineurin-NFAT signaling active. In fast muscle fibers, on the other hand, there is phasic firing of the motor nerve, leading to high amplitude $Ca^{2+}$ transients that are insufficient to activate the calcineurin-NFAT pathway[31, 32]. All NFAT isoforms are important for determining the slow/fast muscle switch. A specific combination of NFAT isoforms determines the slow or fast muscle gene expression[33]. MEF2 is also regulated by calcineurin to induce slow muscle gene expression and the combined

binding of MEF2 and NFAT to slow muscle fiber gene promoters leads to the subsequent gene expression[34]. Calsarcins have been implicated in determining the fast skeletal muscle phenotype. Both calsarcin-2 and -3 are expressed specifically in fast skeletal muscle[35, 36] and knockdown of calsarcin-2 leads to a switch to slow skeletal muscle fibers phenotype by activation of the calcineurin-NFAT pathway[36]. Our results suggest that CHAPb regulates MEF2 levels *in vivo* (chapter 4) and both CHAPa and –b are involved in calcineurin-NFAT signaling (chapter 5 and unpublished results). Therefore, it would be interesting to investigate the function of the CHAP isoforms in determination of skeletal muscle fiber phenotype. This could be achieved by generating tissue-specific (inducible) knockout mice for both isoforms or by overexpression or knockdown of CHAP isoforms *in vitro* in muscle progenitor cells.

*Possible role of CHAP in smooth muscle cells*

Besides expression in adult heart and skeletal muscle, we also found CHAP to be expressed in smooth muscle cells (chapter 2). Additional western blot analysis showed that CHAPa was expressed in these cells (data not shown). During embryonic development we showed expression of CHAP in cardiomyocytes adjacent to the vascular smooth muscle cells (VSMCs) of the vena cava at embryonic day 17.5 (chapter 2). Although CHAPb is the predominant form in striated muscle cells during embryonic development, we cannot exclude CHAPa being expressed in these cells. However, CHAP expression was not detected in smooth muscle cells during development, suggesting that CHAP has no role during VSMC development. In smooth muscle cells contraction is regulated by so-called dense bodies, co-staining with α-actinin will indicate whether CHAP is expressed in dense bodies.

During pathophysiological events it is possible that CHAPb, like in hypertrophic cardiomyocytes, is upregulated. VSMCs respond to hypertension or other stimuli by a phenotypic transition from a contractile state to a synthetic state, leading to increased synthesis of extracellular matrix and migration of VSMCs to the subendothelial layer, where they proliferate to form an artherosclerotic lesion[37]. Cytoskeletal proteins have been implicated in the migration of VSMCs. Phosphorylation of RhoA by cyclic AMP dependent protein kinase leads to migration of VSMCs in vitro[38]. In addition, interleukin-19 inhibits platelet derived growth factor induced VSMC migration by decreasing myosin light chain, RhoA activation and cofilin dephosphorylation[39]. Also CHAPa could function the pathophysiology of VSMCs since contractile proteins have indeed been implicated. For example, SM22α restricts plaque growth by inhibiting the contractile/synthetic phenotypical switch[40]. Furthermore, a role for contractile proteins has also been implicated in determining the vascular stiffness[41]. Both CHAPa and CHAPb could be involved here. Additional experiments in mouse models for atherosclerosis (e.g. ApoE knock out mice) could address this issue.

In summary CHAPa is expressed in adult heart, skeletal and smooth muscle cells, but CHAPb is expressed in embryonic muscle cells only (previous section) and upregulated in pathophysiological circumstances (A. Beqqali, personal communication).

*Additional functions of CHAPb*

Besides expression during heart and skeletal muscle development, we showed that CHAPb is expressed in the small intestine and kidney. In these organs, CHAPb expression is adjacent to microvilli that can be recognized by staining with phalloidin for filamentous actin (chapter 6). Actin dynamics is involved in many cellular processes like cell movement, cell division and cell shape changes[42, 43]. Therefore, CHAPb could also be involved in several other cellular

processes. In chapter 4 we showed that CHAPb is involved in signaling via RhoA-SRF. SRF and RhoA are implicated in several other cellular processes, such as cell polarity, adhesion, cell movement, that are important during development and in pathophysiological situations as cancer[44-46]. Moreover, the CHAP homolog myopodin has been implicated as a tumor suppressor in prostate cancer[47, 48]. Therefore, it would be interesting to investigate the role of CHAPb in these cellular processes by *in vitro* and *in vivo* experiments.

*Conclusions and future directions*

In this thesis, the distribution and function of a novel Z-disc protein CHAP was described. We showed that CHAPa is expressed in adult muscles and has a function in integrity of the Z-disc *in vitro*. CHAPb, on the other hand, is predominantly expressed during development and has a putative function in cardiac and skeletal muscle development. We showed that CHAPb is involved in actin signaling by overexpression *in vivo* and *in vitro*. Moreover, CHAPb is expressed in adult organs and has a putative actin-bundling function. To further explore the function of CHAPa and CHAPb *in vivo* it will be necessary to generate (conditional) CHAP knockout models in mice. Furthermore, investigating the function of CHAP in other transgenic/knockout cardiac development and disease models should reveal more about the putative function of CHAP. The role of CHAP in human development and disease can be unraveled by making use of DNA databases of congenital heart disease patients or HCM/DCM patients, such as the CONCOR database, established ten years ago at the Amsterdam Medical Centre with support of ICIN funding.

# References


(1) Beqqali A, Kloots J, Ward-van Oostwaard D, Mummery C, Passier R. Genome-wide transcriptional profiling of human embryonic stem cells differentiating to cardiomyocytes. *Stem Cells* 2006 August;24(8):1956-67.

(2) Beqqali A, Monshouwer-Kloots J, Monteiro R, Welling M, Bakkers J, Ehler E, Verkleij A, Mummery C, Passier R. CHAP is a newly identified Z-disc protein essential for heart and skeletal muscle function. *J Cell Sci* 2010 April 1;123(Pt 7):1141-50.

(3) Asanuma K, Kim K, Oh J, Giardino L, Chabanis S, Faul C, Reiser J, Mundel P. Synaptopodin regulates the actin-bundling activity of alpha-actinin in an isoform-specific manner. *J Clin Invest* 2005 May;115(5):1188-98.

(4) Weins A, Schwarz K, Faul C, Barisoni L, Linke WA, Mundel P. Differentiation- and stress-dependent nuclear cytoplasmic redistribution of myopodin, a novel actin-bundling protein. *J Cell Biol* 2001 October 29;155(3):393-404.

(5) Beqqali A, Monshouwer-Kloots J, Monteiro R, Welling M, Bakkers J, Ehler E, Verkleij A, Mummery C, Passier R. CHAP is a newly identified Z-disc protein essential for heart and skeletal muscle function. *J Cell Sci* 2010 April 1;123(Pt 7):1141-50.

(6) Asanuma K, Yanagida-Asanuma E, Faul C, Tomino Y, Kim K, Mundel P. Synaptopodin or chestrates actin organization and cell motility via regulation of RhoA signalling. *Nat Cell Biol* 2006 May;8(5):485-91.

(7) Gregorio CC, Antin PB. To the heart of myofibril assembly. *Trends Cell Biol* 2000 Septem ber;10(9):355-62.

(8) Aoki H, Izumo S, Sadoshima J. Angiotensin II activates RhoA in cardiac myocytes: a critical role of RhoA in angiotensin II-induced premyofibril formation. *Circ Res* 1998 April 6;82(6):666-76.

(9) Sakata H, Sakabe M, Matsui H, Kawada N, Nakatani K, Ikeda K, Yamagishi T, Nakajima Y. Rho kinase inhibitor Y27632 affects initial heart myofibrillogenesis in cultured chick blastoderm. *Dev Dyn* 2007 February;236(2):461-72.

(10) Wei L, Zhou W, Croissant JD, Johansen FE, Prywes R, Balasubramanyam A, Schwartz RJ. RhoA sign aling via serum response factor plays an obligatory role in myogenic differentiation. *J Biol Chem* 1998 November 13;273(46):30287-94.

(11) Castellani L, Salvati E, Alema S, Falcone G. Fine regulation of RhoA and Rock is required for skeletal muscle differentiation. *J Biol Chem* 2006 June 2;281(22):15249-57.

(12) Charrasse S, Comunale F, Grumbach Y, Poulat F, Blangy A, Gauthier-Rouviere C. RhoA GTPase regulates M-cadherin activity and myoblast fusion. *Mol Biol Cell* 2006 February;17(2):749-59.

(13) Li S, Czubryt MP, McAnally J, Bassel-Duby R, Richardson JA, Wiebel FF, Nordheim A, Olson EN. Requirement for serum response factor for skeletal muscle growth and maturation revealed by tissue-specific gene deletion in mice. *Proc Natl Acad Sci U S A* 2005 January 25;102(4):1082-7.

(14) Molkentin JD, Lu JR, Antos CL, Markham B, Richardson J, Robbins J, Grant SR, Olson EN. A calcineurin-dependent transcriptional pathway for cardiac hypertrophy. *Cell* 1998 April 17;93(2):215-28.

(15) Wilkins BJ, Molkentin JD. Calcium-calcineurin signaling in the regulation of cardiac hypertrophy. *Biochem Biophys Res Commun* 2004 October 1;322(4):1178-91.

(16) Frey N, Richardson JA, Olson EN. Calsarcins, a novel family of sarcomeric calcineurin-binding pro teins. *Proc Natl Acad Sci U S A* 2000 December 19;97(26):14632-7.

(17) Frey N, Barrientos T, Shelton JM, Frank D, Rutten H, Gehring D, Kuhn C, Lutz M, Rothermel B, Bassel-Duby R, Richardson JA, Katus HA, Hill JA, Olson EN. Mice lacking calsarcin-1 are sensitized to calcineurin signaling and show accelerated cardiomyopathy in response to pathological biomechanical stress. *Nat Med* 2004 December;10(12):1336-43.

(18) Frank D, Kuhn C, van EM, Gehring D, Hanselmann C, Lippl S, Will R, Katus HA, Frey N. Calsarcin-1 protects against angiotensin-II induced cardiac hypertrophy. *Circulation* 2007 November 27;116(22):2587-96.

(19) Passier R, Richardson JA, Olson EN. Oracle, a novel PDZ-LIM domain protein expressed in heart and skeletal muscle. *Mech Dev* 2000 April;92(2):277-84.

(20) Zhou Q, Ruiz-Lozano P, Martone ME, Chen J. Cypher, a striated muscle-restricted PDZ and LIM domain-containing protein, binds to alpha-actinin-2 and protein kinase C. *J Biol Chem* 1999 July 9;274(28):19807-13.

(21) Zheng M, Cheng H, Li X, Zhang J, Cui L, Ouyang K, Han L, Zhao T, Gu Y, Dalton ND, Bang ML,

Peterson KL, Chen J. Cardiac-specific ablation of Cypher leads to a severe form of dilated cardiomyopathy with premature death. *Hum Mol Genet* 2009 February 15;18(4):701-13.

(22) van der Meer DL, Marques IJ, Leito JT, Besser J, Bakkers J, Schoonheere E, Bagowski CP. Zebrafish cypher is important for somite formation and heart development. *Dev Biol* 2006 November 15;299(2):356-72.

(23) Lahoute C, Sotiropoulos A, Favier M, Guillet-Deniau I, Charvet C, Ferry A, Butler-Browne G, Metzger D, Tuil D, Daegelen D. Premature aging in skeletal muscle lacking serum response factor. *PLoS One* 2008;3(12):e3910.

(24) Sanoudou D, Vafiadaki E, Arvanitis DA, Kranias E, Kontrogianni-Konstantopoulos A. Array lessons from the heart: focus on the genome and transcriptome of cardiomyopathies. *Physiol Genomics* 2005 April 14;21(2):131-43.

(25) Beqqali A, van Eldik W, Mummery C, Passier R. Human stem cells as a model for cardiac differentiation and disease. *Cell Mol Life Sci* 2009 March;66(5):800-13.

(26) Arimura T, Hayashi T, Terada H, Lee SY, Zhou Q, Takahashi M, Ueda K, Nouchi T, Hohda S, Shibutani M, Hirose M, Chen J, Park JE, Yasunami M, Hayashi H, Kimura A. A Cypher/ZASP mutation associated with dilated cardiomyopathy alters the binding affinity to protein kinase C. *J Biol Chem* 2004 February 20;279(8):6746-52.

(27) Hayashi T, Arimura T, Itoh-Satoh M, Ueda K, Hohda S, Inagaki N, Takahashi M, Hori H, Yasunami M, Nishi H, Koga Y, Nakamura H, Matsuzaki M, Choi BY, Bae SW, You CW, Han KH, Park JE, Knoll R, Hoshijima M, Chien KR, Kimura A. Tcap gene mutations in hypertrophic cardiomyopathy and dilated cardiomyopathy. *J Am Coll Cardiol* 2004 December 7;44(11):2192-201.

(28) Hassel D, Dahme T, Erdmann J, Meder B, Huge A, Stoll M, Just S, Hess A, Ehlermann P, Weichenhan D, Grimmler M, Liptau H, Hetzer R, Regitz-Zagrosek V, Fischer C, Nurnberg P, Schunkert H, Katus HA, Rottbauer W. Nexilin mutations destabilize cardiac Z-disks and lead to dilated cardiomyopathy. *Nat Med* 2009 November;15(11):1281-8.

(29) Selcen D, Engel AG. Mutations in ZASP define a novel form of muscular dystrophy in humans. *Ann Neurol* 2005 February;57(2):269-76.

(30) Buckingham M, Bajard L, Chang T, Daubas P, Hadchouel J, Meilhac S, Montarras D, Rocancourt D, Relaix F. The formation of skeletal muscle: from somite to limb. *J Anat* 2003 January;202(1):59-68.

(31) Chin ER, Olson EN, Richardson JA, Yang Q, Humphries C, Shelton JM, Wu H, Zhu W, Bassel-Duby R, Williams RS. A calcineurin-dependent transcriptional pathway controls skeletal muscle fiber type. *Genes Dev* 1998 August 15;12(16):2499-509.

(32) McCullagh KJ, Calabria E, Pallafacchina G, Ciciliot S, Serrano AL, Argentini C, Kalhovde JM, Lomo T, Schiaffino S. NFAT is a nerve activity sensor in skeletal muscle and controls activity-dependent myosin switching. *Proc Natl Acad Sci U S A* 2004 July 20;101(29):10590-5.

(33) Calabria E, Ciciliot S, Moretti I, Garcia M, Picard A, Dyar KA, Pallafacchina G, Tothova J, Schiaffino S, Murgia M. NFAT isoforms control activity-dependent muscle fiber type specification. *Proc Natl Acad Sci U S A* 2009 August 11;106(32):13335-40.

(34) Wu H, Naya FJ, McKinsey TA, Mercer B, Shelton JM, Chin ER, Simard AR, Michel RN, Bassel-Duby R, Olson EN, Williams RS. MEF2 responds to multiple calcium-regulated signals in the control of skeletal muscle fiber type. *EMBO J* 2000 May 2;19(9):1963-73.

(35) Frey N, Olson EN. Calsarcin-3, a novel skeletal muscle-specific member of the calsarcin family, inter acts with multiple Z-disc proteins. *J Biol Chem* 2002 April 19;277(16):13998-4004.

(36) Frey N, Frank D, Lippl S, Kuhn C, Kogler H, Barrientos T, Rohr C, Will R, Muller OJ, Weiler H, Bassel-Duby R, Katus HA, Olson EN. Calsarcin-2 deficiency increases exercise capacity in mice through calcineurin/NFAT activation. *J Clin Invest* 2008 November;118(11):3598-608.

(37) Li C, Xu Q. Mechanical stress-initiated signal transduction in vascular smooth muscle cells in vitro and in vivo. *Cell Signal* 2007 May;19(5):881-91.

(38) Rolli-Derkinderen M, Toumaniantz G, Pacaud P, Loirand G. RhoA phosphorylation induces Rac1 release from guanine dissociation inhibitor alpha and stimulation of vascular smooth muscle cell migration. *Mol Cell Biol* 2010 October;30(20):4786-96.

(39) Gabunia K, Jain S, England RN, Autieri MV. Anti-inflammatory cytokine interleukin-19 inhibits smooth muscle cell migration and activation of cytoskeletal regulators of VSMC motility. *Am J Physiol Cell Physiol* 2011 April;300(4):C896-C906.

(40) Feil S, Hofmann F, Feil R. SM22alpha modulates vascular smooth muscle cell phenotype during atherogenesis. *Circ Res* 2004 April 16;94(7):863-5.

(41) Qiu H, Zhu Y, Sun Z, Trzeciakowski JP, Gansner M, Depre C, Resuello RR, Natividad FF, Hunter

WC, Genin GM, Elson EL, Vatner DE, Meininger GA, Vatner SF. Short communication: vascular smooth muscle cell stiffness as a mechanism for increased aortic stiffness with aging. *Circ Res* 2010 September 3;107(5):615-9.

(42) Perrin BJ, Ervasti JM. The actin gene family: function follows isoform. *Cytoskeleton (Hoboken )* 2010 October;67(10):630-4.

(43) Hild G, Bugyi B, Nyitrai M. Conformational dynamics of actin: effectors and implications for biological function. *Cytoskeleton (Hoboken )* 2010 October;67(10):609-29.

(44) Nakaya Y, Sukowati EW, Wu Y, Sheng G. RhoA and microtubule dynamics control cell-basement membrane interaction in EMT during gastrulation. *Nat Cell Biol* 2008 July;10(7):765-75.

(45) Luxenburg C, Pasolli HA, Williams SE, Fuchs E. Developmental roles for Srf, cortical cytoskeleton and cell shape in epidermal spindle orientation. *Nat Cell Biol* 2011 March;13(3):203-14.

(46) Medjkane S, Perez-Sanchez C, Gaggioli C, Sahai E, Treisman R. Myocardin-related transcription factors and SRF are required for cytoskeletal dynamics and experimental metastasis. *Nat Cell Biol* 2009 March;11(3):257-68.

(47) Lin F, Yu YP, Woods J, Cieply K, Gooding B, Finkelstein P, Dhir R, Krill D, Becich MJ, Michalopoulos G, Finkelstein S, Luo JH. Myopodin, a synaptopodin homologue, is frequently deleted in invasive prostate cancers. *Am J Pathol* 2001 November;159(5):1603-12.

(48) Jing L, Liu L, Yu YP, Dhir R, Acquafondada M, Landsittel D, Cieply K, Wells A, Luo JH. Expression of myopodin induces suppression of tumor growth and metastasis. *Am J Pathol* 2004 May;164(5):1799-806.

# Appendix

*Summary*
*Samenvatting*
*List of publications*
*Curriculum vitae*
*Dankwoord*

# Summary

In this thesis we investigated the role of a previously described Z-disc protein CHAP, which we identified by whole-genome wide transcriptome analysis in differentiating cardiomyocytes derived from human embryonic stem cells (hESC). Two isoforms of CHAP exist; a longer isoform CHAPa with a PDZ-domain and nuclear localization signal (NLS) and a shorter isoform CHAPb, which lacks the PDZ-domain. Furthermore, these isoforms differ in their expression; CHAPb is predominantly expressed during embryonic development, whereas CHAPa is expressed in adult stages. We have shown that during mouse embryonic development CHAP is expressed in early cardiac progenitors tissue as indicated by its expression in the cardiac crescent stage which is still maintained in adult hearts. Following expression during early heart development, CHAP expression can be identified in somites, which give rise to skeletal muscle later in life. Furthermore, CHAP co-localizes and interacts with α-actinin-2, a major component of the Z-disc. In recent years, it has become clear that besides its role in contraction, Z-disc proteins may also have additional roles in various signaling pathways, such as sensing changes in stretch or stress on cardiomyocytes. In this thesis we performed experiments in order to study the role of CHAPa and b during embryonic development in chick and mouse and in the adult hearts of mice.

In **chapter 2** we sequenced the *CHAP* isoform in chick (Gallus gallus) and we show that this isoform is homologous to the CHAPa isoform in mouse and human. In addition, we show that the genomic organization of the *CHAP* gene in the chick is comparable to the organization of the CHAP gene in the mouse. We analyzed the expression of *CHAP* during embryonic development of chick embryos in detail and demonstrated that *CHAP* is expressed from the cardiac crescent stage onwards and in later stages in the somites as well, which is comparable to CHAP expression in mouse embryos. Furthermore, we show that *CHAP* is expressed in several muscle groups, such as jaw, eye, tongue and limb muscles in both mouse and chick embryos. Finally, we analyzed the expression of CHAP in adult mice and show that CHAP expression, in addition to cardiomyocytes, can be identified in vascular smooth muscle cells and skeletal muscle cells as well.

From a previous study we know that CHAP plays an important role in the development of the heart and skeletal muscle. In order to investigate the specific role of CHAP in mice, we generated a conventional CHAP knockout (LacZ knockin) and a CHAP conditional knockout targeting contruct in order to create different lines of knockout mice. This is described in **chapter 3**. For this, we successfully modified mouse embryonic stem cells by gene targeting (via homologous recombination), followed by injection in host mouse blastocysts in order to generate chimeric mice. Subsequently, chimeric mice mice were crossbred in order to obtain heterozygous knockout mice (by germline transmission). Although high-percentage chimeras were generated, unfortunately we did not achieve germline transmission for both lines. To investigate the effect of CHAP heterozygosity in cardiomyocytes *in vitro*, we differentiated the CHAP LacZ$^{+/-}$ mouse embryonic stem cells to cardiomyocytes and showed that there was no effect on sarcomeric structure or functional properties (beating frequency) of these cardiomyocytes. Furthermore, we describe the effects of *CHAP* knockdown in chick embryos by injection of *CHAP*-specific morpholino antisense oligonucleotides. Although we could demonstrate effects on cardiac development, these results were not significantly different.

In **chapter 4** we analyzed the role of CHAPa and CHAPb *in vivo* by generating heart-specific CHAP transgenic (Tg) mice. Although we found robust overexpression of CHAPa at the mRNA-level, we did not find an increase of CHAPa Tg protein expression. On the other hand, CHAPb Tg mice displayed both an increase at the mRNA as well as the protein level. Although at one month of age no obvious change in cardiac phenotype was detected, at three month of age the left atria were enlarged and cardiomyocytes of the left ventricle were hypertrophic which coincided with interstitial fibrosis. This phenotype was more severe at 6 months of age. The observed cardiac hypertrophy and interstitial fibrosis was correlated with activation of the fetal gene expression program (ANF, BNP and β-MHC) and collagens, respectively. Furthermore, we showed that expression of both connexin40 and -43 was downregulated in the left atrium of CHAPb Tg mice, which was correlated with prolongation of the conduction from atria to ventricles (PR interval). MRI and single sarcomere measurements showed that the cardiomyocytes of CHAPb Tg hearts were dysfunctional in both contraction and relaxation. Finally, we showed that in CHAPb Tg hearts the presence of actin stress fibers which correlated with activation of the actin signaling pathway.

To investigate the function of CHAPa and CHAPb *in vitro*, we generated CHAPa and CHAPb adenoviruses (AdCHAPa and AdCHAPb). In **chapter 5** we used these viruses to overexpress either isoform in embryonic day 17.5 mouse cardiomyocytes or in a skeletal myoblast cell line (C2C12), which can be differentiated to skeletal muscle cells. As expected, we found that following transduction of these cells with AdCHAPa or AdCHAPb and increase of both CHAP isoform proteins could be detected. We show that overexpression of CHAPa results in disruption of the Z-disc, while the M-band is not affected. *In vitro* overexpression of CHAPb leads to the induction of actin stress fibers, as observed in CHAPb Tg mice. In contrast to our findings in CHAPb Tg mice, we did not observe activation of the actin signaling pathway and the hypertrophic genetic program, following overexpression of CHAPb. In fact, we showed a downregulation of the hypertrophic genes ANF, BNP and β-MHC and a translocation of NFATc2, a key player in cardiac hypertrophy, from the nucleus to the cytoplasm, suggesting that CHAP does not lead to direct activation of hypertrophy *in vitro*.

In **chapter 6** we analyzed the expression of CHAP in adult organs in more detail and show that CHAP is expressed in the brain, kidney and small intestine. Furthermore, we demonstrate that CHAPb is expressed in the villus of the small intestine and kidney tubules, adjacent to actin filament containing micro-villi.

In **chapter 7** we discuss the results of this thesis and give suggestions for future research. For example, it would be interesting to perform genetic studies for mutations in CHAP in patient databases for different cardiac diseases. Furthermore, a possible role of CHAP in the other disease, such as atherosclerosis and cancer could be of interest.

# Samenvatting

In dit proefschrift beschrijven we de functie van een nieuw gen, genaamd Cytoskeletal Heart-enriched Actin-associated Protein (CHAP). CHAP is ontdekt na analyse met behulp van "whole-genome transcriptome arrays" van humane embryonale stamcellen, die gedifferentieerd werden naar hartspiercellen. Er zijn twee varianten van CHAP, CHAPa en CHAPb, waarvan CHAPa het langste eiwit is. Tijdens de ontwikkeling van de muis komt CHAP tot expressie vanaf het vroegste ontwikkelingsstadium van het hart. In een later stadium komt CHAP ook tot expressie in de voorlopercellen van spieren, de somieten. Ook in volwassen muizen komt CHAP tot expressie in het hart. Het hart en skeletspieren zijn zogenaamde dwarsgestreepte spierweefsels. De contractie in deze weefsels wordt gereguleerd door sarcomeren, de kleinste functionele eenheden van dwarsgestreepte spieren. De sarcomeren kunnen ook weer worden opgedeeld in compartimenten, de uiteinden van de sarcomeren worden gemarkeerd door de zogenaamde Z-lijn. Het eiwit α-actinine-2 is een van de meest voorkomende eiwitten in de Z-lijn en bindt allerlei andere eiwitten in de Z-lijn. Waar aanvankelijk werd gedacht dat sarcomeereiwitten alleen betrokken zijn bij de contractie van spiercellen, is het inmiddels duidelijk dat deze eiwitten ook een belangrijke rol kunnen spelen in meerdere biologische processen, zoals het signaleren en overbrengen van stress en stretch. Uit eerdere experimenten weten we dat CHAP gelokaliseerd is in de Z-lijn en dat het een interactie kan aangaan met α-actinine-2. In dit proefschrift hebben we experimenten verricht met het doel om de rol van CHAPa en CHAPb te bestuderen tijdens de embryonale ontwikkeling van de muis en de kip, maar ook in het hart van volwassen muizen.

In **hoofdstuk 2** analyseren we de DNA en eiwit sequentie van CHAP in de kip en laten we zien dat deze het meest overeenkomt met het CHAPa eiwit, zoals dat bekend is in de muis, mens en zebravis. Verder laten we ook zien dat de organisatie van het CHAP gen van de kip vergelijkbaar is met de organisatie van het CHAP gen in de muis. In een volgende stap analyseren we ook de genexpressie van *CHAP* tijdens de ontwikkeling van de kip in detail en laten we zien dat dit een vergelijkbaar expressie patroon geeft met dat van de muis, namelijk een sterke expressie van CHAP in het hart en somieten. Verder laten we zien dat *CHAP* in de kip en de muis tot expressie komt in skelet spieren van de ledematen, kaak, tong en oog. In adulte muizen laten we tot slot zien dat CHAP tot expressie komt in skelet spieren en vasculaire gladde spiercellen.

Uit eerdere studies in zebravissen weten we dat CHAP een belangrijke rol speelt in de ontwikkeling van het hart en skeletspieren. Om vervolgens de specifieke functie van CHAP *in vivo* te kunnen bestuderen in muizen, maken we gebruik van de zogenaamde 'knockout' technologie, waarin het gen wordt uitgeschakeld. Dit wordt beschreven in **hoofdstuk 3.** Om knockout muizen te genereren wordt een allel van het CHAP gen verwijderd in embryonale stam (ES) cellen met behulp van genetische modificatie (homologe recombinatie). Deze gemodificeerde ES cellen worden vervolgens teruggebracht in een muizenembryo, zodat er een mix van gemodificeerde en ongemodificeerde ES cellen ontstaat, resulterend in de geboorte van chimere nakomelingen (muizen afkomstig van beide soorten ES cellen). Deze chimere muizen worden vervolgens verder gekruist met het uiteindelijk doel om kiembaan transmissie te krijgen, wat wil zeggen dat het uitgeschakelde CHAP gen aan de nakomelingen doorgegeven kan worden. We hebben hiervoor twee benaderingen gekozen: een conventionele

knockout muis en een conditionele knockout muis waarbij we het CHAP gen op een gewenste tijd en locatie kunnen uitschakelen. Alhoewel we een hoog percentage chimere muizen hebben verkregen, hebben nakomelingen van deze muizen helaas niet geresulteerd in kiembaan transmissie. Wel laten we zien dat *in vitro* hartspiercel differentiatie van deze gemodificeerde ES cellen, waarvan de expressie van CHAP gehalveerd is (heterozygoot, 1 allel van CHAP is uitgeschakeld), niet leidt tot waarneembare afwijkingen, zoals veranderingen in contractiefrequentie en organisatie van sarcomeren. Tevens beschrijven we in dit hoofdstuk wat de effecten zijn als we *CHAP* expressie remmen door gebruik van *CHAP*-specifieke morpholino antisens-oligonucleotiden in kippen embryos. Alhoewel effecten op de ontwikkeling van het hart waarneembaar waren in meerdere embryos, bleken deze effecten niet significant

In **hoofdstuk 4** bestuderen we de rol van CHAP *in vivo* door CHAPa en CHAPb specifiek tot overexpressie te brengen in het hart van de muis. In beide CHAP transgene muizenlijnen zien we zoals verwachten een verhoogde gen expressie (transcriptie) van CHAP. Echter, in het geval van CHAPa transgene muizen leidt dit niet tot een verhoogd eiwit niveau van CHAPa en een veranderd fenotype. Aangezien CHAPb transgene muizen laten wel een verhoogd en stabiel eiwit niveau van CHAPb in het hart laten zien, hebben we deze verder geanalyseerd. We laten zien dat CHAPb transgene muizen een hartaandoening ontwikkelen (cardiomyopathie met diastole dysfunctie), die ook sterke overeenkomsten vertoont zoals deze bij de mens voorkomt. In CHAPb transgene muizen van 3 maanden zien we dat de harten verdikte kamers en een vergroot linker boezem hebben. Verder kunnen we ook zien dat de individuele hartcellen vergroot (hypertroof) zijn en dat er fibrose (verhoogde afzetting van collageen) tussen de hartcellen aanwezig is. De hypertrofie en fibrose kunnen we bevestigen door te laten zien dat de expressie van genen, specifiek voor hypertrofie en fibose, is verhoogd. In het linker boezem van de CHAPb transgene muizen zien we ook dat de eiwitten die noodzakelijk zijn voor koppeling en communicatie van hartspiercellen, verlaagd zijn in expressie. Ook kunnen we zien dat daardoor de elektrische geleiding van de boezem naar de kamer vertraagd is. Verder laten we zien dat de contractie in deze harten en in individuele hartspiercellen verminderd is. Tot slot laten we zien dat in CHAPb transgene harten er actine bundels worden gevormd en dat de actine signaleringsroute is verhoogd.

In **hoofdstuk 5** bestuderen we de rol van CHAPa en CHAPb door deze tot overexpressie te brengen in cellen. We gebruiken hiervoor skelet spiercellen en hartcellen die we isoleren uit embryonale muizenharten. In deze experimenten is het CHAPa eiwitproduct wel stabiel. Als we CHAPa tot overexpressie brengen in deze cellen dan zien we dat de sarcomeer structuur wordt beïnvloedt: de Z-lijn is niet meer herkenbaar.  Overexpressie van CHAPb heeft de vorming van actine bundels tot resultaat, zoals we ook in CHAPb transgene muizen zien. In deze experimenten kunnen we geen effect op de actine signaleringsroute zien. Verder zien we dat de genen die specifiek zijn voor hypertrofie, en verhoogd waren in CHAPb transgene harten, in deze experimenten juist verlaagd zijn. Tenslotte laten we zien dat het eiwit NFAT, dat een belangrijke rol speelt in de activatie van hypertrofie genen, van de celkern naar het cytoplasma van de cel is verplaats. Dit duidt erop dat in vitro CHAPa en CHAPb niet leidt tot directe activatie van hypertrofie in hartspiercellen

In **hoofdstuk 6** bestuderen we de expressie van CHAP in andere volwassen muizen organen.

We kunnen zien dat CHAPb ook tot expressie komt in de nieren, hersenen, dunne darm en dikke darm. Met behulp van immunohistochemische technieken kunnen we bijvoorbeeld zien dat in de dunne darm CHAP niet lokaliseert in de gladde spierlaag, maar op een specifieke wijze in de darmvlokken. We laten verder zien dat het grenst aan de expressie van actine filamenten. In de nier komt CHAP tot expressie in de nierbuisjes en ook hier zien we dat CHAP expressie grenst aan die van actine filamenten.

In **hoofdstuk 7** tot slot, bespreken we de resultaten van dit onderzoek en geven we suggesties voor vervolg onderzoeken. Zo zou er de mogelijkheid zijn om CHAP te bestuderen in hartaandoeningen bij mensen door gebruik te maken van een DNA database en het opsoren van mogelijke mutaties in CHAP. Verder zou het interessant zijn om de mogelijk rol van CHAP te bestuderen in andere ziektes zoals artheroslerose (aderverkalking) en kanker.

# List of publications

**Willemijn van Eldik**, Abdelaziz Beqqali, Jantine Monshouwer-Kloots, Twan de Vries, Christine Mummery and Robert Passier: *In vitro* overexpression of CHAPa and CHAPb in mouse cardiomyocytes and skeletal muscle cells interferes with Z-disc integrity and decreases fetal gene expression. In preparation.

**Willemijn van Eldik**, Abdelaziz Beqqali, Jantine Monshouwer-Kloots, Brigit den Adel, Daniela Salvatori, Saskia Maas, Nicky Boontje, Jolanda van de Velde, Paul Steendijk, Christine Mummery and Robert Passier: Overexpression of the Z-disc protein CHAPb leads to cardiac hypertrophy and diastolic dysfunction. Submitted

**Willemijn van Eldik** and Robert Passier: Signaling in sarcomeres in cardiac development and disease. Netherlands Heart Journal. Submitted

**Willemijn van Eldik**, Abdelaziz Beqqali, Jantine Monshouwer-Kloots, Christine Mummery, Robert Passier (2011): CHAP is expressed in striated and smooth muscle cells in chick and mouse during embryonic and adult stages. International Journal of Developmental Biology: 55(6): 649-655.

Beqqali A, **van Eldik W**, Mummery C, Passier R. (2009): Human stem cells as a model for cardiac differentiation and disease. Cellular and Molecular Life Sciences: 66(5): 800-813.

# Curriculum vitae

Willemijn van Eldik was born on the 9th of February 1982 in Cothen, The Netherlands. In 2000 she graduated from Revius Lyceum in Doorn (VWO) and in the same year she started with her study biology at the Wageningen University. During her study she carried out two internships to investigate the role of thyroid status on male reproductive function at the department of Human and Animal Physiology (Dr. Katja Teerds) at the Wageningen University and department of Pharmacology and Therapeutics at the McGill University (Dr. Bernard Robaire), Montreal, Canada. In a third internship she investigated the role of the Wnt-pathway on development of colon cancer in the group of Prof. Dr. Hans Clevers at the Hubrecht Institute, Utrecht. In 2006 she graduated and in the same year she started with a PhD-project in the Molecular Biology group (Prof. Dr. Henk Stunnenberg) at the University of Nijmegen, investigating fusion proteins in acute myeloid leukemia. In 2007 she started a PhD-project at the Hubrecht Institute in the group of Prof. Dr. Christine Mummery under the supervision of Dr. Robert Passier. In 2008 the groups of Mummery and Passier moved to the department of Anatomy and Embryology of the Leiden University Medical Center. The results of this investigation are described in this thesis. Currently Willemijn works as a research scientist at RnAsssays.

# Dankwoord

Bloed, zweet en tranen, maar het is af! Dat was nooit gelukt zonder de hulp en steun van een aantal mensen. Deze pagina's wil ik gebruiken om een aantal mensen te bedanken.

Allereerst wil ik Robert bedanken voor de begeleiding tijdens deze jaren. Ik heb het al die jaren erg naar mijn zin gehad in de 'CHAP' groep en ik heb veel van je geleerd. Je eerste AIO in Leiden die gaat promoveren, ik hoop dat er nog veel zullen volgen.

Ook wil ik Christine bedanken voor de kans die je mij hebt geboden om in je lab onderzoek te komen doen.

Appie zonder jou was er geen CHAP geweest! Ook bedankt voor je kritische commentaar bij de papers en hulp bij experimenten. Veel succes in de toekomst met je onderzoek en ik hoop dat er nog veel CHAP papers zullen volgen. Jantine jij hebt me geholpen bij veel experimenten, dankzij jou staan er een aantal mooie figuren in mijn proefschrift!

Andere collega's van de afdeling Anatomie & Embryologie die ik wil bedanken: Daniela en Saskia voor de hulp met muizenexperimenten en voor de analyse van de CHAP transgenen. Brigit en Ernest jullie hulp bij de MRI's hebben een mooi figuur in een artikel opgeleverd. Bert bedankt voor al je gevraagde en ongevraagde advies, voor je hulp bij het coupes snijden, microscopie en het maken van de reconstructies. Ook wil ik Jan en Conny bedanken voor hun hulp bij de experimenten. Bas voor het maken van illustraties. En natuurlijk ook alle andere collega's van Anatomie & Embryologie wil ik bedanken voor de leuke tijd.

Ook wil ik een aantal andere mensen in het LUMC bedanken voor hun hulp. Twan voor de hulp bij het maken van de CHAP adenovirussen. Paul Steendijk voor het maken van de ECG's. De dierverzorgers, Peter, Ilma en Lieke, voor het verzorgen van de muizen.

Ook heb ik hulp gehad van buiten het LUMC en die mensen wil ik ook bedanken. Stieneke voor de hulp bij het manipuleren van de muis ES cellen. Jeroen voor het maken van de transgene muizen. Jolanda en Nicky voor het doen van de sarcomeermetingen, het is een mooie aanvulling bij het transgene paper. I would like to thank Andras Dinnyes for the generation of chimeric mice and Siobhan Loughna for performing the morpholino experiments in the chick embryo's.

En vervolgens wil ik ook een aantal mensen uit mijn directe omgeving bedanken. Meike bedankt dat ik altijd op je paard heb mogen rijden, het was een goede manier om mijn hoofd leeg te maken. En ik vind het echt leuk dat we nu samen kunnen rijden! Ook de mensen van het menclubje, Denise, Maurits, Trudy en Ymkje, voor alle keren dat jullie mij mee wilden nemen op de wagen, het was wel afzien voor jullie. Jolien voor alle leuke dingen die we altijd samen doen. Ik heb goede herinneringen aan onze logeerpartijtjes van vroeger en ik vind het leuk dat we het nog steeds goed kunnen vinden. Aris je bent mijn allergrootste vriend! Ook wil ik Dick en Truus bedanken voor al hun getoonde interesse in mijn werk met muizen.

En dan wil ik tot slot nog een aantal mensen bedanken. Jo voor alle getoonde interesse in

mijn onderzoek en voor alle discussies. Maarten en Geert, ik vind het heel leuk dat jullie mijn paranimfen zijn. Alessandra tu sei la mia cognata preferita! Maarten en Ale ik vind het altijd leuk om bij jullie langs te komen in Brivio. Geert ik ben heel trots op je dat het zo goed gaat met je studie en wens je veel succes in de toekomst met je studie. Oma van Eldik ik voel me zeer vereerd dat ik op uw 97e verjaardag ga promoveren! Tot slot wil ik mijn lieve ouders bedanken voor alle hulp, interesse in mijn onderzoek en onvoorwaardelijke liefde. Jullie staan altijd voor mij klaar, dat waardeer ik heel erg.

Willemijn